

Cell-active Small Molecule Inhibitors of the DNA-damage Repair Enzyme Poly(ADP-ribose) Glycohydrolase (PARG): Discovery and Optimization of Orally Bioavailable Quinazolinedione Sulfonamides

Bohdan Waszkowycz, Kate M. Smith, Alison E McGonagle, Allan M. Jordan, Ben Acton, Emma Fairweather, Louise A. Griffiths, Niall Hamilton, Nicola Hamilton, James Hitchin, Colin P. Hutton, Dominic James, Clifford D. Jones, Stuart Jones, Daniel P. Mould, Helen Small, Alexandra Stowell, Julie Tucker, Ian Waddell, and Donald Ogilvie

J. Med. Chem., **Just Accepted Manuscript** • DOI: 10.1021/acs.jmedchem.8b01407 • Publication Date (Web): 07 Nov 2018

Downloaded from <http://pubs.acs.org> on November 8, 2018

Just Accepted

“Just Accepted” manuscripts have been peer-reviewed and accepted for publication. They are posted online prior to technical editing, formatting for publication and author proofing. The American Chemical Society provides “Just Accepted” as a service to the research community to expedite the dissemination of scientific material as soon as possible after acceptance. “Just Accepted” manuscripts appear in full in PDF format accompanied by an HTML abstract. “Just Accepted” manuscripts have been fully peer reviewed, but should not be considered the official version of record. They are citable by the Digital Object Identifier (DOI®). “Just Accepted” is an optional service offered to authors. Therefore, the “Just Accepted” Web site may not include all articles that will be published in the journal. After a manuscript is technically edited and formatted, it will be removed from the “Just Accepted” Web site and published as an ASAP article. Note that technical editing may introduce minor changes to the manuscript text and/or graphics which could affect content, and all legal disclaimers and ethical guidelines that apply to the journal pertain. ACS cannot be held responsible for errors or consequences arising from the use of information contained in these “Just Accepted” manuscripts.

1
2
3 **Cell-active Small Molecule Inhibitors of the DNA-damage Repair Enzyme**
4
5
6 **Poly(ADP-ribose) Glycohydrolase (PARG): Discovery and Optimization of**
7
8
9 **Orally Bioavailable Quinazolinedione Sulfonamides**
10

11
12
13
14 Bohdan Waszkowycz^{†,#}, Kate M. Smith^{†,#}, Alison E. McGonagle^{†,#}, Allan M. Jordan^{†,#,*}, Ben Acton[†],
15
16 Emma E. Fairweather[†], Louise A. Griffiths[†], Niall M. Hamilton[†], Nicola S. Hamilton[†], James R.
17
18 Hitchin[†], Colin P. Hutton[†], Dominic I. James[†], Clifford D. Jones[§], Stuart Jones[†], Daniel P. Mould[†],
19
20 Helen F. Small[†], Alexandra I. J. Stowell[†], Julie A. Tucker^{‡,∞}, Ian D. Waddell[†] and Donald J. Ogilvie[†].
21
22

23 [†]Cancer Research UK Manchester Institute, The University of Manchester, Alderley Park,
24
25 Maccelsfield, SK10 4TG, UK
26
27

28 [§]Oncology Innovative Medicines Unit, AstraZeneca, Alderley Park, Macclesfield, Cheshire, SK10
29
30 4TG, UK
31
32

33 [‡]Structure and Biophysics, Discovery Sciences, AstraZeneca, Alderley Park, Macclesfield, Cheshire,
34
35 SK10 4TG, UK
36
37

38 [∞]Current address: Centre for Immunology and Infection, Department of Biology and HYMS,
39
40 University of York, Heslington, York, YO10 5DD, UK
41
42
43
44
45
46
47
48
49
50
51
52
53
54
55
56
57
58
59
60

ABSTRACT

DNA damage repair enzymes are promising targets in the development of new therapeutic agents for a wide range of cancers and potentially other diseases. The enzyme poly(ADP-ribose) glycohydrolase (PARG) plays a pivotal role in the regulation of DNA repair mechanisms; however the lack of potent drug-like inhibitors for use in cellular and in vivo models has limited the investigation of its potential as a novel therapeutic target. Using the crystal structure of human PARG in complex with the weakly active and cytotoxic anthraquinone **8a**, novel quinazolinedione sulfonamides PARG inhibitors have been identified by means of structure-based virtual screening and library design. 1-Oxetan-3-ylmethyl derivatives **33d** and **35d** were selected for preliminary investigations in vivo. X-ray crystal structures help rationalize the observed structure-activity relationships of these novel inhibitors.

INTRODUCTION

Exploiting the DNA damage response for cancer therapy relies on the fact that rapidly proliferating cancer cells have higher incidences of DNA damage, defective DNA repair pathways, genomic instability, or a combination of these facets.^{1,2,3} Poly(ADP-ribosylation) is a post-translational modification that plays an important role in the repair of damaged sections of DNA.^{4,5,6} Poly(ADP-ribose) polymerases (PARPs), in particular PARP1, signal the presence of DNA damage and facilitate DNA repair (Figure 1). Upon DNA damage, PARP1 binds to single-strand break (SSB) sites and autoribosylates using NAD⁺ as a substrate, to form poly(ADP-ribose) (PAR) chains. These PAR chains serve to recruit DNA repair proteins, such as XRCC1, to the site of DNA damage. Poly(ADP-ribose) glycohydrolase (PARG) systematically degrades the ADP-ribose polymers on the PARP enzyme, which is essential for DNA repair to occur; however, the precise order of events in this catalytic cycle is still unknown. Figure 1 shows how inhibiting PARG leads to the persistence of PAR chains, with predicted consequences on NAD recycling, PARP recycling, and SSB repair. Although PARP inhibitors have received much attention as cancer therapies,^{7,8} with olaparib approved by the FDA,⁹ the dearth of selective, cell-permeable small molecule PARG inhibitors has hampered

assessment of the therapeutic potential of targeting PARG in human cancer.^{10,11} Additionally, whilst there are 17 known PARP family members, of which only a subset are inhibited by the PARP inhibitors, no close homologs of PARG exist.⁴ This provides an attractive target for drug discovery, given the cell's apparent reliance on this single enzyme in nuclear DNA damage repair.¹²

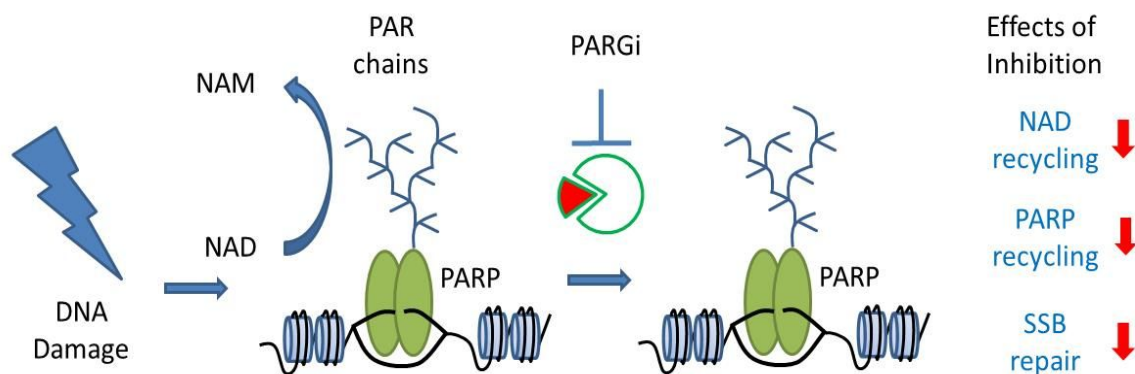


Figure 1. Consequences of PARG inhibition in DNA SSB repair

Crystal structures of the bacterial, protozoal, and mammalian PARG catalytic domains have served to elucidate the structural basis of PAR substrate recognition and catalytic mechanism.^{13,14,15,16,17,18,19} The C-terminal catalytic domain of PARG comprises a macrodomain, an evolutionarily conserved subunit that binds ADP-ribose and is involved in the regulation of PAR turnover and signalling,²⁰ with a PARG-specific catalytic loop. PARG demonstrates a preference for hydrolyzing the long, unbranched chains of PAR, which interact with an extended substrate binding site that is mostly solvent-exposed and polar in character.

To date, identification of potent and selective PARG inhibitors has been hampered by the lack of a suitable HTS-compatible assay system, prompting our recent development of a robust Homogeneous Time-Resolved Fluorescence (HTRF) based assay format.²¹ Inhibitors reported in the literature include: ADP-ribose mimetics (e.g., ADP-HPD, **1**),²² tannins (e.g., mono-galloyl glucose, **2**),²³ salicylanilides (**3**),²⁴ rhodanine-based compounds (**4**),²⁵ and phenolic hydrazide hydrazones (**5**)²⁶ (Figure 2). These compounds are typically weakly potent, non-specific inhibitors with poor cell permeability, only demonstrating activity in cell lysates.¹¹ For example, compounds **3** and **4** did not demonstrate significant PARG inhibitory activity in our biochemical assay (activities > 70 μ M in our

hands). Although compound **4** contains the known pan-assay interference (PAINS)²⁷ motif rhodanine, it has been successfully crystallized in complex with protozoal PARG, demonstrating binding to the ADP-ribose site.²⁴

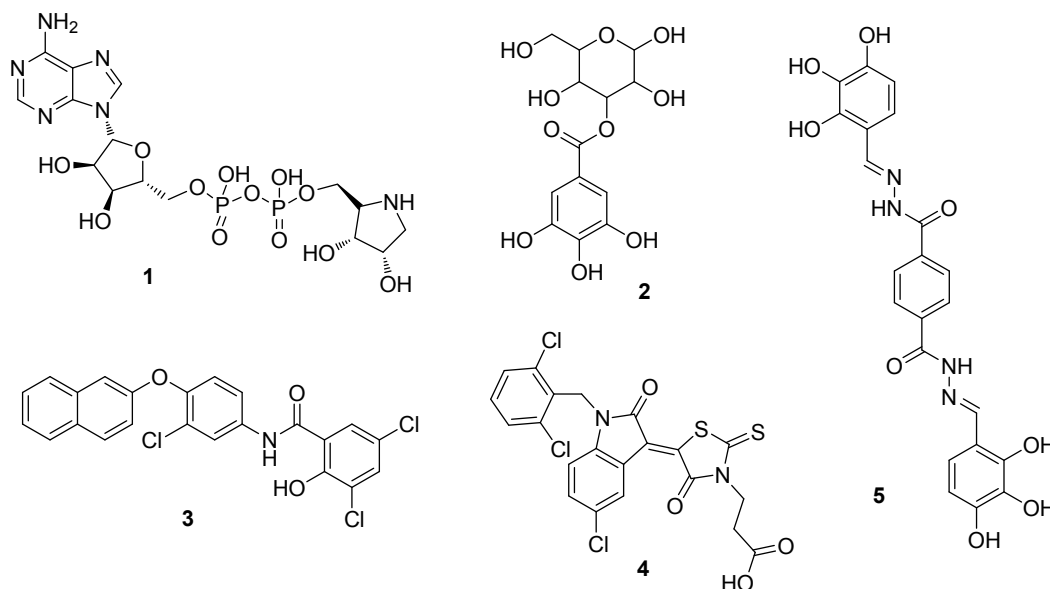


Figure 2. Reported PARG inhibitors

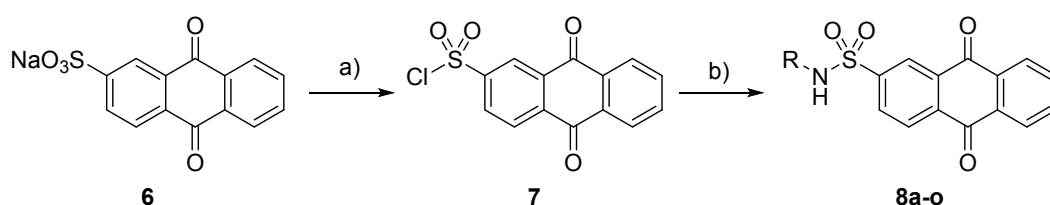
Given the lack of drug-like, cell permeable inhibitors reported to date, there remains a need for selective tool compounds with improved physicochemical properties to validate the therapeutic potential of PARG inhibition.¹¹ To address this need, we recently reported the first cell-active chemical probes against this enzyme.^{12,28,29} Herein, we describe the early discovery of several novel lead-like chemotypes arising from a programme of virtual screening and structure-guided library design, inspired by the crystal structure of a weakly active HTS hit bound to human PARG. We further report our efforts to optimize one of these chemotypes in order to afford more potent *in vitro* tool compounds, and derivatives with physicochemical properties suitable for preliminary *in vivo* pharmacokinetic (PK) assessment.

CHEMISTRY

For preliminary hit expansion, compounds were generally prepared using traditional chlorosulfonation techniques to prepare the sulfonyl chloride, which was then used for sulfonamide formation.

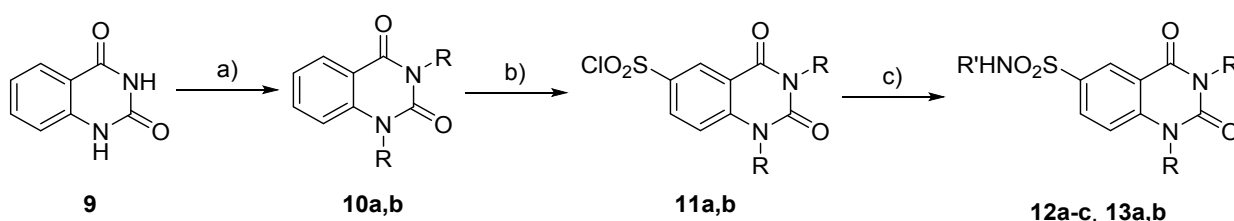
1
2
3 Anthraquinones **8a–o** were prepared in this manner as detailed in Scheme 1, as was compounds **16**
4 described in Scheme 3, with purification by preparative HPLC leading to variable recoveries of
5 material. Symmetrically substituted quinazolidiones **12a–c**, **13a,b** were prepared by alkylation of
6 the quinazolidione, followed by chlorosulfonation and sulfonamide formation (Scheme 2). For the
7 unsymmetrically substituted quinazolidiones **22a–h**, a route was developed which installed the
8 acetyl protected alkyl sulfonamide and allowed diversification in the final step, as detailed in Scheme
9
10
11
12
13
14
15
16
17
18
19
20
21
22
23
24
25
26
27
28
29
30
31
32
33
34
35
36
37
38
39
40
41
42
43
44
45
46
47
48
49
50
51
52
53
54
55
56
57
58
59
60

Scheme 1:^a Synthesis of analogues **8a–o**



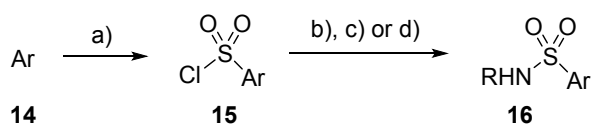
^aReagents: a) SOCl_2 , DMF, reflux, 53%; b) RNH_2 , Et_3N , DCM, 15%–quant.

Scheme 2:^a Synthesis of **12a–c**, **13a,b**

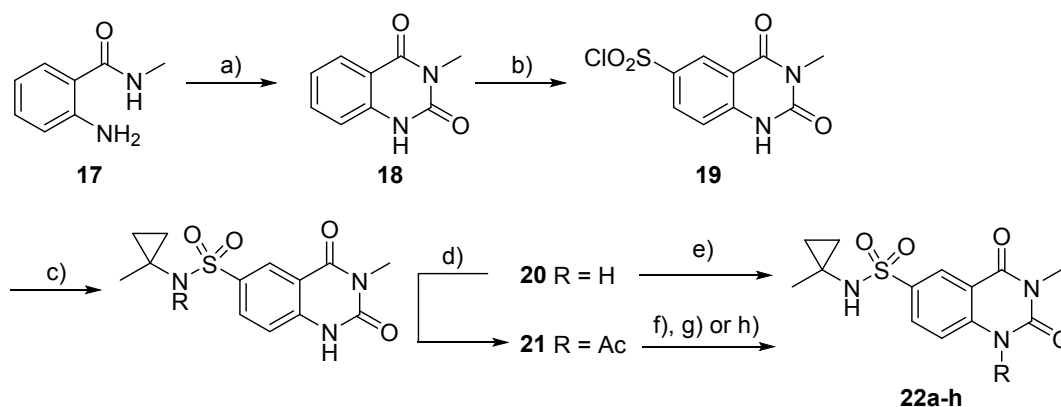


^aReagents: a) RI , K_2CO_3 , DMF, 30–41%; b) ClSO_3H , 60 °C, 64–67%; c) $\text{R}'\text{NH}_2$, Et_3N , DCM, 18–76%.

Scheme 3:^a Synthesis of **16**



^aReagents: a) ClSO_3H , 60 °C, 70%; b) RNH_2 , $i\text{-Pr}_2\text{NEt}$, THF, DCM, 43%.

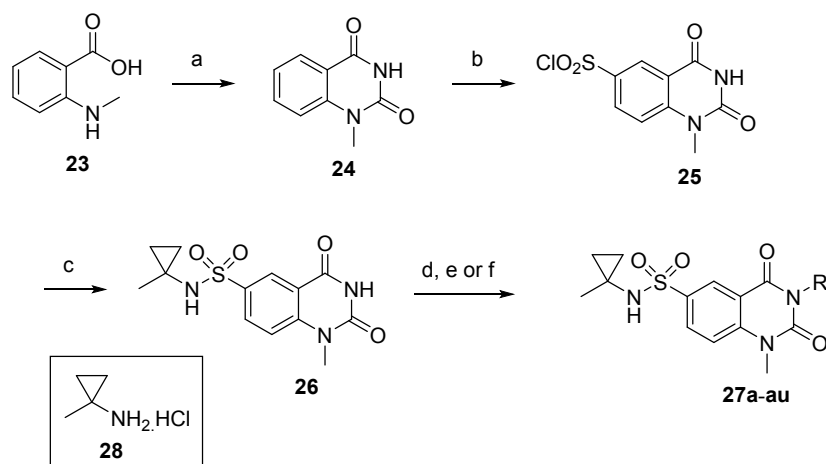
Scheme 4:^a Synthesis of Analogues **22a–t**

^aReagents: a) CDI, DMF, 140 °C, 90%; b) ClSO₃H, 60 °C, 99%; c) 1-methylcyclopropanamine hydrochloride, Et₃N, DCM, 89%; d) Ac₂O, pyridine, DMAP, 83%; e) BrCH₂CN, Cs₂CO₃, DMF, 75%; f) R-X (where X = I or Br), K₂CO₃, DMF, then NH₃, THF, 28–88%; g) R-X (where X = Cl, Br or I), K₂CO₃, DMF, then K₂CO₃, MeOH 20–32%; h) R-OH, DIAD, PS-PPh₃, DMF, then K₂CO₃, MeOH, 93%.

Scheme 5 describes the synthesis of **27a–au**, with elaboration at the N3 vector. The quinazolinedione core was formed from N-methylantranilic acid and sodium cyanate. Subsequent chlorosulfonylation and sulfonamide formation afforded key intermediate **26**, which was alkylated to give 1-methyl-3-substituted quinazolinediones **27a–au**. Scheme 6 shows the synthesis of quinazolinediones with elaboration at both N1 and N3 vectors. Chlorosulfonylation of isatoic anhydride afforded **30**. Careful temperature control in the subsequent sulfonamide formation was vital to minimize anhydride ring-opening with amine **28**. Once the sulfonamide formation was complete at a low temperature, the appropriate primary amine was added to the reaction mixture and warmed to room temperature (RT) to induce anhydride ring-opening and decarboxylation to give amide intermediates **31a–d**. Ring closure to afford quinazolinediones **32a–d** was carried out using triphosgene, and subsequent alkylation at N1 afforded compounds **33–36**. In some cases, Mitsunobu reaction using diisopropylazodicarboxylate (DIAD) resulted in an inseparable mixture of product and reduced DIAD by-product. Fortunately, this problem was surmounted by using di-(4-chlorobenzyl)azodicarboxylate (DCAD),³⁰ as the hydrazine by-product in this case is easily removed by trituration. The approach to

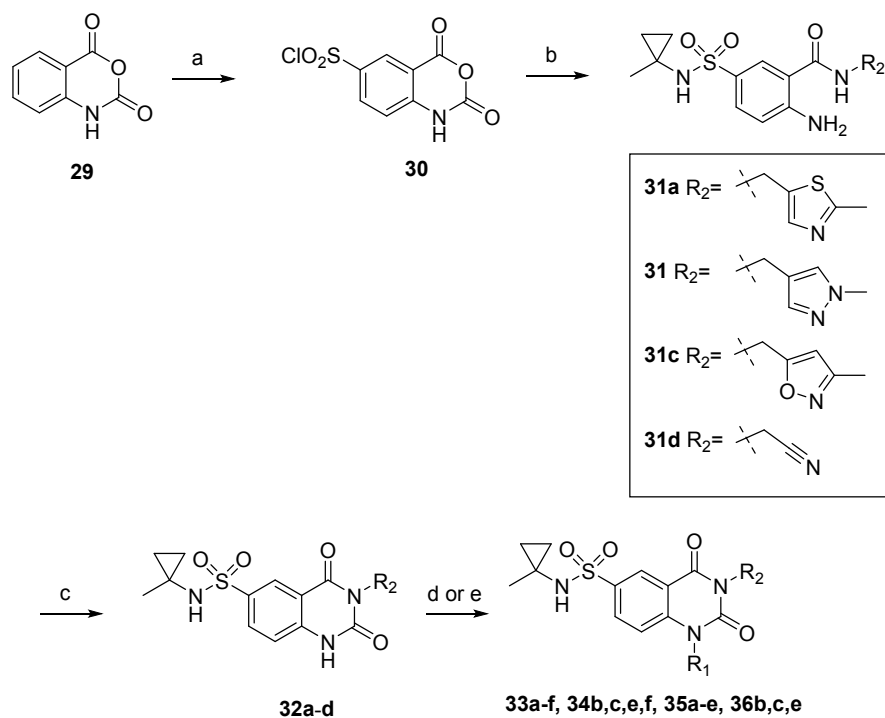
3-(5-methyl-1,3,4-thiadiazol-2-yl)methyl quinazolinediones **41a** and **41e** was slightly different (Scheme 7). The 3-substituent bearing the thiadiazole was introduced prior to the chlorosulfonylation reaction as there are no free sites on the five-membered heteroaryl ring that can undergo chlorosulfonylation in this case.

Scheme 5: Synthesis of **27a-at**^a



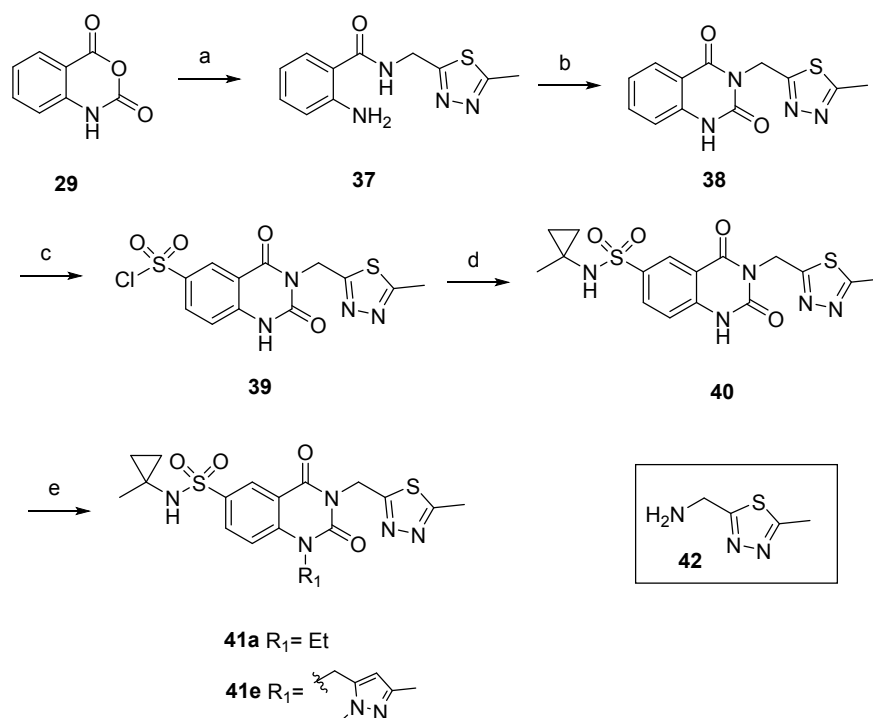
^aReagents and conditions: (a) NaOCN, NaOH, AcOH, H₂O, 50 °C, 1 h, 79%; (b) ClSO₃H, 50 °C, 16 h, quant.; (c) amine **28**, Et₃N, DCM, RT, 3 h, 93%; (d) (i) NaH, DMF, RT, 5 min, (ii) R-X (X= Br, Cl, I, OTs), RT, 6–59%; (e) R-OH, DIAD (or DCAD), PS-PPh₃, DMF, RT, 10–21%; (f) R-B(OH)₂, Cu(OAc)₂, Et₃N, 4Å molecular sieves, DCM, RT, 18%.

Scheme 6: Synthesis of **33–36**^a



^aReagents and conditions: (a) ClSO₃H, 50 °C, 4 h, 79%; (b) (i) amine **28**, Et₃N, DCM, -10 °C, 30 min, (ii) R₂-NH₂, Et₃N, -10 °C-RT, 18 h, 20-67%; (c) triphosgene, THF, 0 °C-RT, 18 h 78-97%; (d) (i) NaH, DMF, RT, 5 min, (ii) R₁-X (X= Br, I, OMs, OTs), RT; (e) R₁-OH, DIAD (or DCAD), PS-PPh₃, DMF, RT, 16-75%.

Scheme 7: Synthesis of **41a** and **41e**^a



Reagents and conditions: (a) amine **42**, Et_3N , DMF, 60 °C for 5 h, then RT for 16 h, 65%; (b) triphosgene, THF, 0 °C–RT, 18 h, 58%; (c) ClSO_3H , 50 °C, 2 h, 69%; (d) amine **28**, Et_3N , DCM, 0 °C–RT, 18 h, 32%; (e) EtI , K_2CO_3 , DMF, μW , 80 °C, 20 min, 20% for **41a**; and 5-(chloromethyl)-1,3-dimethyl-1H-pyrazole, K_2CO_3 , DMF, μW , 80 °C, 20 min, 44% for **41e**.

RESULTS AND DISCUSSION

Crystallographic binding mode and initial optimization of anthraquinone 8a

The low druggability of PARG was highlighted by a high-throughput screen at AstraZeneca, comprising 1.4 million compounds, which resulted in only three confirmed hits of related chemical structure, exemplified by the anthraquinone derivative **8a** (Figure 3). Despite this compound's modest inhibitory potency ($\text{EC}_{50} = 81 \mu\text{M}$) in an HTRF biochemical assay, we were encouraged by its approximately equipotent activity in an acute (1 h) cell-based proof-of-mechanism PAR chain persistence assay,^{21,31} where the compound was shown to block the PARG-mediated degradation of PAR chains in a dose-dependent manner. However, the limited solubility of the compound precluded an accurate estimation of EC_{50} , and further progression of this anthraquinone derivative was additionally hampered by the observation of non-specific 72 h cytotoxicity at cell-active doses.

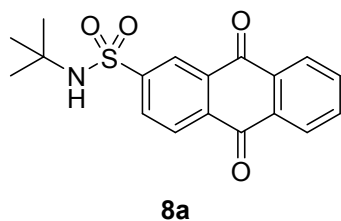


Figure 3. Anthraquinone HTS hit **8a**.

Determination of the co-crystal structure of **8a** with the catalytic domain of human PARG at 1.9 Å resolution confirmed the direct interaction of the inhibitor with the PAR binding site, and revealed some unexpected binding contacts that prompted our efforts to pursue structure-guided optimization of this series. As was previously reported, the substrate binding site in human PARG comprises an extended, relatively solvent-exposed channel.^{15, 16} The anthraquinone **8a** is observed to bind in the region occupied by the adenine moiety of the truncated PAR analogue, ADP-ribose (Figure 4). However, the plane of the anthraquinone ring system is oriented approximately orthogonal to that of the adenine moiety of ADP-ribose, with the result that **8a** is highly solvent-exposed compared to the relatively well-buried adenine. The significant difference in the shape of the binding site between the two crystal structures can be attributed to Phe902 adopting a different rotamer when bound to **8a** compared with ADP-ribose (Figure 4C). As a consequence, the anthraquinone core of **8a** is able to form extensive face-to-face aromatic stacking interactions with both Phe902 and Tyr795. Although this rotamer of Phe902 is incompatible with substrate binding, in the published *apo* structure of human PARG (PDB 4A0D) both rotamers of Phe902 are observed, highlighting the flexibility of this side chain.¹⁶

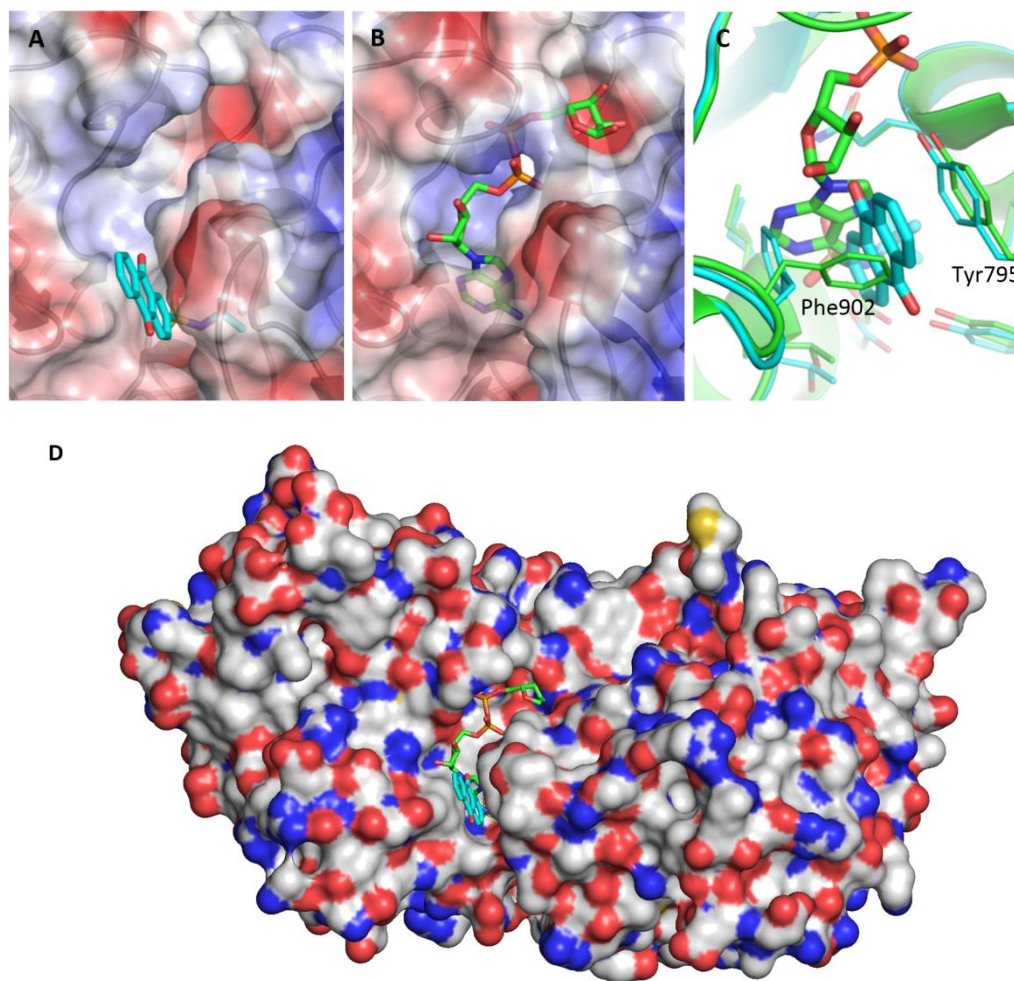


Figure 4. Comparison of the X-ray crystal structures of the catalytic domain of (A) human PARG bound to **8a** (PDB accession code 6HMM) and (B) ADP-ribose (PDB 4B1H), shown in the same coordinate frame. Protein solvent-accessible surfaces are coloured by electrostatic potential. (C) Detail of relative binding orientations of **8a** (cyan carbon atoms) and ADP-ribose (green) highlights movement of Phe902. (D) **8a** and ADP Ribose bound to entire PARG domain, colored by atom type.

The binding mode of **8a** is anchored by a network of three hydrogen bonds from the sulfonamide moiety to the sidechain of Glu727 and the backbones of Ile726 and Gln754, with the *tert*-butyl group deeply buried in a mainly hydrophobic cavity (Figure 5). We note that in the crystal structure of PARG in complex with ADP-ribose, the adenine moiety forms hydrogen bonds to the Glu727 sidechain and Ile726 backbone *NH* (as well as, several water-mediated contacts); hence, this is a rare example of a sulfonamide moiety mimicking the hydrogen-bond network of adenine.

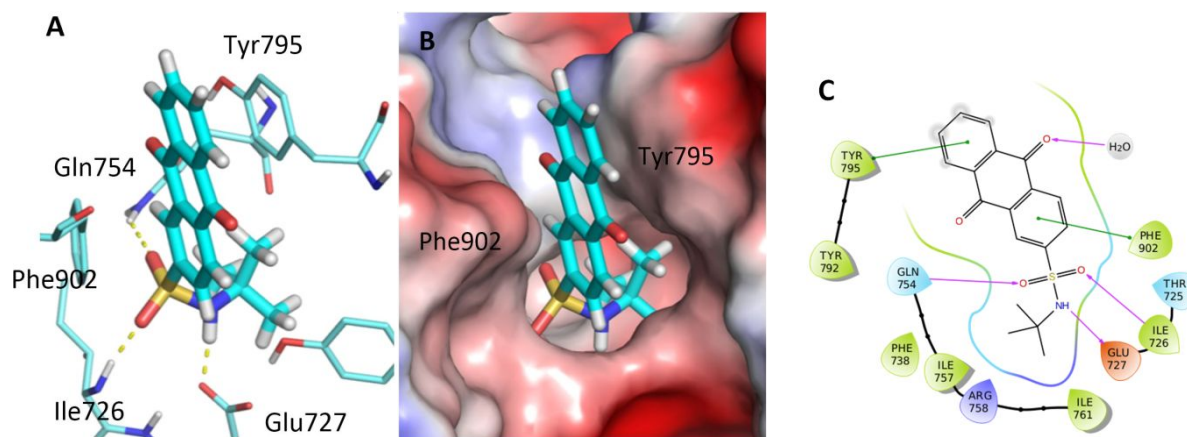
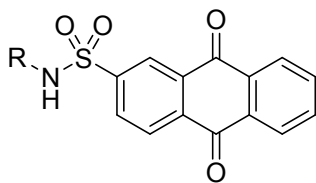


Figure 5. (A) Detail of the hydrogen-bonding environment around **8a** (PDB accession code 6HMM). (B) Protein solvent-accessible surface highlights the exposure to solvent of the anthraquinone core and the buried pocket around the *tert*-butyl moiety. Hydrogen atoms modelled using Maestro (Schrödinger LLC). (C) Protein-ligand interaction diagram with hydrogen bonds indicated by pink arrows and aromatic interactions by green arrows.

Optimization of **8a** focused on a series of hydrophobic and polar replacements of the *tert*-butyl moiety to explore the limits of the constrained binding pocket observed around the *N*-alkyl sulfonamide head-group (Scheme 1, Table 1). A preference was observed for compact branched or cyclic alkyl groups, notably for the simple cyclopropyl **8f**, and particularly the methylcyclopropyl and cyanocyclopropyl derivatives (**8h** and **8i**), which yielded single-digit micromolar biochemical activities. A series of unbranched polar-substituted groups (e.g., **8j–n**) were designed to probe a narrow solvent-filled channel extending from the *tert*-butyl pocket, but these all proved ineffective. *N*-Methylation of the sulfonamide, or replacement with alternative linkers such as amides and the reversed sulfonamide abolished activity (data not shown), emphasizing a strict requirement for the specific network of hydrogen-bonding contacts observed in the crystal structure. In summary, the steep SAR highlighted the limited opportunities for optimization of the *N*-alkyl sulfonamide moiety. Although an encouraging improvement in activity had been achieved for **8i** and **8h** compared with **8a**, cell toxicity remained an issue with this series and was presumed to be related to the anthraquinone ring system, a motif reminiscent of known DNA intercalators.³²

Table 1.^a Initial optimization of the sulfonamide *N*-alkyl moiety of **8a**

Compound	R	PARG Biochemical EC ₅₀ /μM	PARG Cell EC ₅₀ /μM
8a	<i>tert</i> -butyl	81 (21)	~30
8b	Methyl	>30 ^b	<i>nd</i>
8c	Ethyl	110 (7.1)	<i>nd</i>
8d	1,1-dimethylpropyl	49 (27)	<i>nd</i>
8e	Cyclopropylmethyl	24 (5.2)	<i>nd</i>
8f	Cyclopropyl	13 (5.3)	22 (6.8)
8g	Cyclobutyl	>50 ^b	<i>nd</i>
8h	1-methylcyclopropyl	6.0 (2.3)	6.6 (3.5)
8i	1-cyanocyclopropyl	3.3 (2.3)	19 (5.2)
8j	Carbamoylmethyl	>150	<i>nd</i>
8k	2-carbamoylethyl	>150	<i>nd</i>
8l	2-hydroxyethyl	>150	<i>nd</i>
8m	2-methoxyethyl	>150	<i>nd</i>
8n	2-methoxy-1,1-dimethyl-ethyl	>150	<i>nd</i>
8o	2-cyanoethyl	88 (18)	<i>nd</i>

1
2
3 ^aBiological data are stated as the geometric mean of at least three independent determinations unless
4 otherwise stated, with standard deviations quoted in parentheses. *nd* = not determined.
5
6
7

8 ^bMaximum concentration limited by interference and/or solubility issues.
9
10

11 *Scaffold-hopping by virtual screening and library design*

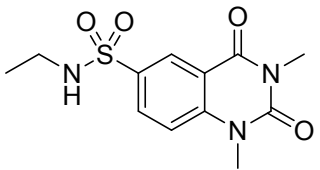
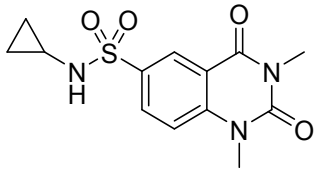
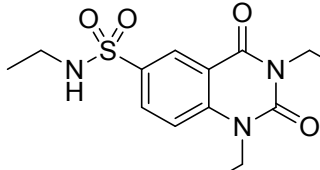
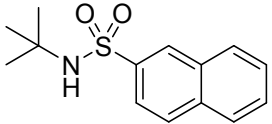
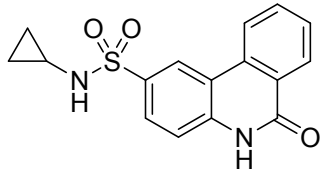
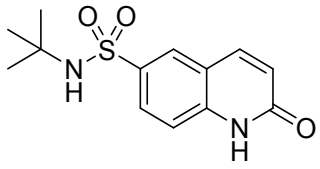
12
13

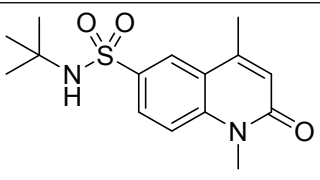
14
15
16
17 In parallel with elaboration of the anthraquinone sulfonamide moiety, a structure-based virtual
18 screening campaign was initiated to identify alternatives to the anthraquinone ring system that might
19 obviate the observed cell toxicity and prove more amenable to optimization. As the hydrogen-bonding
20 network observed around the sulfonamide appeared to be a key pharmacophore, we decided to retain
21 this moiety while exploring alternative bi- and tricyclic ring systems that would maintain the observed
22 stacking interactions with Tyr795 and Phe902, and introduce more drug-like physical properties.
23
24
25
26
27
28
29

30 To this end, commercially available screening libraries were initially triaged to identify and select all
31 aryl sulphonamides bearing a variety of aliphatic *N*-substituents. These selections were then filtered
32 for suitable drug-like properties and any PAINS or undesirable structural motifs removed. These
33 approaches yielded around thirty one thousand putative hits which were then docked into the induced
34 cavity observed in the X-ray structure of **8a** bound to human PARG (Glide SP docking, Schrodinger,
35 LLC, New York). Manual inspection of the top 5 docking poses per ligand ensured maintenance of
36 the key sulphonamide binding motif and credible binding modes and from this manual analysis, a set
37 of 68 compounds was selected for purchase and assessment, based on an assessment of binding mode,
38 site complementarity and docking score.
39
40
41
42
43
44
45
46
47
48
49

50 The biochemical affinity of these initial compounds proved to be very weak, with the notable
51 exception of the quinazolidinedione **12e** (Table 2). Replacing the sulfonamide *N*-cyclopropyl
52 substituent of **12e** with *N*-ethyl (**12d**, **13c**) resulted in a large drop in activity, consistent with the SAR
53 observed for the anthraquinone scaffold (Table 1). The only other *N*-cyclopropyl example in Table 2,
54 the tricyclic scaffold **43**, displayed modest activity but with significantly reduced ligand efficiency
55
56
57
58
59
60

1
2
3 compared with **12e**. While some examples with the *N*-*tert*-butyl moiety, such as **44** and **45**, were of
4
5 similar activity to the anthraquinone **8a**, other bicyclic systems proved to be inactive (**16**). Table 2.^a
6
7 Example hits from the initial virtual screen of commercial compounds.
8
9

Compound	Structure	PARG Biochemical EC ₅₀ /μM
12d		>150
12e		11 (4.0)
13c		140 (30)
16		>150
43		50 (9.8)
44		110 (26)

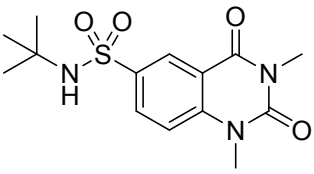
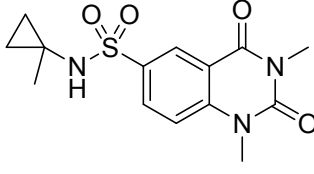
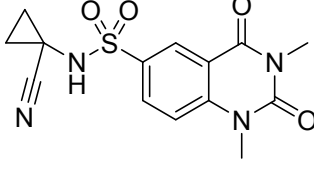
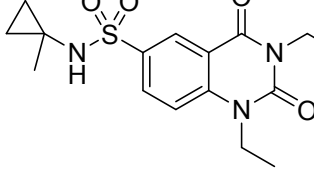
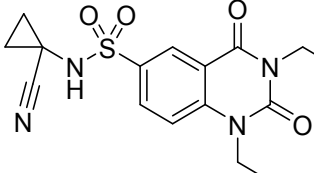
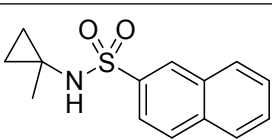
45		57 (25)
----	---	---------

^aBiological data are stated as the geometric mean of at least three independent determinations, with standard deviations quoted in parentheses.

To determine if the weak level of activity for these compounds was a consequence of sub-optimal *N*-alkyl substitution on the sulfonamide, analogues of selected cores were synthesized with the preferred *N*-alkyl substituents identified from the optimization of **8a**, e.g., methylcyclopropyl and cyanocyclopropyl (Scheme 2 and Scheme 3, Table 3). This modification resulted in a significant gain in biochemical activity for the quinazolinones **12b**, **12c**, **13a** and **13b**, which demonstrated a greater than 20-fold improvement compared with the *tert*-butyl analogue **12a**, and were accompanied by an increase in biochemical lipophilic ligand efficiency (LLE)³³ from a value of 2.1 for **12a** to 3.9 and 4.7 for **12b** and **12c**, respectively. Notably, the quinazolinones also demonstrated a similar level of potency in the cell assay, with the best examples achieving low micromolar potency. However, *N*-methylcyclopropyl derivatives of other ring systems such as the naphthalene **16** did not achieve levels of activity to justify further consideration. From docking studies, the quinazolinone scaffold hop was predicted to achieve very similar binding modes to the anthraquinone **8a**, while offering different vectors for enhancing binding affinity through additional protein interactions (Figure 6).

Table 3.^a Optimization of sulfonamide *N*-alkyl groups for hits from the first round of virtual screening.

Compound	Structure	PARG Biochemical	PARG Cell EC ₅₀ /μM
----------	-----------	---------------------	-----------------------------------

		EC ₅₀ /μM	
12a		110 (30)	<i>nd</i>
12b		3.9 (1.7)	1.8 (1.1)
12c		5.0 (1.6)	14 (3.8)
13a		1.5 (0.56)	1.1 (0.53)
13b		1.8 (0.50)	5.6 (3.0)
16		>150	<i>nd</i>

^aBiological data are stated as the geometric mean of at least three independent determinations, with standard deviations quoted in parentheses. *nd* = not determined.

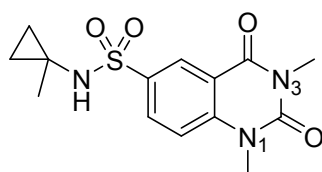
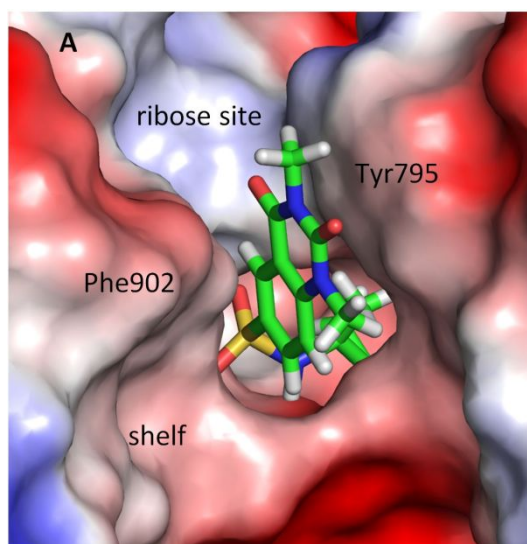


Figure 6. Predicted binding modes of quinazolinedione **12b** (docked into PDB accession code 6HMM) The N1 position presents a vector towards solvent and the shelf adjacent to Phe902, while the N3 position presents a vector toward the pocket occupied by the ribose moiety of ADP.

The requirement for specific *N*-alkyl sulfonamide substituents, such as *tert*-butyl and cyclopropyl, in order to achieve significant levels of potency suggested that potentially useful scaffold hops may have been missed in the original virtual screening campaign because of the limited commercial availability of appropriate sulfonamides. Therefore, a second round of virtual screening was initiated based on docking virtual libraries generated from the in silico enumeration of a diverse set of commercially available aryl sulfonyl chlorides with several of our preferred alkyl amines. A further set of scaffold hops was designed on the basis of 2D similarity to the active cores identified previously. Synthesis of selected examples from these approaches resulted in a chemically diverse set of additional scaffolds, several of which displayed promising levels of activity, though none proved to be superior in potency or lipophilic ligand efficiency to the quinazolinediones (Supporting Information Table S2). Note that for synthetic expediency, no attempt was made to optimize fully the substituents around each distinct ring system; rather, the aim of the exercise was to perform a rapid exploration of synthetically

tractable SAR to understand whether any particular ring systems were significantly favored or disfavored. In general, we observed that fully aromatic/delocalized bicyclic cores were preferred over partially saturated ring systems, consistent with the modelled binding modes in which the aromatic core is tightly stacked between Tyr795 and Phe902. Among aromatic systems, there appears to be a preference for one or more hydrogen bond acceptor groups such as a carbonyl oxygen (as in the quinazolinedione **12b**) or a nitrogen lone pair (as in the quinoline **S12**, Supporting Information Table S2). In contrast, incorporation of a nitrogen atom in the benzo ring bearing the sulfonamide resulted in between 3 and 5-fold loss of activity (e.g., compound **S1**, Supporting Information Table S2). We note that, in the X-ray crystal structure of PARG in complex with **8a**, a number of polar protein atoms are located in close proximity to the anthraquinone ring system, including the potential hydrogen bond donor Tyr795 *OH*, and it may be that a combination of hydrogen bonding (perhaps through water) and enhanced π -stacking interactions account for the preferences seen for certain ring systems over others.

Overall, by utilizing this approach, we succeeded in moving from an unattractive HTS hit to several lead-like scaffolds displaying improved ligand efficiency and physicochemical properties. Comparison of the initial hit compound **8a** with **12b** reveals a reduction in molecular weight and LogP, with associated increases in LE and LLE (Table 4). In addition, the scaffold hop is devoid of the acute non-specific cytotoxicity of the parent anthraquinone. On the basis of its promising potency, synthetic tractability and favorable physicochemical profile, the quinazolinedione series was prioritized as an attractive starting-point for further optimization.

Table 4. Comparison of measured and predicted physicochemical properties of representative compounds.

Compound	MW	Measured LogD _{7.4}	Calculated LogP ^a	Turbidimetric Solubility (μ M)	LE ^b	LLE ^c	Cytotoxicity (μ M)
8a	343.4	<i>Nd</i>	3.18	20	0.23	0.91	16 (2)
12b	323.4	1.73	1.50	>100	0.34	3.9	>30

1
2
3
4
5
6 ^aXlogP calculated using Dotmatics Elemental package (Dotmatics, Bishops Stortford, UK). ^bLigand
7
8 Efficiency calculated from biochemical EC₅₀ (i.e., LE = 1.4(*p*EC₅₀)/HAC, where HAC is the number
9
10 of heavy atoms). ^cRef 33. *nd* = not determined.

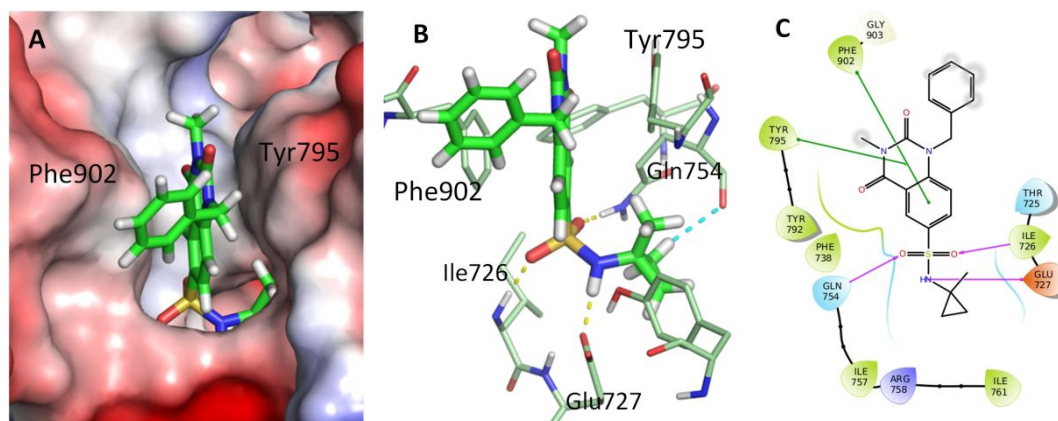
11 12 13 *Optimization of quinazolinedione N1 position*

14
15
16 Initial exploration of the SAR around the quinazolinedione ring system focused on substitution at the
17
18 N1 position (Scheme 4), as this vector presented an opportunity for interaction with a solvent-exposed
19
20 shelf adjacent to Phe902 (Figure 6). Methylene-linked saturated and aromatic ring systems were of
21
22 interest as a strategy to improve binding affinity, as modelling suggested these would readily access
23
24 the Phe902 shelf; while more conformationally flexible groups were deemed likely to extend into
25
26 solvent and thus, would be more useful to modulate physicochemical properties.

27
28
29 In general, substitution at N1 yielded relatively modest gains in biochemical and cellular EC₅₀, (Table
30
31 5) with the ethyl analogue **22a** similar in potency to the parent methyl **12b**. Incorporation of more
32
33 polar groups, such as in **22b** and **22c**, resulted in low micromolar compounds with improved LLE. We
34
35 were pleased to observe that simple lipophilic groups such as the prop-2-ynyl **22d** and
36
37 cyclopropylmethyl **22f** yielded our first sub-micromolar compounds in both enzyme and cell assays.
38
39 This level of cellular potency represents a significant advance in the identification of cell-active
40
41 PARG tool compounds when compared with our original HTS hit and also other inhibitors described
42
43 in the literature.

44
45
46 In comparison with **22f**, larger carbocyclic substituents (e.g., **22g** and **22h**) did not result in any
47
48 further gain in potency. The predicted binding mode of the benzylic derivative **22h** was confirmed by
49
50 soaking the compound into pre-formed crystals of human PARG, resulting in a 2.9 Å resolution X-ray
51
52 crystal structure (Figure 7). The compound was observed to bind similarly to **8a**, with the
53
54 quinazolinedione ring system well aligned with the anthraquinone of **8a** and forming aromatic
55
56 stacking interactions with Tyr795 and Phe902. The sulfonamide moiety forms the same network of
57
58 three hydrogen bonds as observed for **8a**, with the *N*-methylcyclopropyl group occupying a similar
59
60

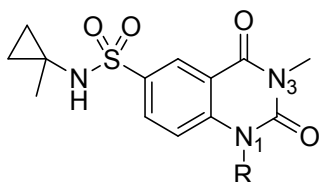
1
2
3 location to the *tert*-butyl of **8a**. As these groups are very similar in size, the significant improvement
4 in activity observed for the methylcyclopropyl may be due to the greater π -character of the
5 cyclopropyl ring:³⁴ we note close non-bonded contacts between the cyclopropyl ring and the
6 sidechains of Gln754 and Glu727, with a potential CH \cdots O hydrogen bond to the backbone carbonyl of
7 Gln754. The N1 benzyl group partly occupies the Phe902 shelf, stacking against the Phe902–Gly903
8 peptide bond. The interaction between the benzyl group and the Phe902 shelf appears sub-optimal in
9 terms of shape complementarity, which likely accounts for the modest potency of **22h** and suggested
10 opportunities for further optimization. Pleasingly, the determined crystallographic structure of this
11 derivative closely matched the binding mode predicted by modelling, facilitating the prioritization of
12 latter derivatives (such as the improved analogue **22f**) for synthesis and precluding the requirement
13 for extensive iterative crystallographic determination.



31
32
33
34
35
36
37
38
39
40
41
42
43
44
45
46
47
48
49
50
51
52
53
54
55
56
57
58
59
60

Figure 7. X-ray crystal structure of **22h** bound to the catalytic domain of human PARG at 2.9 Å resolution (PDB accession code 6HMN) (A) Interaction of the N1-benzyl moiety with the Phe902 shelf. (B) Detail of the hydrogen-bonding environment around the sulfonamide, with a putative CH \cdots O interaction highlighted by the cyan dashed line. Hydrogen atoms modelled using Maestro (Schrödinger LLC). (C) Ligand interaction diagram coloured as in Figure 5.

Table 5.^a Evaluation of quinazolinedione N1 substituents.

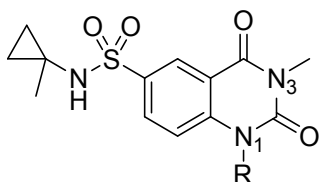


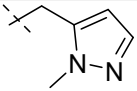
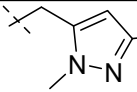
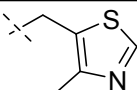
Compound	R	Biochemical EC ₅₀ /μM	Cell EC ₅₀ /μM
20	H	4.0 (2.0)	8.1 (9.2)
12b	methyl	3.9 (1.7)	1.8 (1.1)
22a	ethyl	1.3 (1.9)	3.6 (1.3)
22b	2-methoxyethyl	1.1 (0.13)	6.1 (3.1)
22c	2-(dimethylamino)ethyl	2.0 (0.77)	6.4 (5.3)
22d	prop-2-ynyl	0.71 (0.17)	0.25 (0.088)
22e	cyanomethyl	2.8 (1.6)	8.9 (4.5)
22f	cyclopropylmethyl	0.44 (0.18)	0.62 (0.62)
22g	cyclohexylmethyl	0.56 (0.28)	2.7 (1.6)
22h	benzyl	1.3 (0.62)	2.3 (0.97)

^aBiological data are stated as the geometric mean of at least three independent determinations, with standard deviations quoted in parentheses. nd = not determined.

We determined to further investigate structure-activity relationships (SAR) at the N1 position of the quinazolinone, as this vector presented a good opportunity for interaction with a solvent-exposed shelf adjacent to Phe902. It can be seen from the crystal structure of **22h** in complex with PARG that the N1 vector projects away from the PARG active site towards solvent (Figure 7). A library of more elaborate N1-quinazolinones (with N3 fixed as methyl) was therefore synthesized to explore whether the interactions with this shelf could be optimized in order to boost affinity. Further N1 variations are also shown in Table 6.

Table 6.^a Evaluation of quinazolinone N1 substituents.



Compound	R	Biochemical EC ₅₀ /μM
22i	2-F-Bn	1.4 (1.0)
22j	3-F-Bn	1.6 (0.80)
22k	4-F-Bn	0.53 (0.40)
22l	2-OMe-Bn	3.2 (0.17)
22m	3-OMe-Bn	0.86 (0.77)
22n	4-OMe-Bn	0.45 (0.13)
22o	2-Pyridylmethyl	5.8 (1.8)
22p	3-Pyridylmethyl	1.3 (0.26)
22q	4-Pyridylmethyl	2.4 (0.85)
22r		1.2 (0.37)
22s		0.38 (0.19)
22t		0.18 (0.058)

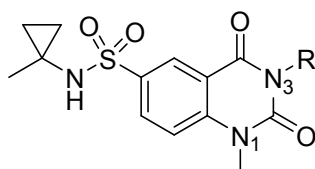
^aBiological data are stated as the geometric mean of at least three independent determinations, unless otherwise stated, with standard deviations quoted in parentheses.

The results in Table 6 show that substitution at the 4-position of the phenyl ring of the benzyl derivatives was usually favored over the 2- or 3-substituted analogues. Although the SAR was generally quite flat, only modest improvements in potency were observed compared to the parent N1-benzyl analogue **22h**. No improvement was observed with pyridylmethyl derivatives **22o-q**. However, significant improvements were obtained with methylene-linked 5-membered heteroaryl substituents. Pyrazole derivative **22r** showed low micromolar activity, and this was enhanced further by methylation at the 3-position (**22s**). Bis-methylated thiazole derivative **22t** gave the most potent quinazolinone in the series. Modelling suggested that these substituted 5-membered heterocycles achieved improved lipophilic contacts with the Phe902 shelf compared with benzyl derivative **22h**. Although some polar protein sites are accessible in this region, it was not apparent from the SAR that any productive hydrogen-bonding interactions were being achieved.

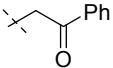
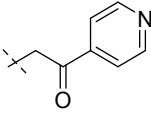
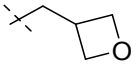
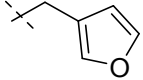
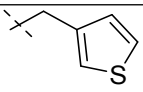
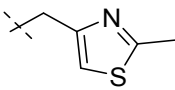
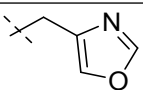
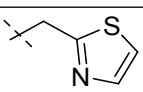
Exploring the N3 vector

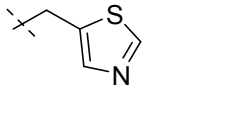
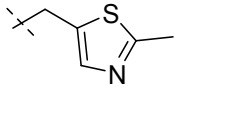
We then turned our attention to exploring the SAR at the N3 vector of the quinazolinone. Although this vector also points primarily towards solvent, its proximity to the ribose binding pocket suggested that additional productive binding interactions may be achievable. A library with a range of substituents at N3 (with N1 fixed as methyl) was modelled into the crystal structure of PARG (PDB accession code 6HMN), and a selection of analogues was prepared in order to investigate what is tolerated at this position. A representative set of N3 variations is shown in Table 7.

Table 7. Elaboration at the N3 vector



Compound	R	PARG Biochemical EC ₅₀ (μM) ^a
26	H	5.2 (1.2)

12b	Me	3.9 (1.7)
27a	Et	4.0 (1.3)
27b	Cyclopropylmethyl	4.6 (0.27)
27c	Cyclohexylmethyl	>150
27d	Ph	23 (4.5)
27e	Bn	26 (2.8)
27f	2-Pyridylmethyl	16 (3.4)
27g	3-Pyridylmethyl	2.5 (1.0)
27h	4-Pyridylmethyl	8.0 (0.64)
27i		1.6 (0.12)
27j		1.7 (0.18)
27k	Propargyl	3.0 (2.0)
27l	Cyanomethyl	1.1 (0.81)
27m		7.0 (4.6)
27n		6.0 (1.5)
27o		20 (0)
27p		10 (0.78)
27q		21 (1.2)
27r		13 (4.0)

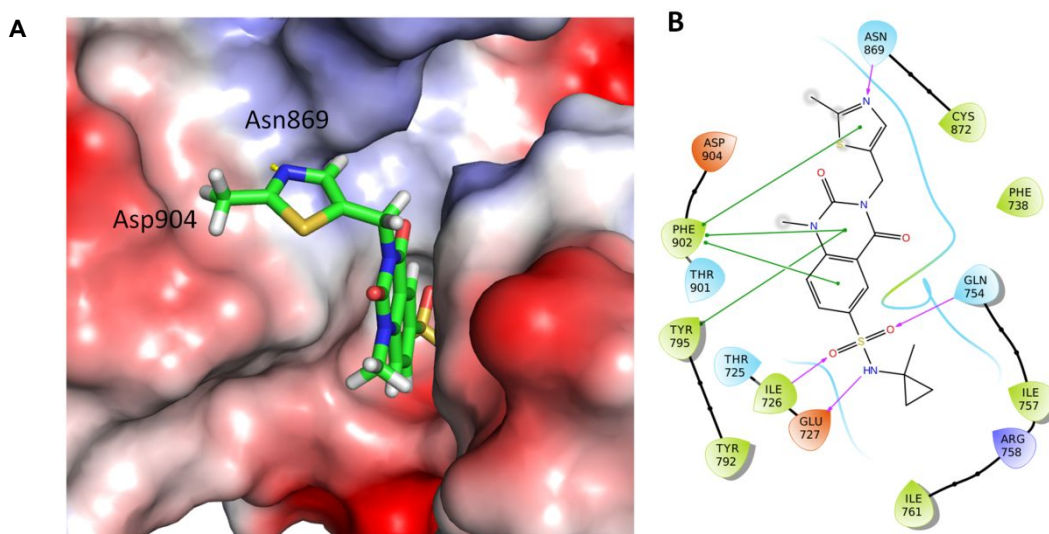
27s		1.2 (0.60)
27t		0.48 (0.36)

^aAll EC_{50} data are means of at least $n = 4$ independent measurements, with standard deviations quoted in parentheses.

We initially investigated lipophilic alkyl and aryl groups, and found that these gave either no improvement over the 3-methyl analogue **12b**, or were detrimental to activity, consistent with the generally polar nature of the protein surface in this region. However, introducing polarity to the substituent at the N3-position yielded promising compounds with activity in the low micromolar range (e.g., **27g**, **27i**, **27j** and **27l**). Modelling studies suggested that the hydrogen bond acceptor atom common to these groups may form a hydrogen bond with Asn869. The difference in activity observed across the pyridyl isomers suggested that the position of this hydrogen bond acceptor was important, and this was further demonstrated using a series of methylene-linked heterocyclic substituents at N3. Initial exploration with this motif resulted in moderate potencies. However, moving from thiazol-2-ylmethyl derivative **27r** (13 μ M) to thiazol-5-yl isomer **27s** resulted in a 10-fold improvement in potency to 1.2 μ M. Methylation of the thiazole (**27t**) gave a further boost to potency to yield a sub-micromolar inhibitor.

Determination of the X-ray crystal structure of **27t** bound to the human PARG catalytic domain revealed that the quinazolinone sulfonamide exhibited a similar binding mode to that observed for the N1-benzyl derivative **22h** (Figure 8). The N3 substituent of **27t** accesses a narrow solvent-exposed ledge above Phe902, potentially making a favorable edge-to-face stacking interaction with the Phe902 sidechain. The crystal structure confirmed the hypothesis that the N atom in the thiazole ring can make a hydrogen bond interaction with the Asn869 sidechain, as had been suggested by modelling. This explains the noticeable gain in potency for this specific thiazole isomer compared to other heterocycles lacking an appropriately positioned hydrogen bond acceptor (e.g., **27q**). The reduced affinity noted for furan **27n** and oxazole **27q** is in line with the weaker hydrogen bonding strength

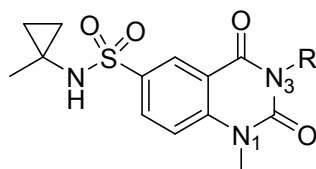
1
2
3 expected from an aromatic oxygen atom compared with a nitrogen lone pair. The 2-methyl group on
4 the thiazole ring of **27t** makes an additional hydrophobic contact with the β -carbon of the Asp904
5 sidechain. Overall, this data suggests that the complementarity in shape and properties of the 2-
6 methylthiazole substituent enables productive binding to an apparently unpromising, narrow shelf on
7 the protein surface. Overall, this data suggests that the complementarity in shape and properties of the 2-
8 methylthiazole substituent enables productive binding to an apparently unpromising, narrow shelf on
9 the protein surface. The relatively limited conformational flexibility around the N3 methylene, due to
10 the protein surface. The relatively limited conformational flexibility around the N3 methylene, due to
11 the steric restrictions imposed by the adjacent carbonyl oxygens of the quinazolinone core, may
12 also help to stabilize the observed binding mode. The relatively limited conformational flexibility around the N3 methylene, due to
13 the steric restrictions imposed by the adjacent carbonyl oxygens of the quinazolinone core, may
14 also help to stabilize the observed binding mode. The relatively limited conformational flexibility around the N3 methylene, due to
15 also help to stabilize the observed binding mode.



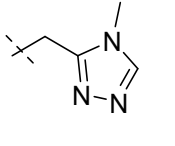
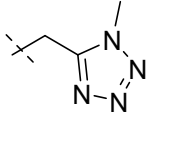
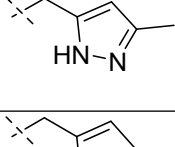
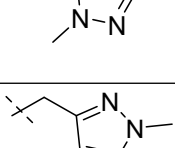
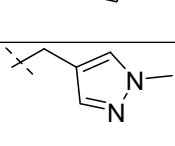
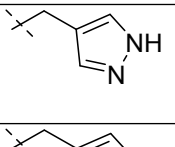
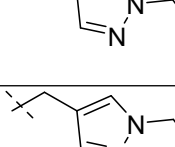
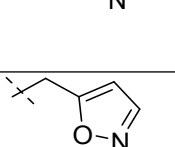
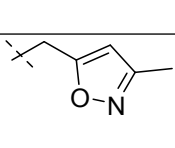
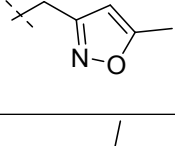
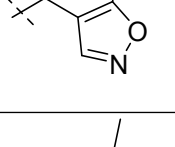
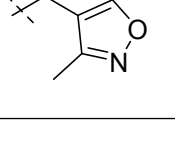
38 Figure 8. (A) Crystal structure of **27t** bound to human PARG at 2.06 Å resolution (PDB accession
39 code 6HMK). Hydrogen atoms modelled using Maestro (Schrödinger LLC); (B) Protein-ligand
40 interaction diagram with hydrogen bonds indicated by pink arrows and aromatic interactions by green
41 arrows.
42
43
44
45

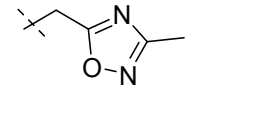
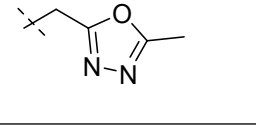
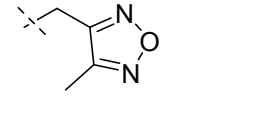
46
47 The data in Table 7 indicated that the SAR at the N3 vector of the quinazolinone was steeper than
48 at the N1 vector. Changing the position of the nitrogen atom in the heteroaryl ring evidently had a
49 significant effect on the PARG activity, and we were keen to explore the interaction of the nitrogen
50 with Asn869 further. A focused set of quinazolinones substituted at the N3 position with
51 methylene-linked 5-membered N-containing heterocycles was therefore synthesized (Table 8).
52
53
54
55
56
57

58 Table 8. Exploring the interaction with Asn869: focused N3 library
59
60



Compound	R	PARG Biochemical EC ₅₀ (μM) ^a
27t		0.48 (0.36)
27u		0.48 (0.17)
27v		0.91 (0.49)
27w		12 (7.0)
27x		2.3 (1.2)
27y		2.7 (0.65)
27z		0.88 (0.27)
27aa		0.47 (0.12)
27ab		4.0 (0.43)
27ac		3.3 (0.85)

27ad		3.1 (1.2)
27ae		3.0 (0.75)
27af		3.2 (0.97)
27ag		4.1 (1.1)
27ah		12 (0.29)
27ai		0.39 (0.28)
27aj		0.38 (0.20)
27ak		0.45 (0.19)
27al		0.37 (0.027)
27am		1.2 (0.77)
27an		0.47 (0.17)
27ao		5.2 (0.91)
27ap		0.77 (0.24)
27aq		0.62 (0.30)

27ar		5.0 (2.8)
27as		1.8 (0.63)
27at		2.1 (1.3)

^aAll EC_{50} data are means of at least $n = 4$ independent measurements, with standard deviations quoted in parentheses.

The X-ray crystal structure of **27t** bound to PARG (Figure 8) showed that the methyl group on the thiazole ring was in close contact with the β -carbon of the sidechain of Asp904. The protein surface in this region is relatively polar due to the proximity of the carboxylate moiety of Asp904, as well as the backbone carbonyls of Thr901 and Phe902; hence, we hoped that the introduction of a more polar substituent in place of the methyl group would allow formation of an additional hydrogen bond. Disappointingly, however, aminothiazole **27u** showed no improvement in potency compared to **27t**. Methylation at the 4-position of the thiazole (**27v**) was tolerated with only a modest loss in PARG inhibitory activity, while the 4-phenyl analogue **27w** resulted in a significant reduction in activity, likely due to steric clashes with both the protein and the quinazolinone core. Having prepared a broad range of methylene-linked heteroaryl substituents, we observed that the best examples (with activities $<0.5 \mu\text{M}$) contained a nitrogen atom at the position essential for maintenance of the key hydrogen bond interaction with Asn869. The importance of having the correct orientation of the nitrogen lone pair is demonstrated by the striking differences in PARG activity observed between regioisomer pairs **27ah** and **27ai**, and **27an** and **27ao**. Although des-methyl analogue **27aj** showed a similar biochemical activity to **27ai**, it displayed a significant drop-off in cell activity (data not shown), probably due to low permeability. Overall, 3-pyrazolylmethyl and 3-isoxazolylmethyl substituents emerged as interesting, less lipophilic alternatives to the 3-thiazolylmethyl substituent of **27t**. Interestingly, introduction of a nitrogen lone pair *ortho* to the methylene linker is generally detrimental to PARG activity (e.g., **27y**, **27ad**, **27ae**, **27ah**, **27ao** and **27ar**), likely as a result of

conformational strain due to the unfavorable electrostatic interaction of the lone pair with the carbonyl oxygen atoms of the quinazolinedione core in the bound conformation.

Figure 9 summarizes the key SAR at the N3 vector of the quinazolinedione. A methylene-linked 5-membered heterocycle has been used as an example, however, the model is equally applicable to 3-substituents containing pyridyl (**27g**), ketone (**27i** and **27j**), and nitrile (**27l**) functional groups. As noted earlier, overall the SAR is much steeper at the quinazolinedione N3 vector compared to the N1 vector, with specific pendant functional groups enabling a significant boost in PARG inhibition.

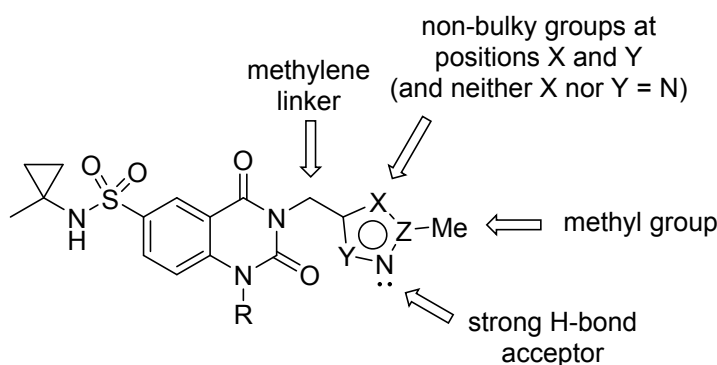
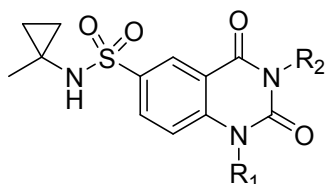


Figure 9. Key SAR at the 3-position of the quinazolinedione

Simultaneous elaboration at both the N1 and N3 vectors

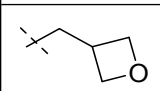
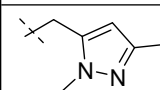
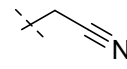
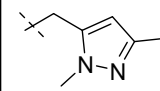
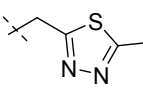
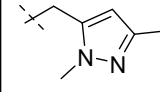
With a better understanding of the SAR at the N1 and N3 vectors in isolation, we next investigated the effect of combining the optimized N1 and N3 substituents in the same compound in a bid to further increase potency. A representative set of N1,N3-substituted quinazolinediones is shown in Table 9.

Table 9. Simultaneous elaboration at both N1 and N3 vectors



Compound	R ₂	R ₁	PARG Biochemical	PARG Cell EC ₅₀ (μM) ^a	Hu (Mo) Mic CL _{int}

			EC ₅₀ (μM) ^a		(μL/min/mg) ^b
33a		ethyl	0.17 (0.074)	0.078 (0.020)	35
33b		propargyl	0.052 (0.0093)	0.13 (0.031)	42
33c		cyclopropylmethyl	0.029 (0.0076)	0.056 (0.019)	81
33d			0.069 (0.044)	0.25 (0.066)	9.2 (16)
33e			0.023 (0.014)	0.088 (0.041)	34
33f			0.0060 (0.0017)	0.020 (0.0077)	97
34b		propargyl	0.045 (0.018)	0.082 (0.039)	100
34c		cyclopropylmethyl	0.019 (0.0043)	0.028 (0.013)	160
34e^c			0.026 (0.0055)	0.037 (0.013)	79
34f^d			0.0048 (0.0023)	0.0092 (0.0040)	140
35a		ethyl	0.33 (0.11)	0.12 (0.020)	26
35b		propargyl	0.10 (0.076)	0.076 (0.020)	72
35c		cyclopropylmethyl	0.055	0.049	80

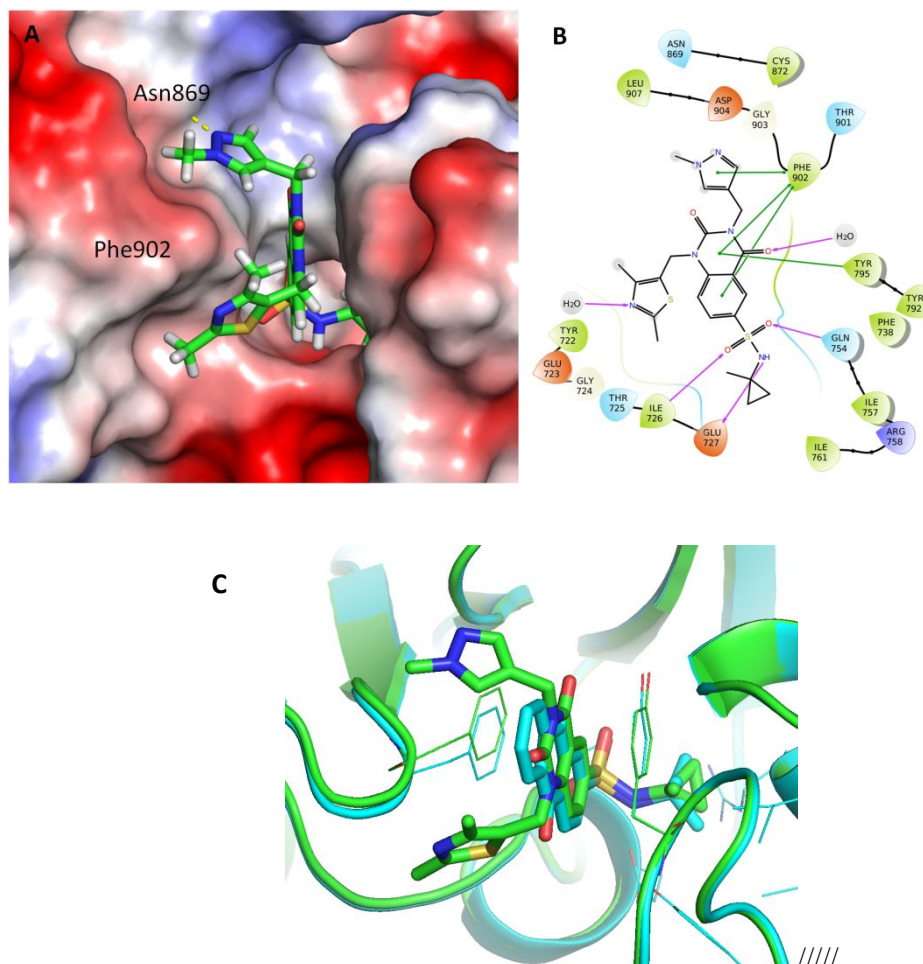
			(0.023)	(0.0097)	
35d			0.34 (0.058)	0.28 (0.067)	19 (22)
35e			0.038 (0.013)	0.12 (0.025)	37
36b		propargyl	0.25 (0.029)	0.27 (0.12)	10 (63)
36c		cyclopropylmethyl	0.28 (0.097)	0.56 (0.042)	20
36e			0.27 (0.14)	1.1 (0.41)	17 (36)
41a		ethyl	0.24 (0.036)	0.12 (0.059)	17 (30)
41e			0.064 (0.018)	0.27 (0.14)	15 (35)

^aAll biochemical and cellular EC_{50} data are means of at least $n = 4$ independent measurements, with standard deviations quoted in parentheses; ^bhuman microsomal clearance (mouse microsomal clearance is shown in brackets for selected compounds); ^cin vitro tool compound **34e** (PDD00017273)³⁵ is available to purchase; ^d**34f** has previously been reported as PDDX-04/PDD00017272³⁶

Combining substitution at both N1 and N3 vectors led to a significant improvement in potency, and biochemical EC_{50} s as low as 4.8 nM were achieved (compound **34f**). For 3-pyrazolylmethyl quinazolinediones (**33a–f**) up to a 100-fold increase in potency was achieved over the 1-methyl analogue (**27ai**). Pleasingly, in our cellular proof-of-mechanism PAR chain persistence assay,³¹ the inhibition of PARG in cells was in line with the biochemical EC_{50} values.³⁷

The X-ray crystal structure of **33f** was solved in complex with the catalytic domain of human PARG (Figure 10), and revealed the same binding configuration of the quinazolinedione core and

1
2
3 sulfonamide as observed for **27t**. For **33f**, the N1 and N3 substituents adopt a “pincer” configuration
4
5 around the Phe902 sidechain. The pyrazole nitrogen makes the key hydrogen bonding interaction with
6
7 Asn869, and the dimethylthiazole moiety at N1 forms extensive hydrophobic contacts with the
8
9 Phe902 shelf, consistent with earlier modelling studies.
10
11
12



44
45
46
47
48
49
50
51
52
53
54
55
56
57
58
59
60

Figure 10. (A) Crystal structure of **33f** bound to human PARG at 2.25 Å resolution (PDB accession code 6HML). Hydrogen atoms modelled using Maestro (Schrödinger LLC); (B) Protein-ligand interaction diagram with key hydrogen bond interactions highlighted (pink arrows); (C) Overlay of crystal structures of **33f** (green carbons and ribbons) with **8a** (blue carbons and ribbons), showing maintenance of initial binding mode.

Encouraged by these good levels of potency in the biochemical and cellular assays, we obtained in vitro human microsomal clearance data to assess which derivatives might be candidates for further studies in vivo. Quinazolidiones **34b**, **34c**, **34e**, **34f**, bearing a 3-(2-methylthiazol-5-yl)methyl

1
2
3 group, showed excellent potency in our biochemical and cellular assays, however, their in vitro
4
5 microsomal stabilities were poor, which we attributed to their high lipophilicity (e.g., **34f** calculated
6
7 $\log P^{39} = 4.7$). Despite high intrinsic clearance, **34e** has been extensively characterised as a potent and
8
9 selective chemical probe and used as an in vitro tool compound to study the effects of small molecule
10
11 inhibition of PARG,^{12,38} to evaluate the chemotherapeutic potential of PARG inhibitors. 3-(1-
12
13 Methylpyrazol-4-yl)methyl derivatives **33a-f** maintained a similar level of potency to the 3-(2-
14
15 methylthiazol-5-yl)methyl compounds, but were slightly less lipophilic (e.g., **33f** calculated $\log P^{39} =$
16
17 3.6), and consequently, showed significantly better stability in human liver microsomes, although
18
19 clearance remained moderate–high. In contrast to the majority of the 3-(1-methylpyrazol-4-yl)methyl
20
21 quinazolinediones, 1-oxetan-3-ylmethyl derivative **33d** had low clearance in vitro and was a useful
22
23 candidate for further investigation. 3-(3-Methylisoxazol-5-yl)methyl quinazolinediones **35a-e**
24
25 exhibited a slight reduction in potency in our biochemical and cellular assays compared to 3-(1-
26
27 methylpyrazol-4-yl)methyl derivatives **33**, whilst maintaining a similar level of in vitro microsomal
28
29 stability. A selection of 3-(5-methyl-1,3,4-thiadiazol-2-yl) and 3-cyanomethyl quinazolinediones **36b-**
30
31 **e**, **41a** and **41e** also showed good potency and human microsomal stability, unfortunately, however,
32
33 their high in vitro mouse clearance precluded them from further studies.
34
35
36

37 *Cytotoxicity and Selectivity*

38
39
40 Pleasingly, all compounds which showed a cell activity of $<0.3 \mu\text{M}$ in this series (exemplified by **33d**,
41
42 **33e**, **34e** and **35d**) showed more than a 100-fold window to cytotoxicity in HeLa cells after 72 h of
43
44 exposure at PARG cell-active doses.
45
46

47
48 The selectivity of a set of quinazolinedione derivatives (**22f**, **33e**, **34c**, **33e** and **35f**) was investigated
49
50 by measuring activity against PARP1 and ARH3, a functionally-related glycohydrolase enzyme.
51
52 Encouragingly, none of the compounds tested showed any activity in either the PARP1 and ARH3
53
54 assays, giving EC_{50} values of $>150 \mu\text{M}$ and $>100 \mu\text{M}$, respectively.
55
56

57 *Pharmacokinetic investigations*

1
2
3 1-Oxetan-3-ylmethyl derivatives **33d** and **35d** showed no cytotoxicity, and a good balance of cell
4
5 potency and human and mouse microsomal stability and were therefore selected for further profiling.
6
7 For the preliminary pharmacokinetic (PK) investigations, mice were dosed intravenously or orally,
8
9 and tail vein blood samples were analyzed at regular time-points (Table 10).
10
11

12 Table 10. In vitro and in vivo parameters for **33d** and **35d**
13
14

	33d	35d
Solubility (μM)	>100	>100
Caco2 A–B mean P_{app} (10^{-6} cm/s); (efflux ratio)	1.0 (34)	1.9 (21)
Mo Hep CL_{int} ($\mu\text{L}/\text{min}/10^6$ cells)	24	25
CYP inhibition (IC_{50} , μM , 5 isoforms) ^a	>10	>25
IV AUC (h.ng/mL) ^b	250	90
IV $T_{1/2}$ (min)	22	12
IV V_D (L/kg)	1.4	2.5
CL_{iv} (L/h/kg)	4.0	10
F (%)	41	25

15
16
17
18
19
20
21
22
23
24
25
26
27
28
29
30
31
32
33
34
35
36
37
38
39 ^aCYP1A, CYP2C19, CYP2C9, CYP2D6 and CYP3A4 isoforms tested; ^bmale CD-1 mice were dosed
40 intravenously ($n=2$) at a nominal dose level of 1 mg/kg, or orally ($n=2$) at a nominal dose level of 5 mg/kg.
41
42

43 The in vivo PK data showed that both compounds were cleared rapidly, with **35d** having an IV
44 clearance greater than liver blood flow, indicating that extra-hepatic clearance mechanisms might be
45 involved. Despite this, we were pleased to see moderate levels of bioavailability (F), especially as the
46 in vitro data had shown high hepatocyte clearance, low permeability and high efflux.
47
48
49
50
51

52 CONCLUSION

53
54 To date, the elucidation of the precise role of PARG in DNA damage repair and its potential as a
55 novel therapeutic target has been severely limited by the lack of drug-like tool compounds suitable for
56 use in cellular and in vivo models. Starting from a weakly active HTS hit **8a**, we have identified
57
58
59
60

1
2
3 several lead-like scaffold hops that show a significant improvement in affinity in biochemical and
4 cellular assays, without the non-specific cellular toxicity of the parent anthraquinone. With the ligand
5 binding site highly solvent-exposed, the tight binding interactions around the *N*-alkyl sulfonamide
6 moiety of **8a** proved to be an essential pharmacophore that was exploited successfully by pursuing a
7 structure-based design approach. An initial virtual screen identified a number of scaffold hops of
8 interest; however, the steep SAR around the sulfonamide necessitated the synthesis of a specific set of
9 *N*-alkyl groups in order to achieve a satisfactory level of potency. By pursuing a focused library
10 design strategy, a number of structurally diverse bicyclic ring systems were found to be tolerated in
11 the aromatic cleft between Tyr795 and Phe902, with the quinazolinedione scaffold deemed of
12 particular interest based on level of activity, drug-like profile, and potential for further substitution to
13 target additional features on the protein surface. High resolution crystal structures of some key
14 compounds bound to human PARG helped to explain the observed SAR and to guide further design.
15 Excellent levels of potency have been achieved, and in vitro tool compounds such as **34e**, with low
16 nanomolar cellular activity, have been provided to elucidate the biological effects of PARG inhibition.
17 These novel PARG inhibitors show no non-mechanistic toxicity, are selective over PARP1 and a
18 functionally-related glycohydrolase (ARH3), and represent promising lead compounds for the
19 discovery of a novel class of chemotherapeutics. Preliminary investigations of 1-oxetan-3-ylmethyl
20 derivatives **33d** and **35d** in vivo also demonstrated encouraging levels of oral bioavailability. Further
21 progress on these efforts will be reported in due course.

22 23 24 25 26 27 28 29 30 31 32 33 34 35 36 37 38 39 40 41 42 43 44 **EXPERIMENTAL SECTION**

45 46 47 **General Chemistry**

48
49
50 Flash chromatography was performed using pre-packed silica gel cartridges (KP-Sil SNAP, Biotage,
51 Hengoed UK or RediSep Rf, Isco). Thin layer chromatography was conducted on 5 × 10 cm plates
52 coated with Merck Type 60 F₂₅₄ silica gel to a thickness of 0.25 mm. All reagents obtained from
53 commercial sources were used without further purification. Anhydrous solvents were obtained from
54 the Sigma-Aldrich Chemical Company Ltd. or Fisher Chemicals Ltd., and used without further
55
56
57
58
59
60

1
2
3 drying. HPLC grade solvents were obtained from Fisher Chemicals Ltd. All compounds were >95%
4
5 purity as determined by examination of the LC–MS chromatograms at two independent pHs and the
6
7 ¹H NMR spectra, unless otherwise specifically indicated. Where Cl or Br were present, expected
8
9 isotopic distribution patterns were observed. Proton (¹H) and carbon (¹³C) NMR spectra were
10
11 recorded on a 300 MHz Bruker spectrometer. Solutions were typically prepared in either
12
13 deuteriochloroform (CDCl₃) or deuterated dimethylsulfoxide (DMSO-d₆) with chemical shifts
14
15 referenced to tetramethylsilane (TMS) or deuterated solvent as an internal standard. ¹H NMR data are
16
17 reported indicating the chemical shift (δ), the integration (e.g., 1H), the multiplicity (s, singlet; d,
18
19 doublet; t, triplet; q, quartet; m, multiplet; br., broad; dd, doublet of doublets; etc.) and the coupling
20
21 constant (*J*) in Hz (app implies apparent coupling on broadened signals). Deuterated solvents were
22
23 obtained from Goss. LC–MS analyses were performed on a Waters Acquity UPLC system fitted with
24
25 BEH C18 1.7 μ M columns (2.1 \times 50 mm) and with UV diode array detection (210–400 nm). Positive
26
27 and negative mass ion detection was performed using a Waters SQD detector. Analyses were
28
29 performed with either buffered acidic or basic solvents, with gradients as detailed in the Supporting
30
31 Information. Some compounds were purified by preparative HPLC on a Waters FractionLynx MS
32
33 autopurification system, with a Waters XBridge 5 μ m C18, 100 mm \times 19 mm i.d. column, running at
34
35 a flow rate of 20 mL/min with UV diode array detection (210–400 nm) and mass-directed collection
36
37 using both positive and negative mass ion detection. Purifications were performed using buffered
38
39 acidic or basic solvent systems as appropriate. Compound retention times on the system were
40
41 routinely assessed using a 30–50 μ L test injection and a standard gradient, then purified using an
42
43 appropriately chosen focused gradient as detailed in the Supporting Information, based upon observed
44
45 retention time.
46
47
48
49

50
51 Compounds **12d,e**, **13c**, **16b**, **43–45** (Table 2) were purchased from either ChemBridge, ChemDiv or
52
53 Princeton BioMolecular Research.
54

55 56 **9,10-Dioxoanthracene-2-sulfonyl chloride (7)** 57 58 59 60

1
2
3 Thionyl chloride (20 mL, 274 mmol) and DMF (1 mL) were sequentially added to 9,10-
4 anthraquinone-2-sulfonic acid, sodium salt, monohydrate (5 g, 16 mmol) in a flask under nitrogen.
5
6 The reaction mixture was heated at reflux for 2 h. The reaction mixture was left to cool to ambient
7
8 temperature overnight and a precipitate formed. The reaction mixture was poured onto stirring ice and
9
10 EtOAc (50 mL) was added to rinse the flask into the ice solution. The precipitate was filtered and
11
12 dried in the vacuum oven to yield a pale yellow solid, **7** (2.6 g, 53%). ¹H NMR (300 MHz, CDCl₃) δ
13
14 9.00 (d, *J*=2.0 Hz, 1H), 8.60 (d, *J*=8.3 Hz, 1H), 8.35–8.47 (m, 3H), 7.89–7.96 (m, 2H). LC–MS *m/z*
15
16 305.5 [M + H]⁺.
17
18
19

20 **N-tert-Butyl-9,10-dioxo-anthracene-2-sulfonamide (8a)**

21
22 Triethylamine (91 μL, 0.65 mmol) and *tert*-butylamine (68.5 μL, 0.65 mmol) were added sequentially
23
24 to a solution of **7** (100 mg, 0.33 mmol) in DCM (5 mL) at ambient temperature. The reaction mixture
25
26 was stirred at ambient temperature overnight. The reaction mixture was diluted with DCM (5 mL),
27
28 washed with water (10 mL) and saturated aq. sodium bicarbonate solution (10 mL). The organic phase
29
30 was passed through a hydrophobic frit and evaporated to dryness. The crude product was purified by
31
32 preparative HPLC (high pH) and lyophilized to dryness to yield **8a** as a white solid (48 mg, 43%). ¹H
33
34 NMR (300 MHz, DMSO-*d*₆) δ 8.61 (d, *J*=1.8 Hz, 1H), 8.39 (d, *J*=8.2 Hz, 1H), 8.31 (dd, *J*=1.9, 8.1
35
36 Hz, 1H), 8.22–8.28 (m, 2H), 7.94–8.02 (m, 3H), 1.14 (s, 9H). ¹³C NMR (75 MHz, DMSO-*d*₆) δ 181.8,
37
38 181.7, 149.3, 135.0, 134.82, 134.77, 133.8, 133.1, 131.3, 128.1, 126.9, 124.4, 53.8, 29.8. HRMS (ESI)
39
40 *m/z* [M + Na]⁺ calcd for C₁₈H₁₇NO₄NaS: 366.0770. Found: 366.0765.
41
42
43
44

45 **N-Methyl-9,10-dioxo-anthracene-2-sulfonamide (8b)**

46
47 Methylamine solution (2 M in THF) (0.82 mL, 1.6 mmol) was added dropwise to a solution of **7** (100
48
49 mg, 0.33 mmol) in DCM (5 mL) cooled to 0 °C. The reaction mixture was allowed to warm to
50
51 ambient temperature and stirred for 2 h. The reaction mixture was diluted with DCM (5 mL) and
52
53 washed with water (10 mL), before passing through a hydrophobic frit and evaporating to dryness to
54
55 yield **8b** as a beige solid (76 mg, 77%). ¹H NMR (300 MHz, DMSO-*d*₆) δ 8.52 (d, *J*=1.8 Hz, 1H),
56
57 8.42 (d, *J*=8.1 Hz, 1H), 8.21–8.29 (m, 3H), 7.90–8.03 (m, 3H), 2.48 (d, *J*=3.7 Hz, 3H). LC–MS *m/z*
58
59 302.1 [M + H]⁺.
60

N-Ethyl-9,10-dioxo-anthracene-2-sulfonamide (8c)

Compound **8c** was prepared in a manner analogous to that for **8b**, purified by preparative HPLC (high pH) (white solid, 26 mg, 26%). ¹H NMR (300 MHz, DMSO-d₆) δ 8.54 (d, *J*=1.9 Hz, 1H), 8.41 (d, *J*=8.2 Hz, 1H), 8.22–8.29 (m, 3H), 7.88–8.02 (m, 3H), 2.86 (q, *J*=7.2 Hz, 2H), 1.00 (t, *J*=7.2 Hz, 3H). LC–MS *m/z* 316.0 [M + H]⁺.

N-(1,1-Dimethylpropyl)-9,10-dioxo-anthracene-2-sulfonamide (8d)

Compound **8d** was prepared in a manner analogous to that for **8b** (beige solid, 88 mg, quant.). ¹H NMR (300 MHz, CDCl₃) δ 8.83 (d, *J*=1.9 Hz, 1H), 8.46 (d, *J*=8.2 Hz, 1H), 8.34–8.43 (m, 2H), 8.31 (dd, *J*=1.9, 8.2 Hz, 1H), 7.85–7.91 (m, 2H), 4.62 (s, 1H), 1.61 (q, *J*=7.5 Hz, 2H), 1.23 (s, 6H), 0.88 (t, *J*=7.4 Hz, 3H). LC–MS *m/z* 356.9 [M – H][–]. LC-MS purity, 90-95%.

N-(Cyclopropylmethyl)-9,10-dioxo-anthracene-2-sulfonamide (8e)

Triethylamine (40 μL, 0.29 mmol) and cyclopropanemethylamine (23 μL, 0.27 mmol) were added sequentially to a solution of **7** (75 mg, 0.24 mmol) in DCM (5 mL) cooled to 0 °C. After addition of the reagents the cooling was removed and the reaction mixture was allowed to warm to ambient temperature and stirred for 3 h. The reaction mixture was diluted with DCM (5 mL) and washed with water (10 mL) and saturated aq. sodium bicarbonate solution (10 mL), before passing through a hydrophobic frit and evaporating to dryness. The crude product was purified by automated column chromatography, eluent 0–5% MeOH in DCM to yield **8e** as a pale yellow solid (54 mg, 64%). ¹H NMR (300 MHz, DMSO-d₆) δ 8.56 (d, *J*=1.6 Hz, 1H), 8.39 (d, *J*=8.0 Hz, 1H), 8.17–8.32 (m, 4H), 7.94–8.01 (m, 2H), 2.74 (t, *J*=6.5 Hz, 2H), 0.72–0.86 (m, 1H), 0.29–0.37 (m, 2H), 0.05–0.12 (m, 2H). LC–MS *m/z* 340.5 [M – H][–].

N-Cyclopropyl-9,10-dioxo-anthracene-2-sulfonamide (8f)

Compound **8f** was prepared in a manner analogous to that for **8e**, stirring at ambient temperature for 1.5 h (pale yellow solid, 39 mg, 49%). ¹H NMR (300 MHz, DMSO-d₆) δ 8.56 (d, *J*=1.8 Hz, 1H), 8.43 (d, *J*=8.1 Hz, 1H), 8.34 (s, 1H), 8.23–8.31 (m, 3H), 7.95–8.01 (m, 2H), 2.16–2.26 (m, 1H), 0.37–0.55

(m, 4H). ¹³C NMR (75 MHz, DMSO-d₆) δ 181.8, 181.7, 145.2, 135.5, 133.8, 133.11, 133.08, 131.9, 128.2, 127.0, 124.9, 117.7, 38.7, 38.5, 24.1, 5.2. HRMS (ESI) *m/z* [M + Na]⁺ calcd for C₁₇H₁₃NO₄NaS: 350.0457. Found: 350.0449.

N-Cyclobutyl-9,10-dioxo-anthracene-2-sulfonamide (8g)

Compound **8g** was prepared in a manner analogous to that for **8a** (beige solid, 60 mg, 77%). ¹H NMR (300 MHz, DMSO-d₆) δ 8.54 (d, *J*=1.9 Hz, 1H), 8.39 (d, *J*=8.1 Hz, 1H), 8.20–8.30 (m, 4H), 7.93–8.03 (m, 2H), 3.72 (quin, *J*=8.2 Hz, 1H), 1.86–2.00 (m, 2H), 1.65–1.85 (m, 2H), 1.40–1.55 (m, 2H). LC-MS *m/z* 340.5 [M – H]⁻.

N-(1-Methylcyclopropyl)-9,10-dioxo-anthracene-2-sulfonamide (8h)

Triethylamine (181 μL, 1.3 mmol) and 1-methylcyclopropanamine hydrochloride (70 mg, 0.65 mmol) were added sequentially to a solution of **7** (100 mg, 0.33 mmol) in DCM (5 mL) at 0 °C. The reaction mixture was allowed to warm to ambient temperature and stirred for 1.5 h. The reaction mixture was diluted with DCM (10 mL), 2 M HCl (10 mL) was added and the reaction mixture stirred for 10 min. The organic phase was separated, the aqueous phase further extracted with DCM (10 mL) and the combined organic phase passed through a hydrophobic frit and evaporated to dryness. The resulting solid was triturated with diethyl ether, filtered and dried to yield **8h** as a pale yellow solid, (100 mg, 89%). ¹H NMR (300 MHz, DMSO-d₆) δ 8.55 (d, *J*=1.9 Hz, 1H), 8.52 (s, 1H), 8.40 (dd, *J*=0.4, 8.1 Hz, 1H), 8.21–8.29 (m, 3H), 7.93–8.01 (m, 2H), 1.11 (s, 3H), 0.54–0.70 (m, 2H), 0.35–0.51 (m, 2H). ¹³C NMR (75 MHz, DMSO-d₆) δ 181.74, 181.68, 147.8, 135.3, 134.83, 134.78, 133.8, 133.10, 133.06, 131.4, 128.2, 126.9, 124.5, 124.1, 117.7, 31.1, 24.0, 13.1. HRMS (ESI) *m/z* [M + Na]⁺ calcd for C₁₈H₁₅NO₄NaS: 364.0614. Found: 364.0607. LC-MS purity, 90-95%.

N-(1-Cyanocyclopropyl)-9,10-dioxo-anthracene-2-sulfonamide (8i)

Triethylamine (75 μL, 0.54 mmol) and 1-amino-1-cyclopropanecarbonitrile hydrochloride (32 mg, 0.27 mmol) were added sequentially to a solution of **7** (75 mg, 0.24 mmol) in DCM (5 mL) cooled to 0 °C. After addition of the reagents the cooling was removed and the reaction mixture was allowed to warm to ambient temperature and continue stirring. After 5 h, further 1-amino-1-

1
2
3 cyclopropanecarbonitrile hydrochloride (32 mg, 0.27 mmol) and triethylamine (75 μ L, 0.54 mmol)
4 were added to the reaction mixture which was left to stir at ambient temperature for 48 h. LC–MS
5 indicated ~50% conversion to the desired product. The reaction mixture was heated at reflux for 5 h,
6
7 no further conversion to product observed by LC–MS. The reaction mixture was diluted with DCM
8 (10 mL) and water (10 mL), separated and the organic phase washed with saturated aq. sodium
9 bicarbonate (10 mL), then passed through a hydrophobic frit and evaporated to dryness. The crude
10 product was purified by preparative HPLC (high pH) to yield **8i** as a cream solid (31 mg, 35%). ¹H
11 NMR (300 MHz, DMSO-*d*₆) δ 8.58 (d, *J*=1.6 Hz, 1H), 8.43 (d, *J*=8.2 Hz, 1H), 8.31 (dd, *J*=1.9, 8.2
12 Hz, 1H), 8.23–8.29 (m, 2H), 7.96–8.02 (m, 2H), 1.39–1.45 (m, 2H), 1.20–1.27 (m, 2H). ¹³C NMR (75
13 MHz, DMSO-*d*₆) δ 181.7, 181.5, 144.8, 135.8, 135.0, 134.9, 133.8, 133.04, 132.96, 132.0, 128.4,
14 127.03, 126.99, 125.1, 119.4, 117.7, 21.9, 15.8. HRMS (ESI) *m/z* [M + Na]⁺ calcd for C₁₈H₁₂N₂O₄S:
15 375.0410. Found: 375.0403.

2-[(9,10-Dioxo-2-anthryl)sulfonylamino]acetamide (**8j**)

31
32 Compound **8j** was prepared in a manner analogous to that for **8h**, stirring at ambient temperature for 4
33 h, the crude product was purified by preparative HPLC (high pH) (cream solid, 12 mg, 15%). ¹H
34 NMR (300 MHz, DMSO-*d*₆) δ 8.55 (d, *J*=1.7 Hz, 1H), 8.38 (d, *J*=8.1 Hz, 1H), 8.20–8.30 (m, 4H),
35 7.93–8.03 (m, 2H), 7.34 (br. s, 1H), 7.05 (br. s, 1H), 3.32 (s, 2H). LC–MS *m/z* 343.5 [M – H][–]. LC-
36 MS purity, 90-95%.

3-[(9,10-Dioxo-2-anthryl)sulfonylamino]propanamide (**8k**)

37
38 Compound **8k** was prepared in a manner analogous to that for **8h**, stirring at ambient temperature for
39 4 h (pale yellow solid, 27 mg, 32%). ¹H NMR (300 MHz, DMSO-*d*₆) δ 8.54 (d, *J*=1.8 Hz, 1H), 8.41
40 (d, *J*=8.1 Hz, 1H), 8.23–8.30 (m, 3H), 8.10 (t, *J*=5.9 Hz, 1H), 7.94–8.01 (m, 2H), 7.31 (br. s, 1H),
41 6.83 (br. s, 1H), 2.95–3.05 (m, 2H), 2.23 (t, *J*=7.3 Hz, 2H). LC–MS *m/z* 357.5 [M – H][–]. LC-MS
42 purity, 90-95%.

N-(2-Hydroxyethyl)-9,10-dioxo-anthracene-2-sulfonamide (**8l**)

1
2
3 Compound **8l** was prepared in a manner analogous to that for **8a**, the crude product was triturated with
4 DCM/diethyl ether and the filtrate isolated and dried in at 40 °C in a vacuum oven (cream solid, 59.5
5 mg, 79%). ¹H NMR (300 MHz, DMSO-d₆) δ 8.55 (d, *J*=1.9 Hz, 1H), 8.40 (d, *J*=8.1 Hz, 1H), 8.19–
6 8.33 (m, 3H), 8.11 (t, *J*=5.8 Hz, 1H), 7.93–8.03 (m, 2H), 4.72 (t, *J*=5.5 Hz, 1H), 3.38 (q, *J*=6.0 Hz,
7 2H), 2.88 (q, *J*=5.9 Hz, 2H). LC–MS *m/z* 330.2 [M – H]⁻.
8
9
10
11
12
13

14 **N-(2-Methoxyethyl)-9,10-dioxo-anthracene-2-sulfonamide (8m)**

15
16
17 Compound **8m** was prepared in a manner analogous to that for **8a**, stirring at ambient temperature for
18 2 h (cream solid, 42 mg, 53%). ¹H NMR (300 MHz, DMSO-d₆) δ 8.55 (d, *J*=1.9 Hz, 1H), 8.39 (d,
19 *J*=8.1 Hz, 1H), 8.19–8.31 (m, 4H), 7.94–8.01 (m, 2H), 3.30 (t, *J*=5.6 Hz, 2H), 3.11 (s, 3H), 3.01 (t,
20 *J*=5.5 Hz, 2H). LC–MS *m/z* 344.4 [M – H]⁻.
21
22
23
24
25

26 **N-(2-Methoxy-1,1-dimethyl-ethyl)-9,10-dioxo-anthracene-2-sulfonamide (8n)**

27
28
29 Compound **8n** was prepared in a manner analogous to that for **8h**, stirring at ambient temperature
30 overnight, the crude product was purified by preparative HPLC (high pH) (beige solid, 26 mg, 31%).
31
32 ¹H NMR (300 MHz, DMSO-d₆) δ 8.61 (d, *J*=1.6 Hz, 1H), 8.38 (d, *J*=8.1 Hz, 1H), 8.21–8.32 (m, 3H),
33 7.92–8.05 (m, 3H), 3.14 (s, 2H), 2.99 (s, 3H), 1.11 (s, 6H). LC–MS *m/z* 372.5 [M – H]⁻.
34
35
36
37
38

39 **N-(2-Cyanoethyl)-9,10-dioxo-anthracene-2-sulfonamide (8o)**

40
41
42 Compound **8o** was prepared in a manner analogous to that for **8a**, stirring at ambient temperature for 2
43 h (cream solid, 40 mg, 52%). ¹H NMR (300 MHz, DMSO-d₆) δ 8.49–8.59 (m, 2H), 8.41 (d, *J*=8.1 Hz,
44 1H), 8.21–8.34 (m, 3H), 7.93–8.03 (m, 2H), 3.08 (app. q, *J*=6.2 Hz, 2H), 2.65 (t, *J*=6.4 Hz, 2H).
45
46 LC–MS *m/z* 339.6 [M – H]⁻.
47
48
49
50

51 **1,3-Dimethylquinazoline-2,4(1H,3H)-dione (10a)**

52
53 A suspension of benzoyleneurea (2.0 g, 12 mmol) in DMF (24 mL) was treated with potassium
54 carbonate (8.5 g, 62 mmol) and was left to stir, under nitrogen at ambient temperature, for 30 min.
55
56 The solution was then treated with iodomethane (2.3 mL, 37 mmol) and stirred at ambient
57
58 temperature for 2 h. The suspension was filtered, water (40 mL) and EtOAc (40 mL) were added to
59
60

1
2
3 the filtrate. The organic layer was separated, washed with brine (2 × 20 mL), dried over MgSO₄ and
4 concentrated to give **1-10a** as a white solid (0.96 g, 41%). ¹H NMR (300 MHz, DMSO-d₆) δ 8.06 (dd,
5 *J*=1.7, 7.8 Hz, 1H), 7.81–7.75 (m, 1H), 7.47 (d, *J*=8.5 Hz, 1H), 7.31 (app. t, *J*=7.5 Hz, 1H), 3.53 (s,
6 3H), 3.32 (s, 3H).
7
8
9

10 11 12 **1,3-Diethylquinazoline-2,4(1H,3H)-dione (10b)**

13
14
15 Compound **10b** was prepared in a manner analogous to that for **10a** (white solid, 807 mg, 30%). ¹H
16 NMR (300 MHz, DMSO-d₆) δ 8.07 (dd, *J*=1.6, 7.9 Hz, 1H), 7.78 (ddd, *J*=1.8, 7.3, 8.5 Hz, 1H), 7.51
17 (d, *J*=8.6 Hz, 1H), 7.30 (app. t, *J*=7.5 Hz, 1H), 4.15 (q, *J*=7.2 Hz, 2H), 3.99 (q, *J*=7.2 Hz, 2H), 1.22 (t,
18 *J*=7.1 Hz, 3H), 1.16 (t, *J*=7.1 Hz, 3H).
19
20
21
22

23 24 **1,3-Dimethyl-2,4-dioxo-1,2,3,4-tetrahydroquinazoline-6-sulfonyl chloride (11a)**

25
26 Chlorosulfonic acid (1.7 mL, 25 mmol) was added portionwise to stirring **10a** (960 mg, 5.1 mmol)
27 cooled to 5–10 °C. The reaction mixture was heated at 60 °C for 4 h. The reaction mixture was cooled
28 and poured into crushed ice, causing the formation of an off-white precipitate. The precipitate was
29 filtered, washed with water and dried in the vacuum oven to give **11a** as a white solid (0.98 g, 67%).
30
31 ¹H NMR (300 MHz, DMSO-d₆) δ 8.25 (d, *J*=2.1 Hz, 1H), 7.93 (dd, *J*=2.2, 8.7 Hz, 1H), 7.42 (d, *J*=8.8
32 Hz, 1H), 3.52 (s, 3H), 3.31 (s, 3H).
33
34
35
36
37
38
39

40 41 **1,3-Diethyl-2,4-dioxo-1,2,3,4-tetrahydroquinazoline-6-sulfonyl chloride (11b)**

42
43 Compound **11b** was prepared in a manner analogous to that for **11a** (white solid, 657 mg, 64%). ¹H
44 NMR (300 MHz, DMSO-d₆) δ 8.26 (d, *J*=2.5 Hz, 1H), 7.92 (dd, *J*=2.1, 8.7 Hz, 1H), 7.46 (d, *J*=8.9
45 Hz, 1H), 4.14 (q, *J*=6.8 Hz, 2H), 3.99 (q, *J*=7.0 Hz, 2H), 1.25–1.13 (m, 6H).
46
47
48

49 50 **N-tert-Butyl-1,3-dimethyl-2,4-dioxo-quinazoline-6-sulfonamide (12a)**

51
52 **11a** (100 mg, 0.35 mmol), *tert*-butylamine (50 μL, 0.52 mmol) and triethylamine (0.10 mL, 0.69
53 mmol) in DCM (5 mL) was stirred at ambient temperature for 1 h. The reaction mixture was diluted
54 with 2 M HCl (5 mL) and DCM (5 mL) and stirred vigorously for 10 min, then filtered through a
55 hydrophobic frit. The organic layer was concentrated to dryness and the crude product purified by
56
57
58
59
60

1
2
3 preparative HPLC (high pH) to yield **12a** as a white solid (83 mg, 73%). ¹H NMR (300 MHz, DMSO-
4 d₆) δ 8.44 (d, *J*=2.3 Hz, 1H), 8.12 (dd, *J*=2.4, 8.9 Hz, 1H), 7.70 (s, 1H), 7.63 (d, *J*=8.9 Hz, 1H), 3.55
5 (s, 3H), 3.32 (s, 3H), 1.10 (s, 9H). LC-MS *m/z* 325.4 [M + H]⁺.
6
7
8

9 **1,3-Dimethyl-N-(1-methylcyclopropyl)-2,4-dioxo-quinazoline-6-sulfonamide (12b)**

10
11 Compound **12b** was prepared in a manner analogous to that for **12a** (white solid, 91 mg, 76%). ¹H
12 NMR (300 MHz, DMSO-d₆) δ 8.41 (d, *J*=2.3 Hz, 1H), 8.19 (s, 1H), 8.07 (dd, *J*=2.3, 8.9 Hz, 1H), 7.65
13 (d, *J*=8.9 Hz, 1H), 3.56 (s, 3H), 3.33 (s, 3H), 1.07 (s, 3H), 0.49–0.69 (m, 2H), 0.32–0.47 (m, 2H).
14
15 LC-MS *m/z* 324.5 [M + H]⁺. ¹³C NMR (75 MHz, DMSO-d₆) δ 160.7, 150.5, 142.8, 136.7, 132.5,
16
17 126.4, 117.7, 115.8, 114.8, 31.0, 30.9, 28.3, 23.9, 12.9. HRMS (ESI) *m/z* [M + Na]⁺ calcd for
18
19 C₁₄H₁₇N₃O₄NaS: 346.0832. Found: 346.0825. LC-MS purity, 90-95%.
20
21
22
23
24
25

26 **N-(1-Cyanocyclopropyl)-1,3-dimethyl-2,4-dioxo-quinazoline-6-sulfonamide (12c)**

27
28 Compound **12c** was prepared in a manner analogous to that for **12a**, the crude product was purified by
29 automated column chromatography, eluent 0–100% EtOAc in *iso*-hexane (white solid, 21 mg, 18%).
30
31 ¹H NMR (300 MHz, DMSO-d₆) δ 9.27 (br. s, 1H), 8.46 (s, 1H), 8.13 (d, *J*=8.9 Hz, 1H), 7.71 (d, *J*=8.9
32
33 Hz, 1H), 3.57 (s, 3H), 1.38–1.54 (m, 2H), 1.15–1.32 (m, 2H). 3H N-CH₃ not observed (under water
34
35 peak). LC-MS *m/z* 335.5 [M + H]⁺.
36
37
38
39

40 **1,3-Diethyl-N-(1-methylcyclopropyl)-2,4-dioxo-quinazoline-6-sulfonamide (13a)**

41
42 Compound **13a** was prepared in a manner analogous to that for **12a** using **11b**, the reaction mixture
43 was stirred at ambient temperature overnight and the crude product purified by automated column
44 chromatography, eluent 0–100% EtOAc in *iso*-hexane (white solid, 52 mg, 47%). ¹H NMR (300
45
46 MHz, DMSO-d₆) δ 8.42 (d, *J*=2.3 Hz, 1H), 8.20 (s, 1H), 8.06 (dd, *J*=2.3, 8.9 Hz, 1H), 7.70 (d, *J*=8.9
47
48 Hz, 1H), 4.17 (q, *J*=6.9 Hz, 2H), 3.99 (q, *J*=6.9 Hz, 2H), 1.23 (t, *J*=7.1 Hz, 3H), 1.18 (t, *J*=7.1 Hz,
49
50 3H), 1.08 (s, 3H), 0.52–0.64 (m, 2H), 0.36–0.44 (m, 2H). LC-MS *m/z* 351.6 [M + H]⁺.
51
52
53
54
55

56 **N-(1-Cyanocyclopropyl)-1,3-diethyl-2,4-dioxo-quinazoline-6-sulfonamide (13b)**

1
2
3 Compound **13b** was prepared in a manner analogous to that for **12a** using **11b**, the reaction mixture
4 was heated at 50 °C overnight and the crude product purified by automated column chromatography,
5 eluent 0–100% EtOAc in *iso*-hexane (white solid, 36 mg, 44%). ¹H NMR (300 MHz, DMSO-*d*₆) δ
6 9.26 (s, 1H), 8.47 (d, *J*=2.3 Hz, 1H), 8.12 (dd, *J*=2.3, 9.0 Hz, 1H), 7.76 (d, *J*=9.0 Hz, 1H), 4.19 (q,
7 *J*=7.1 Hz, 2H), 4.00 (q, *J*=7.0 Hz, 2H), 1.40–1.49 (m, 2H), 1.13–1.31 (m, 8H). LC–MS *m/z* 363.6 [M
8 + H]⁺.
9
10
11
12
13
14
15

16 **N-(1-Methylcyclopropyl)naphthalene-2-sulfonamide (16)**

17
18 To a solution of 2-naphthylsulfonyl chloride (100 mg, 0.44 mmol) in THF (5 mL) cooled in an ice
19 bath, was added a mixture of *N,N*-diisopropylethylamine (0.17 mL, 0.95 mmol) and 1-
20 methylcyclopropanamine hydrochloride (0.050 mL, 0.46 mmol) in DCM (3 mL) the mixture was
21 stirred at ambient temperature overnight. The mixture was diluted with water (10 mL) and extracted
22 with DCM (2 × 10 mL) dried over sodium sulfate and evaporated to dryness. The crude product
23 mixture was purified by preparative HPLC (high pH) to yield **16** as a white solid (50 mg, 43%). ¹H
24 NMR (300 MHz, DMSO-*d*₆) δ 8.45 (d, *J*=1.5 Hz, 1H), 8.09–8.20 (m, 3H), 8.02–8.07 (m, 1H), 7.80
25 (dd, *J*=1.9, 8.7 Hz, 1H), 7.64–7.74 (m, 2H), 1.04 (s, 3H), 0.52–0.69 (m, 2H), 0.29–0.43 (m, 2H).
26 LC–MS *m/z* 262.1 [M + H]⁺.
27
28
29
30
31
32
33
34
35
36
37
38

39 **3-Methyl-1H-quinazoline-2,4-dione (18)**

40
41 A solution of 2-amino-*N*-methylbenzamide (15 g, 0.10 mol) and 1,1-carbonyldiimidazole (21 g, 0.13
42 mol) in DMF (150 mL) was heated at 135–145 °C overnight. The reaction showed 30% starting
43 material by LC–MS, so more 1,1-carbonyldiimidazole (14 g, 0.086 mol) was added and the reaction
44 mixture was heated at 140 °C overnight. The reaction showed complete conversion so was cooled and
45 poured into ice/water (300 mL) and stirred for 10 min. The suspension was filtered and the product
46 was washed with water. The solid was dried in the vacuum oven at 50 °C overnight to give **18** as a
47 white solid (16 g, 90%). ¹H NMR (300 MHz, DMSO-*d*₆) δ 11.44 (br. s, 1H), 7.93 (dd, *J*=1.5, 7.8 Hz,
48 1H), 7.65 (app. t, *J*=7.7 Hz, 1H), 7.23–7.15 (m, 2H), 3.33 (s, 3H).
49
50
51
52
53
54
55
56
57
58
59
60

3-Methyl-2,4-dioxo-1,2,3,4-tetrahydroquinazoline-6-sulfonyl chloride (19)

1
2
3 **18** (15 g, 0.085 mol) was added portionwise with cooling to chlorosulfonic acid (60 mL, 0.9 mol)
4 maintaining the temperature <20 °C. The reaction mixture was heated to 60 °C and stirred for 2 h then
5 allowed to cool. The reaction mixture was added carefully to ice (500 mL) over 30 min. The resultant
6 precipitate was stirred for 30 min, collected by filtration and washed with water. The solid was dried
7 in the vacuum oven to give **19** as a white solid (23 g, 99%). ¹H NMR (300 MHz, DMSO-d₆) δ 11.54
8 (s, 1H), 8.15 (d, *J*=2.1 Hz, 1H), 7.83 (dd, *J*=2.0, 8.4 Hz, 1H), 7.13 (d, *J*=8.5 Hz, 1H), 3.25 (s, 3H).

16 **3-Methyl-N-(1-methylcyclopropyl)-2,4-dioxo-1,2,3,4-tetrahydroquinazoline-6-sulfonamide (20)**

19 **19** (12 g, 44 mmol) and 1-methylcyclopropanamine hydrochloride (5.2 g, 48 mmol) were slurried in
20 DCM (120 mL) at 20 °C. Triethylamine (13 mL, 96 mmol) was added over 15 min: this was
21 exothermic and the temperature was allowed to rise to 34 °C. As the reaction cooled, a precipitate
22 formed. The mixture was stirred for 2 h at ambient temperature, then 1 M HCl (100 mL) was added
23 and the mixture stirred for 25 min. The product was filtered from the biphasic mixture and washed
24 with water (100 mL). The solid was dried in the vacuum oven to give **20** as a white solid (12 g, 89%).
25 ¹H NMR (300 MHz, DMSO-d₆) δ 11.83 (br. s, 1H), 8.32 (d, *J*=2.2 Hz, 1H), 8.13 (s, 1H), 7.99 (dd,
26 *J*=2.2, 8.6 Hz, 1H), 7.32 (d, *J*=8.6 Hz, 1H), 1.06 (s, 3H), 0.62–0.55 (m, 2H), 0.42–0.35 (m, 2H). ¹³C
27 NMR (75 MHz, DMSO-d₆) δ 161.5, 150.2, 141.9, 136.5, 132.5, 126.4, 116.1, 113.7, 30.9, 27.2, 23.9,
28 13.0. HRMS (ESI) *m/z* [M + Na]⁺ calcd for C₁₃H₁₅N₃O₄NaS: 332.0675. Found: 332.0667.

40 **N-((3-Methyl-2,4-dioxo-1,2,3,4-tetrahydroquinazolin-6-yl)sulfonyl)-N-(1-**
41 **methylcyclopropyl)acetamide (21)**

45 **20** (11 g, 36 mmol) was slurried in pyridine (30 mL) and 4-dimethylaminopyridine (430 mg, 3.5
46 mmol) was added. Acetic anhydride (34 mL, 356 mmol) was added over 10 min and the resultant
47 thick slurry was stirred overnight at ambient temperature. The reaction mixture was diluted with
48 EtOAc (25 mL) and filtered. The solid was washed with EtOAc (25 mL). The solid was transferred to
49 a conical flask and slurried in water (40 mL) at 60 °C for 2 h. The slurry was cooled to 35 °C and
50 filtered, washing with water (20 mL). The solid was dried in the vacuum oven to give **21** (10 g, 83%).
51 ¹H NMR (300 MHz, DMSO-d₆) δ 11.91 (br. s, 1H), 8.39 (d, *J*=2.3 Hz, 1H), 8.09 (dd, *J*=2.3, 8.7 Hz,
52
53
54
55
56
57
58
59
60

1
2
3 1H), 7.33 (d, $J=8.8$ Hz, 1H), 3.26 (s, 3H), 2.23 (s, 3H), 1.54 (s, 3H), 1.25–1.16 (m, 2H), 1.10–0.97 (m,
4
5 2H).

6
7
8 **1-Ethyl-3-methyl-N-(1-methylcyclopropyl)-2,4-dioxo-quinazoline-6-sulfonamide (22a)**
9

10 Potassium carbonate (47 mg, 0.34 mmol) was added to a solution of **21** (100 mg, 0.28 mmol) and
11 iodoethane (34 μ L, 0.43 mmol) in DMF (3 mL), the reaction mixture was stirred at ambient
12 temperature overnight, followed by heating at 50 °C for 3.5 h. EtOAc (25 mL) and water (25 mL)
13 were added to the reaction mixture, the organic phase was separated, passed through a hydrophobic
14 frit and evaporated to dryness. The crude intermediate was solubilized in THF (5 mL) and conc. aq.
15 NH₃ (2 mL) was added, the reaction mixture was heated at 50 °C for 29 h. The reaction mixture was
16 evaporated to dryness and the crude product was purified by automated column chromatography,
17 eluent 0–50% EtOAc in *iso*-hexane to yield **22a** as a yellow solid (27 mg, 28%). ¹H NMR (300 MHz,
18 CDCl₃) δ 8.74 (d, $J=2.3$ Hz, 1H), 8.15 (dd, $J=2.3, 8.9$ Hz, 1H), 7.32 (d, $J=8.9$ Hz, 1H), 4.95 (s, 1H),
19 4.25 (q, $J=7.1$ Hz, 2H), 3.51 (s, 3H), 1.39 (t, $J=7.2$ Hz, 3H), 1.26 (s, 3H), 0.74–0.83 (m, 2H), 0.47–
20 0.55 (m, 2H). ¹³C NMR (75 MHz, DMSO-*d*₆) δ 160.6, 150.0, 141.8, 136.6, 132.6, 126.7, 115.5, 115.0,
21 30.9, 28.2, 23.9, 13.0, 12.3. HRMS (ESI) m/z [M + Na]⁺ calcd for C₁₅H₁₉N₃O₄NaS: 360.0988. Found:
22 360.0979.
23
24
25
26
27
28
29
30
31
32
33
34
35
36
37
38

39 **1-(2-Methoxyethyl)-3-methyl-N-(1-methylcyclopropyl)-2,4-dioxo-quinazoline-6-sulfonamide**
40
41 **(22b)**
42

43 A solution of **21** (75 mg, 0.19 mmol), potassium carbonate (32 mg, 0.23 mmol) and 2-bromoethyl
44 methylether (27 μ L, 0.29 mmol) in DMF (3 mL) was stirred at ambient temperature overnight.
45 Methanol (3 mL) and potassium carbonate (13 mg, 0.10 mmol) were added to the reaction mixture,
46 which was stirred at ambient temperature for 2 h. Water (10 mL) and brine (10 mL) were added to the
47 reaction mixture, which was then extracted with EtOAc (50 mL), the organic phase was separated,
48 passed through a hydrophobic frit and evaporated to dryness. The crude product was purified by
49 preparative HPLC (high pH) to yield **22b** as a white solid (14 mg, 20%). ¹H NMR (300 MHz, CDCl₃)
50 δ 8.69 (d, $J=2.3$ Hz, 1H), 8.09 (dd, $J=2.3, 9.0$ Hz, 1H), 7.53 (d, $J=9.0$ Hz, 1H), 4.95 (s, 1H), 4.35 (t,
51
52
53
54
55
56
57
58
59
60

1
2
3 $J=5.3$ Hz, 2H), 3.73 (t, $J=5.3$ Hz, 2H), 3.49 (s, 3H), 3.32 (s, 3H), 1.24 (s, 3H), 0.73–0.80 (m, 2H),
4
5 0.46–0.54 (m, 2H). HRMS (ESI) m/z $[M + Na]^+$ calcd for $C_{16}H_{21}N_3O_5NaS$: 390.1094. Found:
6
7 390.1084.
8
9

10 **1-[2-(Dimethylamino)ethyl]-3-methyl-N-(1-methylcyclopropyl)-2,4-dioxo-quinazoline-6-**
11 **sulfonamide (22c)**
12
13

14 Compound **22c** was prepared in a manner analogous to that for **22b** (white solid, 18 mg, 25%). 1H
15 NMR (300 MHz, $CDCl_3$) δ 8.73 (d, $J=2.3$ Hz, 1H), 8.14 (dd, $J=2.3, 8.8$ Hz, 1H), 7.38 (d, $J=8.8$ Hz,
16
17 1H), 4.96 (s, 1H), 4.30 (t, $J=7.3$ Hz, 2H), 3.51 (s, 3H), 2.63 (t, $J=7.4$ Hz, 2H), 2.37 (s, 6H), 1.26 (s,
18
19 3H), 0.75–0.81 (m, 2H), 0.47–0.55 (m, 2H). ^{13}C NMR (75 MHz, $DMSO-d_6$) δ 160.6, 150.3, 142.1,
20
21 136.6, 132.5, 115.7, 114.9, 55.7, 45.5, 41.7, 30.9, 28.3, 23.9, 13.0. HRMS (ESI) m/z $[M + H]^+$ calcd
22
23 for $C_{17}H_{25}N_4O_4S$: 381.1591. Found: 381.1578.
24
25
26
27

28 **3-Methyl-N-(1-methylcyclopropyl)-2,4-dioxo-1-prop-2-ynyl-quinazoline-6-sulfonamide (22d)**
29

30 **21** (75 mg, 0.19 mmol), propargyl alcohol (22 μ L, 0.38 mmol) and triphenylphosphine, polymer
31 supported (240 mg, 0.38 mmol) were dissolved in chloroform (3 mL) under nitrogen at ambient
32
33 temperature. After 2 min, diisopropyl azodicarboxylate (76 μ L, 0.38 mmol) was added dropwise and
34
35 the reaction was allowed to stir overnight at ambient temperature. Brine (5 mL) was added to the
36
37 reaction mixture which was then passed through a hydrophobic frit, the resulting aqueous phase was
38
39 washed with DCM (10 mL), the organic phase was evaporated to dryness. The resulting oil was
40
41 solubilized in methanol (3 mL), potassium carbonate (27 mg, 0.19 mmol) was added and the reaction
42
43 mixture stirred at ambient temperature for 4.5 h. Brine (10 mL) and DCM (20 mL) were added to the
44
45 reaction mixture, the organic phase was separated with a hydrophobic frit and evaporated to dryness.
46
47 The crude product was purified by automated column chromatography, eluent 0–80% EtOAc in *iso*-
48
49 hexane to yield **22d** as a white solid, (62 mg, 93%). 1H NMR (300 MHz, $CDCl_3$) δ 8.74 (d, $J=2.3$ Hz,
50
51 1H), 8.19 (dd, $J=2.3, 8.8$ Hz, 1H), 7.49 (d, $J=8.8$ Hz, 1H), 4.99 (d, $J=2.5$ Hz, 2H), 4.98 (br. s, 1H),
52
53 3.52 (s, 3H), 2.36 (t, $J=2.5$ Hz, 1H), 1.26 (s, 3H), 0.75–0.83 (m, 2H), 0.49–0.56 (m, 2H). ^{13}C NMR
54
55 (75 MHz, $DMSO-d_6$) δ 160.4, 149.9, 141.2, 137.3, 132.5, 126.6, 115.9, 115.2, 78.0, 75.7, 33.5, 30.9,
56
57 28.4, 23.9, 13.0. HRMS (ESI) m/z $[M + Na]^+$ calcd for $C_{16}H_{17}N_3O_4NaS$: 370.0832. Found: 370.0823.
58
59
60

1-(Cyanomethyl)-3-methyl-N-(1-methylcyclopropyl)-2,4-dioxo-quinazoline-6-sulfonamide (22e)

20 (50 mg, 0.16 mmol), bromoacetonitrile (12 μ L, 0.18 mmol) and caesium carbonate (58 mg, 0.18 mmol) in DMF (2 mL) was stirred at ambient temperature for 5 h. Water (10 mL) was added and the reaction mixture extracted with EtOAc (2 \times 10 mL), the combined organic phase was passed through a hydrophobic frit and evaporated to dryness. The crude product was purified by preparative HPLC (high pH) to yield **22e** as a pale yellow solid (43 mg, 75%). ^1H NMR (300 MHz, DMSO- d_6) δ 8.44 (d, $J=2.3$ Hz, 1H), 8.37 (br. s, 1H), 8.15 (dd, $J=2.3, 8.8$ Hz, 1H), 7.79 (d, $J=8.8$ Hz, 1H), 5.34 (s, 2H), 3.32 (s, 3H), 1.08 (s, 3H), 0.56–0.62 (m, 2H), 0.36–0.43 (m, 2H). ^{13}C NMR (75 MHz, DMSO- d_6) δ 160.4, 150.0, 140.9, 137.8, 132.7, 126.7, 115.7, 115.6, 115.3, 32.3, 31.0, 28.5, 23.9, 13.0. HRMS (ESI) m/z $[\text{M} + \text{Na}]^+$ calcd for $\text{C}_{15}\text{H}_{16}\text{N}_4\text{O}_4\text{NaS}$: 371.0784. Found: 371.0775.

1-(Cyclopropylmethyl)-3-methyl-N-(1-methylcyclopropyl)-2,4-dioxo-quinazoline-6-sulfonamide (22f)

Compound **22f** was prepared in a manner analogous to that for **22b**, purified by automated column chromatography, eluent 0–30% EtOAc in DCM (white solid, 15 mg, 21%). ^1H NMR (300 MHz, CDCl_3) δ 8.75 (d, $J=2.3$ Hz, 1H), 8.15 (dd, $J=2.3, 8.9$ Hz, 1H), 7.44 (d, $J=8.9$ Hz, 1H), 5.02 (s, 1H), 4.12 (d, $J=6.9$ Hz, 2H), 3.51 (s, 3H), 1.26 (s, 3H), 0.83–0.75 (m, 2H), 0.64–0.49 (m, 6H). ^{13}C NMR (75 MHz, DMSO- d_6) δ 192.6, 160.6, 150.6, 142.2, 136.7, 132.5, 126.7, 117.7, 116.0, 114.9, 47.4, 30.9, 28.4, 23.9, 13.0, 9.4, 3.7. HRMS (ESI) m/z $[\text{M} + \text{H}]^+$ calcd for $\text{C}_{17}\text{H}_{22}\text{N}_3\text{O}_4\text{S}$: 364.1326. Found: 364.1318.

1-(Cyclohexylmethyl)-3-methyl-N-(1-methylcyclopropyl)-2,4-dioxo-quinazoline-6-sulfonamide (22g)

Compound **22g** was prepared in a manner analogous to that for **22b**, the reaction mixture was stirred at ambient temperature for 7 days and purified by automated column chromatography, eluent 0–50% EtOAc in *iso*-hexane (white solid, 25 mg, 32%). ^1H NMR (300 MHz, CDCl_3) δ 8.73 (d, $J=2.3$ Hz, 1H), 8.12 (dd, $J=2.3, 8.9$ Hz, 1H), 7.29 (d, $J=5.0$ Hz, 1H), 4.94 (s, 1H), 4.05 (d, $J=7.1$ Hz, 2H), 3.51 (s, 3H), 1.65–1.85 (m, 6H), 1.27 (s, 3H), 1.15–1.26 (m, 5H), 0.76–0.82 (m, 2H), 0.47–0.56 (m, 2H).

¹³C NMR (75 MHz, DMSO-d₆) δ 160.6, 150.6, 142.4, 136.5, 132.3, 126.6, 124.5, 117.7, 116.2, 114.9, 35.8, 30.9, 29.9, 28.4, 25.8, 25.3, 23.9, 13.0. HRMS (ESI) *m/z* [M + H]⁺ calcd for C₂₀H₂₈N₃O₄S: 406.1795. Found: 406.1787.

1-Benzyl-3-methyl-N-(1-methylcyclopropyl)-2,4-dioxo-quinazoline-6-sulfonamide (22h)

Compound **22h** was prepared in a manner analogous to that for **22a** (white solid, 101 mg, 88%). ¹H NMR (300 MHz, CDCl₃) δ 8.73 (d, *J*=2.3 Hz, 1H), 8.01 (dd, *J*=2.3, 8.8 Hz, 1H), 7.28–7.40 (m, 4H), 7.21–7.25 (m, 2H), 5.43 (s, 2H), 4.90 (s, 1H), 3.58 (s, 3H), 1.24 (s, 3H), 0.68–0.78 (m, 2H), 0.46–0.53 (m, 2H). ¹³C NMR (75 MHz, DMSO-d₆) δ 160.7, 150.9, 142.1, 136.9, 135.8, 132.4, 128.7, 127.3, 126.6, 126.5, 116.0, 115.3, 46.7, 30.9, 28.5, 23.9, 12.9. HRMS (ESI) *m/z* [M + H]⁺ calcd for C₂₀H₂₂N₃O₄S: 400.1326. Found: 400.1316.

1-[(2-Fluorophenyl)methyl]-3-methyl-N-(1-methylcyclopropyl)-2,4-dioxo-quinazoline-6-sulfonamide (22i)

Compound **22i** was prepared in a manner analogous to that for **22a** (white powder, 40%). ¹H NMR (400 MHz, CDCl₃) δ = 8.74 (d, *J*=2.3 Hz, 1H), 8.04 (dd, *J*=2.3, 9.2 Hz, 1H), 7.33–7.21 (m, 2H), 7.17–7.09 (m, 3H), 5.48 (s, 2H), 4.88 (s, 1H), 3.58 (s, 3H), 1.24 (s, 3H), 0.78–0.74 (m, 2H), 0.53–0.48 (m, 2H). LC-MS *m/z* 418.1 [M + H]⁺.

1-[(3-Fluorophenyl)methyl]-3-methyl-N-(1-methylcyclopropyl)-2,4-dioxo-quinazoline-6-sulfonamide (22j)

Compound **22j** was prepared in a manner analogous to that for **22a** (white powder, 55%). ¹H NMR (400 MHz, CDCl₃) δ = 8.72 (d, *J*=2.3 Hz, 1H), 8.01 (dd, *J*=2.3, 9.2 Hz, 1H), 7.36–7.29 (m, 1H), 7.16 (d, *J*=8.7 Hz, 1H), 7.05–6.92 (m, 3H), 5.39 (s, 2H), 4.95 (s, 1H), 3.56 (s, 3H), 1.22 (s, 3H), 0.77–0.72 (m, 2H), 0.52–0.45 (m, 2H). LC-MS *m/z* 416.0 [M – H]⁻.

1-[(4-Fluorophenyl)methyl]-3-methyl-N-(1-methylcyclopropyl)-2,4-dioxo-quinazoline-6-sulfonamide (22k)

1
2
3 Compound **22k** was prepared in a manner analogous to that for **22a** (white powder, 28%). ¹H NMR
4 (400 MHz, CDCl₃) δ = 8.72 (d, *J*=2.3 Hz, 1H), 8.01 (dd, *J*=2.3, 9.2 Hz, 1H), 7.28–7.18 (m, 3H), 7.08–
5 7.00 (m, 2H), 5.37 (s, 2H), 4.93 (s, 1H), 3.55 (s, 3H), 1.22 (s, 3H), 0.77–0.71 (m, 2H), 0.52–0.45 (m,
6 2H). LC–MS *m/z* 416.1 [M – H]⁻.
7
8
9

10
11
12 **1-[(2-Methoxyphenyl)methyl]-3-methyl-N-(1-methylcyclopropyl)-2,4-dioxo-quinazoline-6-**
13 **sulfonamide (22l)**
14
15

16
17 Compound **22l** was prepared in a manner analogous to that for **22a** (white powder, 17%). ¹H NMR
18 (400 MHz, CDCl₃) δ = 8.70 (d, *J*=2.3 Hz, 1H), 7.98 (dd, *J*=2.3, 9.2 Hz, 1H), 7.31–7.19 (m, 2H), 6.97–
19 6.91 (m, 2H), 6.88–6.82 (m, 1H), 5.40 (s, 2H), 4.90 (s, 1H), 3.94 (s, 3H), 3.56 (s, 3H), 1.22 (s, 3H),
20 0.78–0.71 (m, 2H), 0.51–0.42 (m, 2H). LC–MS *m/z* 428.0 [M – H]⁻.
21
22
23
24
25

26
27 **1-[(3-Methoxyphenyl)methyl]-3-methyl-N-(1-methylcyclopropyl)-2,4-dioxo-quinazoline-6-**
28 **sulfonamide (22m)**
29
30

31
32 Compound **22m** was prepared in a manner analogous to that for **22a** (white powder, 45%). ¹H NMR
33 (400 MHz, CDCl₃) δ = 8.71 (d, *J*=1.8 Hz, 1H), 7.99 (dd, *J*=2.3, 8.7 Hz, 1H), 7.29–7.23 (m, 1H), 7.21
34 (d, *J*=8.7 Hz, 1H), 6.85–6.75 (m, 3H), 5.37 (s, 2H), 5.06 (s, 1H), 3.79–3.74 (m, 3H), 3.55 (s, 3H), 1.21
35 (s, 3H), 0.78–0.70 (m, 2H), 0.50–0.38 (m, 2H). LC–MS *m/z* 428.0 [M – H]⁻.
36
37
38
39
40

41
42 **1-[(4-Methoxyphenyl)methyl]-3-methyl-N-(1-methylcyclopropyl)-2,4-dioxo-quinazoline-6-**
43 **sulfonamide (22n)**
44
45

46
47 Compound **22n** was prepared in a manner analogous to that for **22a** (white powder, 20%). ¹H NMR
48 (400 MHz, CDCl₃) δ = 8.71 (d, *J*=2.3 Hz, 1H), 8.00 (dd, *J*=2.3, 8.7 Hz, 1H), 7.29–7.24 (m, 1H), 7.19
49 (d, *J*=8.7 Hz, 2H), 6.87 (d, *J*=8.7 Hz, 2H), 5.34 (s, 2H), 4.90 (s, 1H), 3.78 (s, 3H), 3.55 (s, 3H), 1.22
50 (s, 3H), 0.77–0.69 (m, 2H), 0.50–0.44 (m, 2H). LC–MS *m/z* 876.1 [2M + NH₄]⁺.
51
52
53
54
55

56 **3-Methyl-N-(1-methylcyclopropyl)-2,4-dioxo-1-(2-pyridylmethyl)quinazoline-6-sulfonamide**
57 **(22o)**
58
59
60

1
2
3 Compound **22o** was prepared in a manner analogous to that for **22a** (white powder, 25%). ¹H NMR
4 (400 MHz, CDCl₃) δ = 8.69 (d, *J*=2.3 Hz, 1H), 8.56–8.52 (m, 1H), 8.01 (dd, *J*=2.3, 8.7 Hz, 1H),
5 7.66 (dt, *J*=1.8, 7.8 Hz, 1H), 7.47 (d, *J*=8.7 Hz, 1H), 7.31 (d, *J*=8.2 Hz, 1H), 7.22 (t, *J*=6.1 Hz, 1H),
6 5.49 (s, 2H), 5.28 (s, 1H), 3.54 (s, 3H), 1.20 (s, 3H), 0.76–0.70 (m, 2H), 0.50–0.42 (m, 2H).
7
8 LC–MS *m/z* 401.0 [M + H]⁺.
9
10
11
12

13
14 **3-Methyl-N-(1-methylcyclopropyl)-2,4-dioxo-1-(3-pyridylmethyl)quinazoline-6-sulfonamide**
15
16 **(22p)**
17

18
19 Compound **22p** was prepared in a manner analogous to that for **22a** (yellow powder, 16%). ¹H
20 NMR (400 MHz, CDCl₃) δ = 8.73 (d, *J*=2.3 Hz, 1H), 8.65 (d, *J*=2.3 Hz, 1H), 8.58 (dd, *J*=1.4, 5.0
21 Hz, 1H), 8.04 (dd, *J*=2.5, 8.9 Hz, 1H), 7.63 (br d, *J*=8.2 Hz, 1H), 7.34–7.26 (m, 1H), 7.21 (d, *J*=8.7
22 Hz, 1H), 5.43 (s, 2H), 4.99 (s, 1H), 3.55 (s, 3H), 1.23 (s, 3H), 0.79–0.69 (m, 2H), 0.54–0.46 (m,
23 2H). LC–MS *m/z* 401.0 [M + H]⁺.
24
25
26
27
28

29
30 **3-Methyl-N-(1-methylcyclopropyl)-2,4-dioxo-1-(4-pyridylmethyl)quinazoline-6-sulfonamide**
31
32 **(22q)**
33

34
35 Compound **22q** was prepared in a manner analogous to that for **22a**, yellow powder, 27%). ¹H
36 NMR (400 MHz, CDCl₃) δ = 8.74 (d, *J*=2.3 Hz, 1H), 8.63–8.57 (m, 2H), 8.02 (dd, *J*=2.3, 8.7 Hz,
37 1H), 7.16 (d, *J*=6.0 Hz, 2H), 7.05 (d, *J*=8.7 Hz, 1H), 5.41 (s, 2H), 4.96 (s, 1H), 3.56 (s, 3H), 1.23
38 (s, 3H), 0.77–0.71 (m, 2H), 0.53–0.47 (m, 2H). LC–MS *m/z* 401.0 [M + H]⁺.
39
40
41
42

43
44 **3-Methyl-N-(1-methylcyclopropyl)-1-[(2-methylpyrazol-3-yl)methyl]-2,4-dioxo-quinazoline-6-**
45 **sulfonamide (22r)**
46

47
48 Compound **22r** was prepared in a manner analogous to that for **22d** (white powder, 22%). ¹H NMR
49 (400 MHz, CDCl₃) δ = 8.74 (d, *J*=2.3 Hz, 1H), 8.10 (dd, *J*=2.3, 9.2 Hz, 1H), 7.38 (d, *J*=1.8 Hz,
50 1H), 7.30 (d, *J*=8.7 Hz, 1H), 6.00 (d, *J*=2.3 Hz, 1H), 5.39 (s, 2H), 4.94 (s, 1H), 4.01 (s, 3H), 3.52
51 (s, 3H), 1.24 (s, 3H), 0.79–0.73 (m, 2H), 0.54–0.47 (m, 2H). LC–MS *m/z* 404.0 [M + H]⁺. NMR
52
53
54
55
56
57
58
59
60 purity, 85-90%.

1
2
3 **1-[(2,5-Dimethylpyrazol-3-yl)methyl]-3-methyl-N-(1-methylcyclopropyl)-2,4-dioxo-**
4
5 **quinazoline-6-sulfonamide (22s)**
6

7
8 Compound **22s** was prepared in a manner analogous to that for **22d** (white powder, 13%). ¹H NMR
9
10 (400 MHz, CDCl₃) δ = 8.74 (d, *J*=2.3 Hz, 1H), 8.11 (br dd, *J*=2.3, 9.2 Hz, 1H), 7.29 (d, *J*=8.7 Hz,
11
12 1H), 5.76 (s, 1H), 5.33 (s, 2H), 4.92 (s, 1H), 3.92 (s, 3H), 3.51 (s, 3H), 2.15 (s, 3H), 1.25 (s, 3H),
13
14 0.79–0.74 (m, 2H), 0.53–0.49 (m, 2H). LC–MS *m/z* 418.1 [M + H]⁺.
15

16
17 **1-[(2,4-Dimethylthiazol-5-yl)methyl]-3-methyl-N-(1-methylcyclopropyl)-2,4-dioxo-**
18
19 **quinazoline-6-sulfonamide (22t)**
20

21
22 Compound **22t** was prepared in a manner analogous to that for **22d** (off-white powder, 5%). ¹H
23
24 NMR (300 MHz, DMSO-*d*₆) δ = 8.44 (d, *J*=2.3 Hz, 1H), 8.22 (s, 1H), 8.11 (dd, *J*=2.4, 8.9 Hz, 1H),
25
26 7.67 (d, *J*=8.9 Hz, 1H), 5.45 (s, 2H), 3.34 (s, 3H), 2.49 (s, 3H), 2.47 (s, 3H), 1.08 (s, 3H), 0.66–
27
28 0.56 (m, 2H), 0.43–0.36 (m, 2H). LC–MS *m/z* 435.5 [M + H]⁺.
29

30
31 **1-Methylquinazoline-2,4(1H,3H)-dione (24)**
32

33
34 Sodium cyanate (30 g, 0.46 mol) was added to a slurry of N-methylantranilic acid (50 g, 0.33
35
36 mol) in water (1.75 L) and acetic acid (3.3 mL). The reaction mixture was heated to 50 °C for 1 h.
37
38 The solution was slowly basified by the addition of sodium hydroxide (exothermic). The resulting
39
40 solution was heated to 80 °C and stirred overnight. The reaction mixture was cooled to 0 °C and the
41
42 resultant precipitate collected by filtration. The solid was dissolved in boiling water (200 mL) and
43
44 acidified with conc. sulfuric acid to pH 2. The slurry was cooled to RT and filtered. The solid was
45
46 dried in a vacuum oven to give **24** as a white powder (53 g, 77%). ¹H NMR (300 MHz, DMSO-*d*₆)
47
48 δ = 11.54 (br s, 1H), 8.00 (d, *J*=7.7 Hz, 1H), 7.77 (t, *J*=7.9 Hz, 1H), 7.43 (d, *J*=8.6 Hz, 1H), 7.28 (t,
49
50 *J*=7.5 Hz, 1H), 3.33 (s, 3H).
51

52
53 **1-Methyl-2,4-dioxo-1,2,3,4-tetrahydroquinazoline-6-sulfonyl chloride (25)**
54

55
56 Compound **24** (25 g, 0.14 mol) was added portionwise to chlorosulfonic acid (125 mL, 1.9 mol) at
57
58 50 °C. The reaction mixture was heated to 50 °C and stirred overnight then allowed to cool. The
59
60 reaction mixture was added carefully to ice/water (1.5 L) maintaining the temperature <20 °C. The

1
2
3 resultant precipitate was collected by filtration and dried in an open atmosphere to give **19** as a
4 white powder (44 g, 113% - contains water). ¹H NMR (300 MHz, DMSO-d₆) δ = 11.58 (s, 1H),
5 8.19 (d, *J*=2.1 Hz, 1H), 7.91 (dd, *J*=2.1, 8.6 Hz, 1H), 7.38 (d, *J*=8.7 Hz, 1H), 3.44 (s, 3H).
6
7
8

9
10 **1-Methyl-N-(1-methylcyclopropyl)-2,4-dioxo-1,2,3,4-tetrahydroquinazoline-6-sulfonamide**
11
12 **(26)**
13

14 Triethylamine (8.1 g, 80 mmol) was added to a stirred solution of **25** (11.3 g, 36 mmol) in DCM
15 (250 mL). 1-Methylcyclopropanamine hydrochloride (4.3 g, 40 mmol) was added portionwise over
16 10 min and the reaction mixture was stirred at RT for 3 h. The reaction mixture was poured onto
17 water (250 mL) and filtered to afford **26** as a white powder (10.5 g, 93%). ¹H NMR (300 MHz,
18 DMSO-d₆) δ = 11.83 (br s, 1H), 8.35 (d, *J*=2.4 Hz, 1H), 8.17 (s, 1H), 8.06 (dd, *J*=2.3, 8.8 Hz, 1H),
19 7.61 (d, *J*=8.9 Hz, 1H), 3.48 (s, 3H), 1.07 (s, 3H), 0.64–0.55 (m, 2H), 0.44–0.35 (m, 2H).
20
21
22
23
24
25
26
27

28 **Preparation of Compounds 27a–au**
29

30 **General method A:**
31

32 A solution of **26** (50 mg, 0.16 mmol) in DMF (1 mL) was treated with NaH (60% w/w in mineral oil)
33 (6.6 mg, 0.17 mmol) and the resulting mixture was stirred at RT for 5 min. Alkyl halide, mesylate or
34 tosylate (0.17 mmol) was added (if the alkyl chloride, mesylate or tosylate was used, NaI (5 mg, 0.030
35 mmol) was also added) and the mixture was stirred at RT until analysis revealed complete reaction.
36 Water (2 mL) and ethyl acetate (3 mL) were added and the layers were separated. The organic layer
37 was washed with water (2 × 2 mL) and concentrated under reduced pressure. Purification by mass
38 directed prep. HPLC gave the alkylated products.
39
40
41
42
43
44
45
46
47
48

49 **General method B:**
50

51 A mixture of **26** (50 mg, 0.161 mmol), polymer supported triphenylphosphine (202 mg, 0.32
52 mmol) and alcohol (0.32 mmol) in DMF (1.5 mL) was treated with diisopropyl azodicarboxylate
53 (64 μL, 0.32 mmol) and stirred at RT until analysis revealed complete reaction. The reaction
54 mixture was quenched with water (0.5 mL), filtered and washed with EtOAc. The filtrate was
55 concentrated and purified by prep. HPLC to afford the alkylated products.
56
57
58
59
60

3-Ethyl-1-methyl-N-(1-methylcyclopropyl)-2,4-dioxo-quinazoline-6-sulfonamide (27a)

Prepared by General method A (using the alkyl iodide) to afford a white powder, 59%. ¹H NMR (300 MHz, CDCl₃) δ = 8.73 (d, *J*=2.3 Hz, 1H), 8.17 (dd, *J*=2.3, 8.8 Hz, 1H), 7.32 (d, *J*=8.9 Hz, 1H), 4.97 (s, 1H), 4.18 (q, *J*=7.0 Hz, 2H), 3.67 (s, 3H), 1.32 (t, *J*=7.1 Hz, 3H), 1.26 (s, 3H), 0.84–0.71 (m, 2H), 0.56–0.49 (m, 2H). LC–MS *m/z* 336.6 [M – H][–].

3-(Cyclopropylmethyl)-1-methyl-N-(1-methylcyclopropyl)-2,4-dioxo-quinazoline-6-sulfonamide (27b)

Prepared by General method A (using the alkyl bromide) to afford a white powder, 18%. ¹H NMR (300 MHz, CDCl₃) δ = 8.72 (d, *J*=2.3 Hz, 1H), 8.16 (dd, *J*=2.3, 8.8 Hz, 1H), 7.32 (d, *J*=8.9 Hz, 1H), 5.10 (s, 1H), 4.00 (d, *J*=7.2 Hz, 2H), 3.67 (s, 3H), 1.28–1.22 (m, 4H), 0.81–0.71 (m, 2H), 0.55–0.43 (m, 6H). LC–MS *m/z* 364.5 [M + H]⁺.

3-(Cyclohexylmethyl)-1-methyl-N-(1-methylcyclopropyl)-2,4-dioxo-quinazoline-6-sulfonamide (27c)

Prepared by General method A (using the alkyl bromide) to afford a beige powder, 30%. ¹H NMR (300 MHz, CDCl₃) δ = 8.63–8.59 (m, 1H), 8.48 (br s, 1H), 8.19–8.12 (m, 1H), 7.32 (d, *J*=8.9 Hz, 1H), 3.63 (s, 3H), 3.13 (d, *J*=7.1 Hz, 2H), 1.85–1.65 (m, 7H), 1.28 (s, 3H), 1.24–1.17 (m, 2H), 0.97–0.80 (m, 4H), 0.63 (s, 2H). LC–MS *m/z* 406.6 [M + H]⁺.

1-Methyl-N-(1-methylcyclopropyl)-2,4-dioxo-3-phenyl-quinazoline-6-sulfonamide (27d)

Following the method of Chan et al.,⁴⁰ a mixture of **26** (100 mg, 0.32 mmol), phenylboronic acid (79 mg, 0.65 mmol), copper acetate (59 mg, 0.32 mmol), triethylamine (0.09 mL, 0.65 mmol) and 4 Å molecular sieves was slurried in DCM (2 mL) and stirred at RT for 3 d. The reaction mixture was filtered through celite and the filtrate was concentrated to dryness and partitioned between water (10 mL) and DCM (10 mL). The organic layer was passed through a hydrophobic frit, concentrated to dryness and purified by prep. HPLC to afford **27d** (23 mg, 18%) as a white powder. ¹H NMR (300 MHz, CDCl₃) δ = 8.75 (d, *J*=2.3 Hz, 1H), 8.23 (dd, *J*=2.3, 8.8 Hz, 1H), 7.60–7.48

(m, 3H), 7.40 (d, $J=8.9$ Hz, 1H), 7.32–7.29 (m, 2H), 4.98 (s, 1H), 3.71 (s, 3H), 1.29 (s, 3H), 0.83–0.77 (m, 2H), 0.57–0.52 (m, 2H). LC–MS m/z 386.6 $[M + H]^+$.

3-Benzyl-1-methyl-N-(1-methylcyclopropyl)-2,4-dioxo-quinazoline-6-sulfonamide (27e)

Prepared by General method A (using the alkyl bromide) to afford a white powder, 39%. ^1H NMR (300 MHz, CDCl_3) δ = 8.51 (s, 1H), 7.93 (br d, $J=8.8$ Hz, 1H), 7.37–7.24 (m, 2H), 7.17–7.06 (m, 4H), 5.05 (s, 2H), 4.87 (s, 1H), 3.41 (s, 3H), 1.01 (s, 3H), 0.62–0.47 (m, 2H), 0.35–0.22 (m, 2H). LC–MS m/z 400.5 $[M + H]^+$.

1-Methyl-N-(1-methylcyclopropyl)-2,4-dioxo-3-(2-pyridylmethyl)quinazoline-6-sulfonamide (27f)

Prepared by General method A (using the alkyl bromide HBr salt plus an extra equivalent of base) to afford a white powder, 15%. ^1H NMR (400 MHz, CDCl_3) δ = 8.72 (d, $J=2.3$ Hz, 1H), 8.50 (br d, $J=4.1$ Hz, 1H), 8.16 (dd, $J=2.3, 8.7$ Hz, 1H), 7.66 (dt, $J=1.6, 7.7$ Hz, 1H), 7.32 (d, $J=8.7$ Hz, 2H), 7.19–7.13 (m, 1H), 5.42 (s, 2H), 4.92 (s, 1H), 3.66 (s, 3H), 1.25 (s, 3H), 0.79–0.72 (m, 2H), 0.55–0.47 (m, 2H). LC–MS m/z 401.0 $[M + H]^+$.

1-Methyl-N-(1-methylcyclopropyl)-2,4-dioxo-3-(3-pyridylmethyl)quinazoline-6-sulfonamide (27g)

Prepared by General method A (using the alkyl bromide HBr salt plus an extra equivalent of base) to afford a white powder, 15%. ^1H NMR (400 MHz, CDCl_3) δ = 8.81 (br s, 1H), 8.67 (d, $J=2.3$ Hz, 1H), 8.53 (br d, $J=2.3$ Hz, 1H), 8.13 (dd, $J=2.3, 8.7$ Hz, 1H), 7.92 (br d, $J=7.8$ Hz, 1H), 7.33–7.27 (m, 2H), 5.28 (s, 2H), 5.20 (br s, 1H), 3.64 (s, 3H), 1.21 (s, 3H), 0.80–0.68 (m, 2H), 0.51–0.41 (m, 2H). LC–MS m/z 401.0 $[M + H]^+$.

1-Methyl-N-(1-methylcyclopropyl)-2,4-dioxo-3-(4-pyridylmethyl)quinazoline-6-sulfonamide (27h)

Prepared by General method A (using the alkyl bromide HBr salt plus an extra equivalent of base) to afford a white powder, 19%. ^1H NMR (400 MHz, CDCl_3) δ = 8.72 (d, $J=2.3$ Hz, 1H), 8.61–8.52 (m, 2H), 8.22–8.11 (m, 1H), 7.43 (br d, $J=5.0$ Hz, 2H), 7.32 (d, $J=9.2$ Hz, 1H), 5.27 (s, 2H), 5.01

(s, 1H), 3.65 (s, 3H), 1.24 (s, 3H), 0.81–0.72 (m, 2H), 0.56–0.45 (m, 2H). LC–MS m/z 401.0 [M + H]⁺. LC-MS purity, 90-95%.

1-Methyl-N-(1-methylcyclopropyl)-2,4-dioxo-3-phenacyl-quinazoline-6-sulfonamide (27i)

Prepared by General method A (using the alkyl bromide) to afford a white powder, 37%. ¹H NMR (300 MHz, DMSO-*d*₆) δ = 8.43 (d, J =2.3 Hz, 1H), 8.24 (s, 1H), 8.18–8.09 (m, 3H), 7.78–7.72 (m, 2H), 7.65–7.58 (m, 2H), 5.53 (s, 2H), 3.60 (s, 3H), 1.09 (s, 3H), 0.65–0.59 (m, 2H), 0.44–0.38 (m, 2H). LC–MS m/z 428.2 [M + H]⁺.

1-Methyl-N-(1-methylcyclopropyl)-2,4-dioxo-3-[2-oxo-2-(4-pyridyl)ethyl]quinazoline-6-sulfonamide (27j)

Prepared by General method A (using the alkyl bromide HBr salt plus an extra equivalent of base) to afford a white powder, 6%. ¹H NMR (300 MHz, DMSO-*d*₆) δ = 8.90 (dd, J =1.6, 4.7 Hz, 2H), 8.42 (d, J =2.3 Hz, 1H), 8.24 (s, 1H), 8.16 (dd, J =2.3, 8.9 Hz, 1H), 7.98 (dd, J =1.8, 4.7 Hz, 2H), 7.75 (d, J =8.9 Hz, 1H), 5.56 (s, 2H), 3.60 (s, 3H), 1.09 (s, 3H), 0.66–0.56 (m, 2H), 0.44–0.39 (m, 2H). LC–MS m/z 429.2 [M + H]⁺.

1-Methyl-N-(1-methylcyclopropyl)-2,4-dioxo-3-prop-2-ynyl-quinazoline-6-sulfonamide (27k)

Prepared by General method B to afford a white powder, 13%. ¹H NMR (300 MHz, DMSO-*d*₆) δ = 8.42 (d, J =2.3 Hz, 1H), 8.23 (br s, 1H), 8.10 (dd, J =2.3, 8.9 Hz, 1H), 7.68 (d, J =8.9 Hz, 1H), 4.69 (d, J =2.4 Hz, 2H), 3.57 (s, 3H), 3.22–3.17 (m, 1H), 1.07 (s, 3H), 0.64–0.56 (m, 2H), 0.42–0.37 (m, 2H). LC–MS m/z 348.5 [M + H]⁺.

3-(Cyanomethyl)-1-methyl-N-(1-methylcyclopropyl)-2,4-dioxo-quinazoline-6-sulfonamide (27l)

Prepared by General method A (using the alkyl bromide) to afford a white powder, 21%. ¹H NMR (300 MHz, DMSO-*d*₆) δ = 8.42 (d, J =2.3 Hz, 1H), 8.21 (br s, 1H), 8.12 (dd, J =2.3, 8.9 Hz, 1H), 7.70 (d, J =8.9 Hz, 1H), 4.97 (s, 2H), 3.58 (s, 3H), 1.08 (s, 3H), 0.67–0.52 (m, 2H), 0.47–0.34 (m, 2H). LC–MS m/z 349.5 [M + H]⁺.

1
2
3 **1-Methyl-N-(1-methylcyclopropyl)-3-(oxetan-3-ylmethyl)-2,4-dioxo-quinazoline-6-**
4 **sulfonamide (27m)**
5
6

7
8 Prepared by General method A (using the alkyl tosylate) to afford a white powder, 42%. ¹H NMR
9 (300 MHz, CDCl₃) δ = 8.72 (d, *J*=2.3 Hz, 1H), 8.18 (d, *J*=8.9 Hz, 1H), 7.36–7.30 (m, 1H), 4.96 (s,
10 1H), 4.82–4.74 (m, 2H), 4.71–4.64 (m, 2H), 4.44 (d, *J*=6.7 Hz, 2H), 3.66 (s, 3H), 3.55–3.38 (m,
11 1H), 1.27 (s, 3H), 0.81–0.75 (m, 2H), 0.56–0.49 (m, 2H). LC–MS *m/z* 380.1 [M + H]⁺.
12
13
14
15

16
17 **3-(3-Furylmethyl)-1-methyl-N-(1-methylcyclopropyl)-2,4-dioxo-quinazoline-6-sulfonamide**
18 **(27n)**
19
20

21 Prepared by General method B to afford a white powder, 10%. ¹H NMR (300 MHz, CDCl₃) δ =
22 8.72 (d, *J*=2.3 Hz, 1H), 8.15 (dd, *J*=2.3, 8.8 Hz, 1H), 7.60 (d, *J*=0.7 Hz, 1H), 7.34 (t, *J*=1.6 Hz,
23 1H), 7.30 (d, *J*=8.9 Hz, 1H), 6.55 (s, 1H), 5.12 (s, 1H), 5.11 (s, 2H), 3.65 (s, 3H), 1.24 (s, 3H),
24 0.81–0.73 (m, 2H), 0.54–0.46 (m, 2H). LC–MS *m/z* 390.1 [M + H]⁺.
25
26
27
28
29

30
31 **1-Methyl-N-(1-methylcyclopropyl)-2,4-dioxo-3-(3-thienylmethyl)quinazoline-6-sulfonamide**
32 **(27o)**
33
34

35 Prepared by General method A (using the alkyl bromide) to afford a white powder, 25%. ¹H NMR
36 (300 MHz, DMSO-*d*₆) δ = 8.30 (d, *J*=2.3 Hz, 1H), 8.06 (br s, 1H), 7.96 (dd, *J*=2.3, 8.8 Hz, 1H),
37 7.54 (d, *J*=8.9 Hz, 1H), 7.36–7.32 (m, 1H), 7.31–7.28 (m, 1H), 6.99 (dd, *J*=1.3, 4.9 Hz, 1H), 4.99
38 (s, 2H), 3.44 (s, 3H), 0.95 (s, 3H), 0.51–0.44 (m, 2H), 0.31–0.23 (m, 2H). LC–MS *m/z* 406.1 [M +
39 H]⁺.
40
41
42
43
44
45

46
47 **1-Methyl-N-(1-methylcyclopropyl)-3-[(2-methylthiazol-4-yl)methyl]-2,4-dioxo-quinazoline-6-**
48 **sulfonamide (27p)**
49
50

51 Prepared by General method A (using the alkyl chloride) to afford a white powder, 6%. ¹H NMR
52 (300 MHz, DMSO-*d*₆) δ = 8.42 (d, *J*=2.3 Hz, 1H), 8.22 (s, 1H), 8.11 (dd, *J*=2.3, 8.9 Hz, 1H), 7.68
53 (d, *J*=8.9 Hz, 1H), 7.30 (s, 1H), 5.18 (s, 2H), 3.57 (s, 3H), 2.60 (s, 3H), 1.09 (s, 3H), 0.64–0.56 (m,
54 2H), 0.44–0.37 (m, 2H). LC–MS *m/z* 421.1 [M + H]⁺.
55
56
57
58
59
60

1
2
3 **1-Methyl-N-(1-methylcyclopropyl)-3-(oxazol-4-ylmethyl)-2,4-dioxo-quinazoline-6-**
4
5 **sulfonamide (27q)**
6

7
8 Following the method of Lipshutz et al.,³⁰ a mixture of 1,3-oxazol-4-ylmethanol (38 mg, 0.39
9 mmol), **26** (60 mg, 0.19 mmol) and polymer supported triphenylphosphine (242 mg, 0.39 mmol) in
10 DMF (1 mL) was treated with a solution of bis(4-chlorobenzyl)azodicarboxylate (0.19 mL, 0.39
11 mmol) in DMF (1 mL) and stirred at RT for 2 h. The reaction mixture was filtered and the filter
12 cake washed with EtOAc (2 × 5 mL). The filtrate was concentrated and then DCM (3 mL) was
13 added. The flask was cooled in an ice bath and the resulting hydrazine by-product was collected by
14 filtration and washed with DCM (2 × 5 mL). The DCM filtrate was concentrated and purified by
15 prep. HPLC to afford **12r** (10 mg, 13%) as a white powder. ¹H NMR (300 MHz, DMSO-d₆) δ =
16 8.42 (d, *J*=2.3 Hz, 1H), 8.28 (d, *J*=0.9 Hz, 1H), 8.21 (s, 1H), 8.10 (dd, *J*=2.3, 8.8 Hz, 1H), 8.04 (d,
17 *J*=1.0 Hz, 1H), 7.68 (d, *J*=8.9 Hz, 1H), 5.06 (s, 2H), 3.56 (s, 3H), 1.08 (s, 3H), 0.64–0.56 (m, 2H),
18 0.44–0.37 (m, 2H). LC–MS *m/z* 391.1 [M + H]⁺.
19
20
21
22
23
24
25
26
27
28
29
30

31 **1-Methyl-N-(1-methylcyclopropyl)-2,4-dioxo-3-(thiazol-2-ylmethyl)quinazoline-6-sulfonamide**
32 **(27r)**
33

34
35 Prepared by General method B to afford a white powder, 12%. ¹H NMR (300 MHz, DMSO-d₆) δ =
36 8.43 (d, *J*=2.2 Hz, 1H), 8.34 (s, 1H), 8.12 (dd, *J*=2.2, 8.9 Hz, 1H), 7.73–7.66 (m, 3H), 5.46 (s, 2H),
37 3.59 (s, 3H), 1.08 (s, 3H), 0.65–0.57 (m, 2H), 0.44–0.36 (m, 2H). LC–MS *m/z* 407.5 [M + H]⁺.
38
39
40
41
42

43 **1-Methyl-N-(1-methylcyclopropyl)-2,4-dioxo-3-(thiazol-5-ylmethyl)quinazoline-6-sulfonamide**
44 **(27s)**
45

46
47 Prepared by General method B to afford a white powder, 21%. ¹H NMR (300 MHz, DMSO-d₆) δ =
48 9.00 (s, 1H), 8.43 (d, *J*=2.3 Hz, 1H), 8.20 (s, 1H), 8.09 (dd, *J*=2.3, 8.9 Hz, 1H), 7.93 (s, 1H), 7.66
49 (d, *J*=8.9 Hz, 1H), 5.34 (s, 2H), 3.56 (s, 3H), 1.07 (s, 3H), 0.62–0.56 (m, 2H), 0.42–0.36 (m, 2H).
50 LC–MS *m/z* 407.5 [M + H]⁺. LC-MS purity, 85-90%.
51
52
53
54
55

56 **1-Methyl-N-(1-methylcyclopropyl)-3-[(2-methylthiazol-5-yl)methyl]-2,4-dioxo-quinazoline-6-**
57 **sulfonamide (27t)**
58
59
60

Prepared by General method B to afford a white powder, 16%. ¹H NMR (300 MHz, CDCl₃) δ = 8.73 (d, *J*=2.3 Hz, 1H), 8.16 (dd, *J*=2.4, 8.9 Hz, 1H), 7.75 (s, 1H), 7.30 (d, *J*=8.9 Hz, 1H), 5.38 (s, 2H), 4.99 (s, 1H), 3.66 (s, 3H), 2.65 (s, 3H), 1.25 (s, 3H), 0.80–0.74 (m, 2H), 0.55–0.49 (m, 2H). LC-MS *m/z* 421.0 [M + H]⁺.

3-[(2-Aminothiazol-5-yl)methyl]-1-methyl-N-(1-methylcyclopropyl)-2,4-dioxo-quinazoline-6-sulfonamide (27u)

1. Preparation of alcohol with protected amino group:

(a) Following the method of Leblanc et al.,⁴¹ a mixture of methyl 2-aminothiazole-5-carboxylate (359 mg, 2.3 mmol), hexane-2,5-dione (0.29 mL, 2.5 mmol) and p-toluenesulfonic acid monohydrate (20 mg, 0.11 mmol) in toluene (15 mL) was heated to 80 °C for 3 h and then stirred at reflux for a further 17 h. The reaction mixture was then cooled to RT and concentrated. The crude material was columned, eluting with 0–50% EtOAc in hexane, then flushed with EtOAc to give methyl 2-(2,5-dimethylpyrrol-1-yl)thiazole-5-carboxylate as a pale yellow oil (155 mg, 29%) (50% starting material was also recovered). ¹H NMR (300 MHz, DMSO-*d*₆) δ = 8.43 (s, 1H), 5.94 (s, 2H), 3.88 (s, 3H), 2.25 (s, 6H).

(b) A solution of methyl 2-(2,5-dimethylpyrrol-1-yl)thiazole-5-carboxylate (1.2 g, 5.0 mmol) in THF (40 mL) was cooled to 0 °C and treated slowly with a solution of lithium aluminium hydride (1.0 M in THF, 5.5 mL, 5.5 mmol) and the mixture was stirred at RT for 20 min. The reaction mixture was cooled to 0 °C and carefully quenched with sat. aq. Rochelle's salt (40 mL) and stirred vigorously at RT for 1 h. The mixture was allowed to settle then the clear solution was decanted away from the sticky residue. The sticky residue was washed with EtOAc and decanted (×3) and the layers separated. The aqueous layer was re-extracted with EtOAc, and organic extracts washed with brine, passed through a hydrophobic frit and concentrated to give an amber oil (989 mg, 96%). ¹H NMR (300 MHz, DMSO-*d*₆) δ = 7.65 (t, *J*=0.9 Hz, 1H), 5.86 (s, 2H), 5.71 (t, *J*=5.7 Hz, 1H), 4.71 (dd, *J*=1.0, 5.7 Hz, 2H), 2.19–2.05 (m, 6H). LC-MS purity, 90-95%.

2. Quinazolidinedione alkylation:

1
2
3 General method B was followed to afford crude material which was progressed to the deprotection
4
5 reaction without purification.
6

7 3. Deprotection:

8
9 A mixture of the intermediate from the previous step (100 mg, 0.16 mmol), hydroxylamine
10 hydrochloride (171 mg, 2.5 mmol) and 2 M NaOH (0.82 mL, 1.6 mmol) in EtOH (2 mL), water (2
11 mL) and DMF (2 mL) was heated to reflux for 3 d. The reaction mixture was concentrated and the
12 residue taken up in DCM, then saturated aq. NaHCO₃ and water were added, stirred for 5 min and
13 then passed through a hydrophobic frit and washed with DCM. The combined organics were
14 concentrated and the residue purified by prep. HPLC to give **12v** (8 mg, 12%) as a white powder. ¹H
15 NMR (300 MHz, DMSO-d₆) δ = 8.42 (d, *J*=2.4 Hz, 1H), 8.19 (br s, 1H), 8.08 (dd, *J*=2.3, 8.8 Hz, 1H),
16 7.65 (d, *J*=8.9 Hz, 1H), 6.96–6.82 (m, 3H), 5.06 (s, 2H), 3.56 (s, 3H), 1.07 (s, 3H), 0.64–0.53 (m, 2H),
17 0.45–0.32 (m, 2H). LC–MS *m/z* 422.2 [M + H]⁺.
18
19

20 **3-[(2,4-Dimethylthiazol-5-yl)methyl]-1-methyl-N-(1-methylcyclopropyl)-2,4-dioxo-quinazoline-** 21 **6-sulfonamide (27v)**

22 Prepared by General method B to afford a white powder, 4%. ¹H NMR (300 MHz, DMSO-d₆) δ =
23 8.43 (d, *J*=2.2 Hz, 1H), 8.20 (s, 1H), 8.09 (dd, *J*=2.2, 8.9 Hz, 1H), 7.65 (d, *J*=8.9 Hz, 1H), 5.19 (s,
24 2H), 3.56 (s, 3H), 2.51 (3H, s), 2.44 (s, 3H), 1.07 (s, 3H), 0.67–0.55 (m, 2H), 0.43–0.34 (m, 2H).
25 LC–MS *m/z* 435.5 [M + H]⁺.
26
27

28 **1-Methyl-N-(1-methylcyclopropyl)-3-[(2-methyl-4-phenyl-thiazol-5-yl)methyl]-2,4-dioxo-** 29 **quinazoline-6-sulfonamide (27w)**

30 Prepared by General method B to afford a white powder, 6%. ¹H NMR (300 MHz, DMSO-d₆) δ =
31 8.40 (d, *J*=2.3 Hz, 1H), 8.35 (s, 1H), 8.10 (dd, *J*=2.3, 8.9 Hz, 1H), 7.77–7.69 (m, 2H), 7.66 (d, *J*=8.9
32 Hz, 1H), 7.54–7.37 (m, 3H), 5.41 (s, 2H), 3.54 (s, 3H), 2.59 (s, 3H), 1.08 (s, 3H), 0.64–0.55 (m, 2H),
33 0.43–0.36 (m, 2H). LC–MS *m/z* 497.6 [M + H]⁺.
34
35

36 **3-(Isothiazol-5-ylmethyl)-1-methyl-N-(1-methylcyclopropyl)-2,4-dioxo-quinazoline-6-** 37 **sulfonamide (27x)**

38 Prepared by General method B to afford a white powder, 4%. ¹H NMR (300 MHz, DMSO-d₆) δ =
39 8.46–8.42 (m, 2H), 8.21 (s, 1H), 8.13–8.07 (m, 1H), 7.68 (d, *J*=8.9 Hz, 1H), 7.43 (d, *J*=1.7 Hz, 1H),
40
41

5.41 (s, 2H), 3.57 (s, 3H), 1.08 (s, 3H), 0.63–0.57 (m, 2H), 0.42–0.37 (m, 2H). LC–MS m/z 407.1 [M + H]⁺.

1-Methyl-N-(1-methylcyclopropyl)-2,4-dioxo-3-(thiadiazol-4-ylmethyl)quinazoline-6-sulfonamide (27y)

Prepared by General method B to afford a white powder, 24%. ¹H NMR (300 MHz, CDCl₃) δ = 8.75 (d, J =2.2 Hz, 1H), 8.65 (s, 1H), 8.19 (dd, J =2.3, 8.8 Hz, 1H), 7.40–7.32 (m, 1H), 5.81 (s, 2H), 4.92 (s, 1H), 3.68 (s, 3H), 1.27 (s, 3H), 0.82–0.74 (m, 2H), 0.57–0.49 (m, 2H). LC–MS m/z 406.5 [M – H][–].

1-Methyl-N-(1-methylcyclopropyl)-3-[(4-methylthiadiazol-5-yl)methyl]-2,4-dioxo-quinazoline-6-sulfonamide (27z)

Prepared by General method B to afford a white powder, 50%. ¹H NMR (300 MHz, CDCl₃) δ = 8.75 (d, J =2.2 Hz, 1H), 8.20 (dd, J =2.3, 8.9 Hz, 1H), 7.34 (d, J =8.9 Hz, 1H), 5.51 (s, 2H), 4.97 (s, 1H), 3.69 (s, 3H), 2.93 (s, 3H), 1.27 (s, 3H), 0.80–0.74 (m, 2H), 0.56–0.50 (m, 2H). LC–MS m/z 422.3 [M + H]⁺.

1-Methyl-N-(1-methylcyclopropyl)-3-[(5-methyl-1,3,4-thiadiazol-2-yl)methyl]-2,4-dioxo-quinazoline-6-sulfonamide (27aa)

Prepared by General method A (using the alkyl chloride) to afford a white powder, 34%. ¹H NMR (300 MHz, DMSO-*d*₆) δ = 8.43 (d, J =2.3 Hz, 1H), 8.23 (s, 1H), 8.12 (dd, J =2.2, 8.9 Hz, 1H), 7.70 (d, J =8.9 Hz, 1H), 5.50 (s, 2H), 3.58 (s, 3H), 2.68 (s, 3H), 1.08 (s, 3H), 0.64–0.56 (m, 2H), 0.44–0.37 (m, 2H). LC–MS m/z 422.1 [M + H]⁺.

3-(1H-Imidazol-4-ylmethyl)-1-methyl-N-(1-methylcyclopropyl)-2,4-dioxo-quinazoline-6-sulfonamide (27ab)

Prepared by General method B to afford a white powder, 5%. ¹H NMR (300 MHz, DMSO-*d*₆) δ = 8.42 (d, J =2.3 Hz, 1H), 8.26 (s, 1H), 8.09 (dd, J =2.3, 8.9 Hz, 1H), 7.66 (d, J =8.9 Hz, 1H), 7.48 (d, J =0.9 Hz, 1H), 6.95 (s, 1H), 5.07 (s, 2H), 3.56 (s, 3H), 1.07 (s, 3H), 0.62–0.55 (m, 2H), 0.42–0.36 (m, 2H). LC–MS m/z 390.1 [M + H]⁺. LC-MS purity, 85-90%.

1-Methyl-N-(1-methylcyclopropyl)-3-[(3-methylimidazol-4-yl)methyl]-2,4-dioxo-quinazoline-6-sulfonamide (27ac)

1
2
3 Prepared by General method B to afford a white powder, 23%. ¹H NMR (300 MHz, CDCl₃) δ = 8.73
4 (d, *J*=2.3 Hz, 1H), 8.21–8.15 (m, 1H), 7.43 (s, 1H), 7.34–7.30 (m, 2H), 5.27 (s, 2H), 5.00 (s, 1H), 3.87
5 (s, 3H), 3.66 (s, 3H), 1.26 (s, 3H), 0.82–0.71 (m, 2H), 0.55–0.48 (m, 2H). LC–MS *m/z* 404.6 [M +
6 H]⁺.
7
8
9

10
11 **1-Methyl-N-(1-methylcyclopropyl)-3-[(4-methyl-1,2,4-triazol-3-yl)methyl]-2,4-dioxo-**
12 **quinazoline-6-sulfonamide (27ad)**
13

14
15 Prepared by General method A (using the alkyl chloride) to afford a white powder, 6%. ¹H NMR (300
16 MHz, DMSO-*d*₆) δ = 8.43 (d, *J*=2.3 Hz, 1H), 8.40 (s, 1H), 8.23 (s, 1H), 8.13 (dd, *J*=2.4, 8.9 Hz, 1H),
17 7.72 (d, *J*=8.9 Hz, 1H), 5.27 (s, 2H), 3.75 (s, 3H), 3.58 (s, 3H), 1.08 (s, 3H), 0.65–0.57 (m, 2H), 0.44–
18 0.37 (m, 2H). LC–MS *m/z* 405.2 [M + H]⁺.
19
20
21
22

23
24 **1-Methyl-N-(1-methylcyclopropyl)-3-[(1-methyltetrazol-5-yl)methyl]-2,4-dioxo-quinazoline-6-**
25 **sulfonamide (27ae)**
26

27
28 Prepared by General method A (using the alkyl chloride) to afford a white powder, 30%. ¹H NMR
29 (300 MHz, DMSO-*d*₆) δ = 8.43 (d, *J*=2.2 Hz, 1H), 8.23 (s, 1H), 8.16–8.11 (m, 1H), 7.72 (d, *J*=8.9 Hz,
30 1H), 5.46 (s, 2H), 4.17 (s, 3H), 3.58 (s, 3H), 1.08 (s, 3H), 0.64–0.58 (m, 2H), 0.43–0.38 (m, 2H).
31 LC–MS *m/z* 406.1 [M + H]⁺.
32
33
34
35

36
37 **1-Methyl-N-(1-methylcyclopropyl)-3-[(3-methyl-1H-pyrazol-5-yl)methyl]-2,4-dioxo-quinazoline-**
38 **6-sulfonamide (27af)**
39

40
41 Prepared by General method B to afford a white powder, 11%. ¹H NMR (300 MHz, CDCl₃) δ = 8.70
42 (d, *J*=2.3 Hz, 1H), 8.14 (dd, *J*=2.3, 8.8 Hz, 1H), 7.30 (d, *J*=9.1 Hz, 1H), 6.15 (s, 1H), 5.84 (s, 1H),
43 5.26 (s, 2H), 4.68 (br s, 1H), 3.65 (s, 3H), 2.25 (s, 3H), 1.24 (s, 3H), 0.80–0.72 (m, 2H), 0.51–0.44 (m,
44 2H). LC–MS *m/z* 402.2 [M – H][–].
45
46
47
48

49
50 **1-Methyl-N-(1-methylcyclopropyl)-3-[(2-methylpyrazol-3-yl)methyl]-2,4-dioxo-quinazoline-6-**
51 **sulfonamide (27ag)**
52

53
54 Prepared by General method B to afford a white powder, 32%. ¹H NMR (400 MHz, CDCl₃) δ = 8.71
55 (d, *J*=2.3 Hz, 1H), 8.15 (dd, *J*=2.3, 8.7 Hz, 1H), 7.38 (d, *J*=1.8 Hz, 1H), 7.30 (d, *J*=8.7 Hz, 1H), 6.38
56 (d, *J*=1.8 Hz, 1H), 5.29 (s, 2H), 4.93 (s, 1H), 4.08 (s, 3H), 3.64 (s, 3H), 1.23 (s, 3H), 0.79–0.73 (m,
57 2H), 0.55–0.48 (m, 2H). LC–MS *m/z* 404.0 [M + H]⁺.
58
59
60

1
2
3 **1-Methyl-N-(1-methylcyclopropyl)-3-[(1-methylpyrazol-3-yl)methyl]-2,4-dioxo-quinazoline-6-**
4
5 **sulfonamide (27ah)**

6
7 Prepared by General method B to afford a white powder, 11%. ¹H NMR (300 MHz, CDCl₃) δ = 8.75
8 (d, *J*=2.3 Hz, 1H), 8.16 (dd, *J*=2.3, 8.8 Hz, 1H), 7.31 (d, *J*=8.9 Hz, 1H), 7.28–7.26 (m, 1H), 6.29 (d,
9 *J*=2.2 Hz, 1H), 5.32 (s, 2H), 4.95 (s, 1H), 3.86 (s, 3H), 3.67 (s, 3H), 1.26 (s, 3H), 0.81–0.75 (m, 2H),
10 0.55–0.49 (m, 2H). LC–MS *m/z* 404.6 [M + H]⁺.

11
12
13
14
15 **1-Methyl-N-(1-methylcyclopropyl)-3-[(1-methylpyrazol-4-yl)methyl]-2,4-dioxo-quinazoline-6-**
16
17 **sulfonamide (27ai)**

18
19 Prepared by General method B to afford a white powder, 9%. ¹H NMR (300 MHz, DMSO-*d*₆) δ =
20 8.42 (d, *J*=2.3 Hz, 1H), 8.19 (br s, 1H), 8.07 (dd, *J*=2.3, 8.8 Hz, 1H), 7.67 (d, *J*=5.4 Hz, 1H), 7.64 (d,
21 *J*=8.9 Hz, 1H), 7.39 (s, 1H), 4.95 (s, 2H), 3.76 (s, 3H), 3.55 (s, 3H), 1.07 (s, 3H), 0.65–0.52 (m, 2H),
22 0.45–0.33 (m, 2H). LC–MS *m/z* 404.2 [M + H]⁺.

23
24
25
26
27 **1-Methyl-N-(1-methylcyclopropyl)-2,4-dioxo-3-(1H-pyrazol-4-ylmethyl)quinazoline-6-**
28
29 **sulfonamide (27aj)**

30
31 Prepared by General method B to afford a white powder, 29%. ¹H NMR (300 MHz, CDCl₃) δ = 8.72
32 (d, *J*=2.4 Hz, 1H), 8.15 (dd, *J*=2.4, 8.9 Hz, 1H), 7.78 (s, 2H), 7.29 (d, *J*=8.9 Hz, 1H), 5.18 (s, 2H),
33 4.97 (s, 1H), 3.65 (s, 3H), 2.18 (s, 1H), 1.24 (s, 3H), 0.80–0.74 (m, 2H), 0.54–0.48 (m, 2H). LC–MS
34 *m/z* 390.4 [M + H]⁺.

35
36
37
38
39 **3-[(1-Ethylpyrazol-4-yl)methyl]-1-methyl-N-(1-methylcyclopropyl)-2,4-dioxo-quinazoline-6-**
40
41 **sulfonamide (27ak)**

42
43 Prepared by General method B to afford a white powder, 42%. ¹H NMR (300 MHz, CDCl₃) δ = 8.73
44 (d, *J*=2.3 Hz, 1H), 8.15 (dd, *J*=2.3, 8.9 Hz, 1H), 7.65 (s, 1H), 7.60 (s, 1H), 7.35–7.30 (m, 1H), 5.13 (s,
45 2H), 5.06 (br s, 1H), 4.13 (q, *J*=7.3 Hz, 2H), 3.65 (s, 3H), 1.47 (t, *J*=7.3 Hz, 3H), 1.25 (s, 3H), 0.82–
46 0.71 (m, 2H), 0.55–0.49 (m, 2H). LC–MS *m/z* 418.4 [M + H]⁺.

47
48
49
50
51
52
53 **3-[[1-(Cyanomethyl)pyrazol-4-yl]methyl]-1-methyl-N-(1-methylcyclopropyl)-2,4-dioxo-**
54
55 **quinazoline-6-sulfonamide (27al)**

56
57 A solution of **27ak** (45 mg, 0.12 mmol) and sodium hydride (60% w/w in mineral oil, 10 mg, 0.25
58 mmol) in DMF was stirred at ambient temperature for 30 min. Bromoacetonitrile (8.9 μL, 0.13 mmol)
59
60

1
2
3 was then added to the reaction mixture, and the reaction mixture stirred at ambient temperature for 1
4
5 h. Water (1 mL) was carefully added to the reaction mixture followed by 2 M HCl (1 mL). DCM (10
6
7 mL) was added and the mixture was stirred vigorously for 10 min and then passed through a
8
9 hydrophobic frit. The aqueous layer was washed with DCM (5 mL) and the combined organic phase
10
11 concentrated to dryness in vacuo. The crude product was purified by prep. HPLC to yield the desired
12
13 product (6 mg, 12%) as a white powder. ¹H NMR (300 MHz, DMSO-d₆) δ = 8.42 (d, *J*=2.3 Hz, 1H),
14
15 8.08 (dd, *J*=2.3, 8.9 Hz, 1H), 7.87 (s, 1H), 7.65 (d, *J*=8.9 Hz, 1H), 7.57 (s, 1H), 5.42 (s, 2H), 4.98 (s,
16
17 2H), 3.55 (s, 3H), 1.07 (s, 3H), 0.63–0.54 (m, 2H), 0.43–0.33 (m, 2H). LC–MS *m/z* 429.3 [M + H]⁺.

20 **3-(Isoxazol-5-ylmethyl)-1-methyl-N-(1-methylcyclopropyl)-2,4-dioxo-quinazoline-6-sulfonamide**
21
22 **(27am)**

23
24 Prepared by General method A (using the alkyl bromide) to afford a white powder, 29%. ¹H NMR
25
26 (300 MHz, DMSO-d₆) δ = 8.50 (d, *J*=1.8 Hz, 1H), 8.42 (d, *J*=2.3 Hz, 1H), 8.23 (s, 1H), 8.12 (dd,
27
28 *J*=2.3, 8.9 Hz, 1H), 7.70 (d, *J*=8.9 Hz, 1H), 6.49 (d, *J*=1.8 Hz, 1H), 5.29 (s, 2H), 3.57 (s, 3H), 1.08 (s,
29
30 3H), 0.64–0.56 (m, 2H), 0.43–0.37 (m, 2H). LC–MS *m/z* 391.2 [M + H]⁺.

32 **1-Methyl-N-(1-methylcyclopropyl)-3-[(3-methylisoxazol-5-yl)methyl]-2,4-dioxo-quinazoline-6-**
33
34 **sulfonamide (27an)**

35
36 Prepared by General method B to afford a white powder, 38%. ¹H NMR (300 MHz, CDCl₃) δ = 8.73
37
38 (d, *J*=2.3 Hz, 1H), 8.19 (dd, *J*=2.3, 8.8 Hz, 1H), 7.33 (d, *J*=8.9 Hz, 1H), 6.16 (s, 1H), 5.39 (s, 2H),
39
40 4.95 (s, 1H), 3.67 (s, 3H), 2.27 (s, 3H), 1.26 (s, 3H), 0.80–0.75 (m, 2H), 0.55–0.50 (m, 2H). LC–MS
41
42 *m/z* 405.2 [M + H]⁺.

44
45 **1-Methyl-N-(1-methylcyclopropyl)-3-[(5-methylisoxazol-3-yl)methyl]-2,4-dioxo-quinazoline-6-**
46
47 **sulfonamide (27ao)**

48
49 Prepared by General method A (using the alkyl bromide) to afford a white powder, 18%. ¹H NMR
50
51 (400 MHz, CDCl₃) δ = 8.71 (d, *J*=2.3 Hz, 1H), 8.16 (dd, *J*=2.3, 8.7 Hz, 1H), 7.34–7.27 (m, 1H), 6.02
52
53 (s, 1H), 5.31 (s, 2H), 4.94 (s, 1H), 3.65 (s, 3H), 2.37 (s, 3H), 1.24 (s, 3H), 0.79–0.72 (m, 2H), 0.53–
54
55 0.47 (m, 2H). LC–MS *m/z* 446.0 [M + H]⁺.

56
57
58 **1-Methyl-N-(1-methylcyclopropyl)-3-[(5-methylisoxazol-4-yl)methyl]-2,4-dioxo-quinazoline-6-**
59
60 **sulfonamide (27ap)**

1
2
3 Prepared by General method B to afford a white powder, 23%. ¹H NMR (300 MHz, DMSO-d₆) δ =
4
5 8.43 (d, *J*=2.3 Hz, 1H), 8.38 (s, 1H), 8.08 (dd, *J*=2.3, 8.9 Hz, 1H), 7.65 (d, *J*=8.9 Hz, 1H), 4.93 (s,
6
7 2H), 3.55 (s, 3H), 2.51 (s, 3H), 1.07 (s, 3H), 0.64–0.55 (m, 2H), 0.43–0.35 (m, 2H). LC–MS *m/z*
8
9 405.1 [M + H]⁺.

10
11
12 **3-[(3,5-Dimethylisoxazol-4-yl)methyl]-1-methyl-N-(1-methylcyclopropyl)-2,4-dioxo-quinazoline-**
13
14 **6-sulfonamide (27aq)**

15
16 Prepared by General method A (using the alkyl bromide) to afford a white powder, 30%. ¹H NMR
17
18 (300 MHz, DMSO-d₆) δ = 8.43 (d, *J*=2.3 Hz, 1H), 8.07 (dd, *J*=2.4, 8.9 Hz, 1H), 7.64 (d, *J*=8.9 Hz,
19
20 1H), 4.91 (s, 2H), 3.54 (s, 3H), 2.42 (s, 3H), 2.21 (s, 3H), 1.07 (s, 3H), 0.62–0.56 (m, 2H), 0.41–0.35
21
22 (m, 2H). LC–MS *m/z* 417.0 [M – H]⁻.

23
24 **1-Methyl-N-(1-methylcyclopropyl)-3-[(3-methyl-1,2,4-oxadiazol-5-yl)methyl]-2,4-dioxo-**
25
26 **quinazoline-6-sulfonamide (27ar)**

27
28 Prepared by General method B to afford a white powder, 29%. ¹H NMR (300 MHz, DMSO-d₆) δ =
29
30 8.43 (d, *J*=2.3 Hz, 1H), 8.25 (s, 1H), 8.15 (dd, *J*=2.3, 8.9 Hz, 1H), 7.73 (d, *J*=8.9 Hz, 1H), 5.41 (s,
31
32 2H), 3.66–3.52 (m, 3H), 2.30 (s, 3H), 1.09 (s, 3H), 0.65–0.56 (m, 2H), 0.45–0.37 (m, 2H). LC–MS
33
34 *m/z* 406.1 [M + H]⁺.

35
36
37 **1-Methyl-N-(1-methylcyclopropyl)-3-[(5-methyl-1,3,4-oxadiazol-2-yl)methyl]-2,4-dioxo-**
38
39 **quinazoline-6-sulfonamide (27as)**

40
41 Prepared by General method B to afford a white powder, 10%. ¹H NMR (300 MHz, DMSO-d₆) δ =
42
43 8.33 (d, *J*=2.3 Hz, 1H), 8.14 (br s, 1H), 8.04 (dd, *J*=2.3, 8.9 Hz, 1H), 7.62 (d, *J*=8.9 Hz, 1H), 5.24 (s,
44
45 2H), 3.48 (s, 3H), 2.37 (s, 3H), 0.98 (s, 3H), 0.54–0.47 (m, 2H), 0.34–0.27 (m, 2H). LC–MS *m/z*
46
47 406.2 [M + H]⁺.

48
49
50 **1-Methyl-N-(1-methylcyclopropyl)-3-[(4-methyl-1,2,5-oxadiazol-3-yl)methyl]-2,4-dioxo-**
51
52 **quinazoline-6-sulfonamide (27at)**

53
54 Prepared by General method B to afford a white powder, 12%. ¹H NMR (300 MHz, DMSO-d₆) δ =
55
56 8.43 (d, *J*=2.2 Hz, 1H), 8.22 (s, 1H), 8.15–8.09 (m, 1H), 7.70 (d, *J*=8.9 Hz, 1H), 5.31 (s, 2H), 3.57 (s,
57
58 3H), 2.46 (s, 3H), 1.08 (s, 3H), 0.64–0.57 (m, 2H), 0.43–0.38 (m, 2H). LC–MS *m/z* 406.1 [M + H]⁺.

59
60 **2,4-Dioxo-1H-3,1-benzoxazine-6-sulfonyl chloride (30)**

1
2
3 Isatoic acid anhydride **29** (5.0 g, 28 mmol) was added portionwise to stirring chlorosulfonic acid (9
4 mL, 140 mmol) at RT. A slight exotherm was observed during the addition, and the mixture turned
5 very dark brown immediately. The mixture was heated at 50 °C with a base scrubber for 4 h. The
6 reaction mixture was allowed to cool to RT and then added dropwise to stirring ice/water. The
7 precipitated solid was filtered and oven-dried to give **30** (5.8 g, 79%) as a brown solid. ¹H NMR (300
8 MHz, DMSO-d₆) δ = 11.82 (s, 1H), 8.06 (d, *J*=2.0 Hz, 1H), 7.91 (dd, *J*=2.0, 8.5 Hz, 1H), 7.11 (d,
9 *J*=8.5 Hz, 1H).

18 **2-Amino-5-[(1-methylcyclopropyl)sulfamoyl]-N-[(2-methylthiazol-5-yl)methyl]benzamide (31a)**

19
20 A suspension of **30** (1.0 g, 3.8 mmol) in DMF (12 mL) was treated with 1-methylcyclopropanamine
21 hydrochloride **28** (493 mg, 4.6 mmol) and cooled to -10 °C in an ice/ MeOH bath. The suspension
22 was treated dropwise with triethylamine (1.2 mL, 8.4 mmol) and the resulting solution was stirred at
23 -10 °C for 30 min. A solution of (2-methyl-1,3-thiazol-5-yl)methanamine (400 mg, 3.1 mmol) in
24 DMF (5 mL) was added dropwise to the reaction mixture, followed by triethylamine (1.1 mL, 7.6
25 mmol) and the reaction mixture was stirred at RT for 18 h. Water (25 mL) was added and the mixture
26 was extracted with EtOAc (2 × 25 mL), the organic extracts were washed with brine (25 mL),
27 dried (hydrophobic frit) and concentrated. The crude product was purified by automated column
28 chromatography, eluting with 0–5% MeOH in DCM to afford **31a** (286 mg, 20%) as an off-white
29 solid. ¹H NMR (300 MHz, CDCl₃) δ = 7.90 (d, *J*=2.2 Hz, 1H), 7.62 (dd, *J*=2.2, 8.8 Hz, 1H), 7.53 (br s,
30 1H), 7.12 (t, *J*=6.0 Hz, 1H), 6.70 (d, *J*=8.8 Hz, 1H), 6.24 (br s, 2H), 5.11 (s, 1H), 4.71 (d, *J*=5.7 Hz,
31 2H), 3.08 (s, 1H), 2.68 (s, 3H), 1.18 (s, 3H), 0.80–0.72 (m, 2H), 0.47–0.42 (m, 2H).

45 **2-Amino-5-[(1-methylcyclopropyl)sulfamoyl]-N-[(1-methylpyrazol-4-yl)methyl]benzamide (31b)**

46
47 Prepared in the same manner as **31a** using (1-methyl-1H-pyrazol-4-yl)methylamine, to afford the
48 desired product as a white powder, 67%. ¹H NMR (300 MHz, DMSO-d₆) δ = 8.83 (t, *J*=5.7 Hz, 1H),
49 7.87 (d, *J*=2.3 Hz, 1H), 7.58 (s, 1H), 7.55 (s, 1H), 7.46 (dd, *J*=2.2, 8.7 Hz, 1H), 7.35 (s, 1H), 7.09 (br
50 s, 2H), 6.79 (d, *J*=8.8 Hz, 1H), 4.22 (d, *J*=5.7 Hz, 2H), 3.78 (s, 3H), 1.04 (s, 3H), 0.65–0.51 (m, 2H),
51 0.36–0.29 (m, 2H).

58 **2-Amino-5-[(1-methylcyclopropyl)sulfamoyl]-N-[(3-methylisoxazol-5-yl)methyl]benzamide (31c)**

1
2
3 Prepared in the same manner as **32a** using (3-methylisoxazol-5-ylmethyl)amine, to afford the desired
4 product as an off-white powder, 42%. ¹H NMR (300 MHz, CDCl₃) δ = 7.95 (d, *J*=2.1 Hz, 1H), 7.65
5 (dd, *J*=2.2, 9.1 Hz, 1H), 6.99 (br s, 1H), 6.72 (d, *J*=8.6 Hz, 1H), 6.10 (s, 1H), 4.68 (d, *J*=5.7 Hz, 2H),
6 2.29 (s, 3H), 1.22 (s, 3H), 0.79–0.75 (m, 2H), 0.49–0.44 (m, 2H).
7
8
9

10 11 **2-Amino-N-(cyanomethyl)-5-[(1-methylcyclopropyl)sulfamoyl]benzamide (31d)**

12 Prepared in the same manner as **32a**, using aminoacetonitrile bisulfate plus an extra equivalent of
13 trimethylamine, to afford the desired product as a white powder, 35%. ¹H NMR (300 MHz, CDCl₃) δ
14 = 9.18 (t, *J*=5.4 Hz, 1H), 7.94 (d, *J*=2.1 Hz, 1H), 7.64 (s, 1H), 7.51 (dd, *J*=2.1, 8.8 Hz, 1H), 7.24 (s,
15 2H), 6.85 (d, *J*=8.9 Hz, 1H), 4.25 (d, *J*=5.5 Hz, 2H), 1.06 (s, 3H), 0.62–0.56 (m, 2H), 0.38–0.30 (m,
16 2H).
17
18
19
20
21
22
23

24 **N-(1-methylcyclopropyl)-3-[(2-methylthiazol-5-yl)methyl]-2,4-dioxo-1H-quinazoline-6-** 25 **sulfonamide (32a)**

26 A solution of **31a** (283 mg, 0.74 mmol) in THF (8 mL) was cooled in an ice bath (reaction mixture
27 fitted with NaOH scrubber) and treated with triphosgene (110 mg, 0.37 mmol) which caused
28 precipitation of a white solid. The reaction mixture was stirred at RT for 18 h, then quenched with sat.
29 aq. K₂CO₃ (10 mL) and stirred for 3 h. The mixture was extracted with EtOAc (3 × 20 mL) and the
30 organic extracts washed with brine, dried (hydrophobic frit) and concentrated to give **17a** (275 mg,
31 91%) as an off-white solid. ¹H NMR (300 MHz, DMSO-*d*₆) δ = 11.98 (s, 1H), 8.32 (d, *J*=2.2 Hz, 1H),
32 8.14 (s, 1H), 8.01 (dd, *J*=2.2, 8.6 Hz, 1H), 7.61 (s, 1H), 7.33 (d, *J*=8.6 Hz, 1H), 5.19 (s, 2H), 1.06 (s,
33 3H), 0.65–0.51 (m, 2H), 0.45–0.31 (m, 2H).
34
35
36
37
38
39
40
41
42
43
44

45 **N-(1-methylcyclopropyl)-3-[(1-methylpyrazol-4-yl)methyl]-2,4-dioxo-1H-quinazoline-6-** 46 **sulfonamide (32b)**

47 Prepared from **31b** in the same manner as **32a**, with an ether trituration, to afford the desired product
48 as a pale yellow solid, 78%. ¹H NMR (400 MHz, CD₃OD) δ = 8.51 (d, *J*=2.0 Hz, 1H), 8.05–8.03 (m,
49 1H), 7.68 (s, 1H), 7.54 (s, 1H), 7.29 (d, *J*=8.8 Hz, 1H), 5.05 (s, 2H), 3.84 (s, 3H), 1.16 (s, 3H), 0.71–
50 0.67 (m, 2H), 0.43–0.46 (m, 2H).
51
52
53
54
55
56
57

58 **N-(1-Methylcyclopropyl)-3-[(3-methylisoxazol-5-yl)methyl]-2,4-dioxo-1H-quinazoline-6-** 59 **sulfonamide (32c)**

Prepared from **31c** in the same manner as **32a** to afford the desired product as a white solid, 97%. ¹H NMR (400 MHz, DMSO-d₆): δ 12.03 (s, 1H), 8.31 (d, *J*=8.3 Hz, 1H), 8.17 (s, 1H), 8.04–8.02 (m, 1H), 7.36 (d, *J*=8.8 Hz, 1H), 6.33 (s, 1H), 5.16 (s, 2H), 2.17 (s, 3H), 1.07 (s, 3H), 0.58–0.56 (m, 2H), 0.40–0.37 (m, 2H).

3-(Cyanomethyl)-N-(1-methylcyclopropyl)-2,4-dioxo-1H-quinazoline-6-sulfonamide (32d)

Prepared from **31d** in the same manner as **32a**, to afford the desired product as an off-white solid, 84%. ¹H NMR (300 MHz, DMSO-d₆) δ = 12.13 (s, 1H), 8.33 (d, *J*=2.2 Hz, 1H), 8.17 (s, 1H), 8.04 (dd, *J*=2.2, 8.6 Hz, 1H), 7.36 (d, *J*=8.7 Hz, 1H), 4.91 (s, 2H), 1.07 (s, 3H), 0.68–0.51 (m, 2H), 0.42–0.35 (m, 2H).

Preparation of Compounds 33–36

General method C:

A mixture of 3-substituted quinazolinedione (**32a**, **32b**, **32c** or **32d**; 0.21 mmol), K₂CO₃ (34 mg, 0.25 mmol) and alkyl halide, mesylate or tosylate (if the alkyl chloride, mesylate or tosylate was used, NaI (5 mg, 0.030 mmol) was also added) in DMF (2 mL) was heated to 80 °C under microwave irradiation for 20 min. The resulting mixture was diluted with DCM (5 mL) and water (2 mL), stirred vigorously for 10 min, then passed through a hydrophobic frit. The aqueous layer was re-extracted with DCM in a similar manner, and the combined organic extracts were concentrated and purified by prep. HPLC to afford the N1-alkylated product.

1-Ethyl-N-(1-methylcyclopropyl)-3-[(1-methylpyrazol-4-yl)methyl]-2,4-dioxo-quinazoline-6-sulfonamide (33a)

Prepared by General method C (using the alkyl iodide) using **32b** to afford a white powder, 38%. ¹H NMR (300 MHz, DMSO-d₆) δ = 8.43 (d, *J*=2.3 Hz, 1H), 8.20 (s, 1H), 8.06 (dd, *J*=2.3, 8.9 Hz, 1H), 7.70 (d, *J*=9.0 Hz, 1H), 7.67 (s, 1H), 7.39 (s, 1H), 4.95 (s, 2H), 4.17 (q, *J*=6.9 Hz, 2H), 3.76 (s, 3H), 1.23 (t, *J*=7.0 Hz, 3H), 1.07 (s, 3H), 0.62–0.55 (m, 2H), 0.44–0.35 (m, 2H); ¹³C NMR (75 MHz, CDCl₃) δ = 160.3, 149.9, 142.3, 139.8, 136.7, 133.3, 128.9, 124.6, 116.5, 115.9, 114.1, 39.4, 38.9, 35.5, 31.8, 24.6, 14.1, 12.6. HRMS (ESI) *m/z* [M + Na]⁺ calcd for C₁₉H₂₃N₅O₄SNa: 440.1363. Found: 440.1350.

1
2
3 **N-(1-Methylcyclopropyl)-3-[(1-methylpyrazol-4-yl)methyl]-2,4-dioxo-1-prop-2-ynyl-**
4
5 **quinazoline-6-sulfonamide (33b)**
6

7 Prepared by General method B, using **32b** as a starting material, to afford a white powder, 16%. ¹H
8 NMR (300 MHz, DMSO-d₆) δ = 8.44 (d, *J*=2.3 Hz, 1H), 8.24 (br s, 1H), 8.14 (dd, *J*=2.3, 8.8 Hz, 1H),
9
10 7.71 (s, 1H), 7.69 (s, *J*=7.9 Hz, 1H), 7.40 (s, 1H), 4.99 (d, *J*=2.2 Hz, 2H), 4.95 (s, 2H), 3.76 (s, 3H),
11
12 3.40 (s, 1H), 1.08 (s, 3H), 0.65–0.55 (m, 2H), 0.45–0.35 (m, 2H); HRMS (ESI) *m/z* [M + H]⁺ calcd for
13
14 C₂₀H₂₂N₅O₄S: 428.1387. Found: 428.1378.
15
16

17
18 **1-(Cyclopropylmethyl)-N-(1-methylcyclopropyl)-3-[(1-methylpyrazol-4-yl)methyl]-2,4-dioxo-**
19
20 **quinazoline-6-sulfonamide (33c)**
21

22 Prepared by General method B, using **32b** as a starting material, to afford a white powder, 17%. ¹H
23 NMR (300MHz, DMSO-d₆) δ = 8.44 (d, *J*=2.4 Hz, 1H), 8.38 (s, 1H), 8.07 (dd, *J*=2.3, 8.9 Hz, 1H),
24
25 7.80 (d, *J*=8.9 Hz, 1H), 7.68 (s, 1H), 7.39 (s, 1H), 4.96 (s, 2H), 4.08 (d, *J*=6.9 Hz, 2H), 3.76 (s, 3H),
26
27 1.24–1.19 (m, 1H), 1.08 (s, 3H), 0.63–0.56 (m, 2H), 0.52–0.44 (m, 4H), 0.42–0.37 (m, 2H); HRMS
28
29 (ESI) *m/z* [M + H]⁺ calcd for C₂₁H₂₆N₅O₄S: 444.1700. Found: 444.1687.
30
31

32
33 **N-(1-Methylcyclopropyl)-3-[(1-methylpyrazol-4-yl)methyl]-1-(oxetan-3-ylmethyl)-2,4-dioxo-**
34
35 **quinazoline-6-sulfonamide (33d)**
36

37 Prepared by General method C (using the alkyl tosylate), using **32b** as a starting material, to afford a
38 white powder, 43%. ¹H NMR (300 MHz, DMSO-d₆) δ = 8.41 (d, *J*=2.3 Hz, 1H), 8.37 (s, 1H), 8.02 (d,
39
40 *J*=8.9 Hz, 1H), 7.73–7.66 (m, 2H), 7.39 (s, 1H), 4.95 (s, 2H), 4.61 (dd, *J*=6.2, 7.8 Hz, 2H), 4.52–4.44
41
42 (m, 4H), 3.76 (s, 3H), 3.44–3.39 (m, 1H), 1.07 (s, 3H), 0.59 (s, 2H), 0.42–0.37 (m, 2H); ¹³C NMR (75
43
44 MHz, CDCl₃) δ = 160.0, 150.7, 142.4, 140.2, 137.2, 133.3, 131.2, 129.1, 116.2, 116.0, 114.0, 74.7,
45
46 46.1, 38.9, 35.8, 33.9, 31.8, 24.6, 14.1. HRMS (ESI) *m/z* [M + H]⁺ calcd for C₂₁H₂₆N₅O₅S: 444.1649.
47
48 Found: 444.1637.
49
50

51
52 **1-[(2,5-Dimethylpyrazol-3-yl)methyl]-N-(1-methylcyclopropyl)-3-[(1-methylpyrazol-4-**
53
54 **yl)methyl]-2,4-dioxo-quinazoline-6-sulfonamide (33e)**
55

56 Prepared by General method B, using **32b** as a starting material, to afford a white powder, 19%. ¹H
57 NMR (300MHz, DMSO-d₆) δ = 8.44 (d, *J*=2.3 Hz, 1H), 8.21 (s, 1H), 8.02 (dd, *J*=2.4, 8.9 Hz, 1H),
58
59 7.68 (s, 1H), 7.56 (d, *J*=8.9 Hz, 1H), 7.39 (s, 1H), 5.73 (s, 1H), 5.37 (s, 2H), 4.97 (s, 2H), 3.82 (s, 3H),
60

3.76 (s, 3H), 1.99 (s, 3H), 1.07 (s, 3H), 0.62 - 0.55 (m, 2H), 0.42 - 0.35 (m, 2H); ^{13}C NMR (75 MHz, CDCl_3) δ = 159.9, 150.2, 147.7, 142.0, 140.1, 137.6, 137.0, 133.3, 131.2, 128.8, 116.1, 116.0, 114.8, 105.4, 39.5, 38.9, 36.6, 36.0, 31.8, 24.6, 14.1, 13.2. HRMS (ESI) m/z $[\text{M} + \text{H}]^+$ calcd for $\text{C}_{23}\text{H}_{28}\text{N}_7\text{O}_4\text{S}$: 498.1918. Found: 498.1905.

1-[(2,4-Dimethylthiazol-5-yl)methyl]-N-(1-methylcyclopropyl)-3-[(1-methylpyrazol-4-yl)methyl]-2,4-dioxo-quinazoline-6-sulfonamide (33f)

Prepared by General method B, using **32b** as a starting material, to afford a white powder, 21%. ^1H NMR (300 MHz, CDCl_3) δ = 8.72 (d, $J=2.3$ Hz, 1H), 8.12 (dd, $J=2.3, 8.8$ Hz, 1H), 7.64 (s, 1H), 7.57 (s, 1H), 7.27–7.25 (m, 1H), 5.40 (s, 2H), 5.14 (s, 2H), 5.08 (s, 1H), 3.87 (s, 3H), 2.59 (s, 3H), 2.57 (s, 3H), 1.26 (s, 3H), 0.80–0.72 (m, 2H), 0.55–0.48 (m, 2H); HRMS (ESI) m/z $[\text{M} + \text{H}]^+$ calcd for $\text{C}_{23}\text{H}_{27}\text{N}_6\text{O}_4\text{S}_2$: 515.1530. Found: 515.1519. LC-MS purity, 90-95%.

N-(1-Methylcyclopropyl)-3-[(2-methylthiazol-5-yl)methyl]-2,4-dioxo-1-prop-2-ynyl-quinazoline-6-sulfonamide (34b)

Prepared by General method B, using **32a** as a starting material, to afford a white powder, 75%. ^1H NMR (300 MHz, DMSO-d_6) δ = 8.44 (d, $J=2.2$ Hz, 1H), 8.15 (dd, $J=2.3, 8.9$ Hz, 1H), 7.71 (d, $J=8.9$ Hz, 1H), 7.64 (s, 1H), 5.25 (s, 2H), 5.00 (d, $J=2.4$ Hz, 2H), 3.44–3.39 (m, 1H), 2.57 (s, 3H), 1.08 (s, 3H), 0.65–0.54 (m, 2H), 0.48–0.32 (m, 2H); ^{13}C NMR (75 MHz, DMSO-d_6) δ = 166.2, 159.8, 149.27, 142.5, 141.2, 137.6, 132.9, 131.8, 126.6, 116.2, 115.0, 77.8, 75.9, 37.2, 33.6, 30.9, 23.9, 18.7, 13.0. HRMS (ESI) m/z $[\text{M} + \text{H}]^+$ calcd for $\text{C}_{20}\text{H}_{21}\text{N}_4\text{O}_4\text{S}_2$: 445.0999. Found: 445.0987.

1-(Cyclopropylmethyl)-N-(1-methylcyclopropyl)-3-[(2-methylthiazol-5-yl)methyl]-2,4-dioxo-quinazoline-6-sulfonamide (34c)

Prepared by General method B, using **32a** as a starting material, to afford a white powder, 34%. ^1H NMR (300 MHz, DMSO-d_6) δ = 8.43 (d, $J=2.3$ Hz, 1H), 8.08 (dd, $J=2.3, 8.9$ Hz, 1H), 7.81 (d, $J=8.9$ Hz, 1H), 7.62 (s, 1H), 5.25 (s, 2H), 4.09 (d, $J=6.9$ Hz, 2H), 2.57 (s, 3H), 1.22 (br s, 1H), 1.07 (s, 3H), 0.62–0.56 (m, 2H), 0.53–0.43 (m, 4H), 0.43–0.37 (m, 2H); ^{13}C NMR (75 MHz, CDCl_3) δ = 160.1, 150.4, 142.7, 137.0, 133.5, 131.8, 128.9, 128.5, 115.6, 114.8, 108.9, 48.4, 37.2, 31.8, 24.7, 18.9, 14.1, 9.4, 4.2. HRMS (ESI) m/z $[\text{M} + \text{H}]^+$ calcd for $\text{C}_{21}\text{H}_{25}\text{N}_4\text{O}_4\text{S}_2$: 461.1312. Found: 461.1299.

1
2
3 **1-[(2,5-dimethylpyrazol-3-yl)methyl]-N-(1-methylcyclopropyl)-3-[(2-methylthiazol-5-yl)methyl]-**
4
5 **2,4-dioxo-quinazoline-6-sulfonamide (34e)**
6

7 Prepared by General method B, using **32a** as a starting material, to afford a white powder, 43%. ¹H
8 NMR (300 MHz, DMSO-d₆) δ = 8.44 (d, *J*=2.3 Hz, 1H), 8.21 (br s, 1H), 8.03 (dd, *J*=2.3, 8.9 Hz, 1H),
9
10 7.64 (s, 1H), 7.57 (d, *J*=8.9 Hz, 1H), 5.75 (s, 1H), 5.38 (s, 2H), 5.27 (s, 2H), 3.82 (s, 3H), 2.58 (s, 3H),
11
12 1.99 (s, 3H), 1.07 (s, 3H), 0.58 (s, 2H), 0.39 (d, *J*=2.0 Hz, 2H); ¹³C NMR (75 MHz, CDCl₃) δ = 159.8,
13
14 150.1, 147.8, 143.1, 142.0, 137.8, 136.4, 133.5, 131.2, 128.8, 123.9, 115.8, 115.0, 105.4, 39.6, 37.4,
15
16 36.7, 31.8, 24.6, 19.1, 14.1, 13.3. HRMS (ESI) *m/z* [M + H]⁺ calcd for C₂₃H₂₇N₆O₄S₂: 515.1530.
17
18 Found: 515.1518.
19

20
21
22 **1-[(2,4-Dimethylthiazol-5-yl)methyl]-N-(1-methylcyclopropyl)-3-[(2-methylthiazol-5-yl)methyl]-**
23
24 **2,4-dioxo-quinazoline-6-sulfonamide (34f)**
25

26 Prepared by General method B, using **32a** as a starting material, to afford an off-white powder, 27%.
27
28 ¹H NMR (300MHz, DMSO-d₆) δ = 8.44 (d, *J*=1.9 Hz, 1H), 8.23 (s, 1H), 8.12 (dd, *J*=1.8, 8.9 Hz, 1H),
29
30 7.67 (s, 1H), 7.64 (s, 1H), 5.46 (s, 2H), 5.26 (s, 2H), 2.58 (s, 3H), 2.49 (s, 3H), 2.47 (s, 3H), 1.07 (s,
31
32 3H), 0.58 (s, 2H), 0.44–0.36 (m, 2H); ¹³C NMR (75 MHz, CDCl₃) δ = 167.6, 165.3, 159.8, 150.0,
33
34 143.0, 141.7, 137.8, 133.6, 131.2, 129.1, 124.7, 124.4, 115.8, 114.4, 40.8, 37.3, 31.9, 24.6, 23.4, 19.1,
35
36 15.4, 14.1. HRMS (ESI) *m/z* [M + H]⁺ calcd for C₂₃H₂₆N₅O₄S₃ : 532.1141. Found: 532.1129.
37

38
39 **1-Ethyl-N-(1-methylcyclopropyl)-3-[(3-methylisoxazol-5-yl)methyl]-2,4-dioxo-quinazoline-6-**
40
41 **sulfonamide (35a)**
42

43 Prepared by General method C (using the alkyl iodide), using **32c** as a starting material, to afford a
44
45 white powder, 26%. ¹H NMR (300 MHz, DMSO-d₆) δ = 8.43 (d, *J*=2.3 Hz, 1H), 8.23 (br s, 1H), 8.10
46
47 (dd, *J*=2.2, 8.9 Hz, 1H), 7.75 (d, *J*=8.9 Hz, 1H), 6.33 (s, 1H), 5.22 (s, 2H), 4.18 (s, 2H), 2.18 (s, 3H),
48
49 1.24 (t, *J*=7.0 Hz, 3H), 1.09 (s, 3H), 0.60 (s, 2H), 0.41 (d, *J*=2.0 Hz, 2H); ¹³C NMR (75 MHz, CDCl₃)
50
51 δ = 166.3, 160.1, 160.0, 149.70, 142.3, 137.1, 133.7, 129.1, 115.6, 114.4, 104.3, 83.6, 39.7, 36.8,
52
53 31.8, 24.6, 14.1, 12.5, 11.4. HRMS (ESI) *m/z* [M + H]⁺ calcd for C₁₉H₂₃N₄O₅S: 419.1384. Found:
54
55 419.1373.
56

57
58 **N-(1-Methylcyclopropyl)-3-[(3-methylisoxazol-5-yl)methyl]-2,4-dioxo-1-prop-2-ynyl-**
59
60 **quinazoline-6-sulfonamide (35b)**

1
2
3 Prepared by General method C (using the alkyl bromide), using **32c** as a starting material, to afford a
4 white powder, 64%. ¹H NMR (300 MHz, DMSO-d₆) δ = 8.44 (d, *J*=2.2 Hz, 1H), 8.17 (dd, *J*=2.3, 8.8
5 Hz, 1H), 7.74 (d, *J*=8.9 Hz, 1H), 6.35 (s, 1H), 5.22 (s, 2H), 5.01 (d, *J*=2.3 Hz, 2H), 3.46–3.40 (m,
6 1H), 2.18 (s, 3H), 1.09 (s, 3H), 0.64–0.55 (m, 2H), 0.46–0.36 (m, 2H); ¹³C NMR (75 MHz, DMSO-d₆)
7 δ = 166.9, 159.9, 159.7, 149.3, 141.3, 137.6, 132.9, 126.7, 116.2, 115.1, 103.5, 77.8, 75.9, 37.2, 33.7,
8 30.9, 23.9, 13.0, 10.9. HRMS (ESI) *m/z* [M + Na]⁺ calcd for C₂₀H₂₀N₄O₅SNa: 451.1047. Found:
9 451.1033.

10
11
12
13
14
15
16
17
18 **1-(Cyclopropylmethyl)-N-(1-methylcyclopropyl)-3-[(3-methylisoxazol-5-yl)methyl]-2,4-dioxo-**
19 **quinazoline-6-sulfonamide (35c)**

20
21 Prepared by General method C (using the alkyl bromide), using **32c** as a starting material, to afford a
22 white powder, 60%. ¹H NMR (300 MHz, DMSO-d₆) δ = 8.44 (d, *J*=2.3 Hz, 1H), 8.24 (s, 1H), 8.11
23 (dd, *J*=2.3, 8.9 Hz, 1H), 7.84 (d, *J*=8.9 Hz, 1H), 6.32 (s, 1H), 5.23 (s, 2H), 4.09 (d, *J*=6.9 Hz, 2H),
24 2.18 (s, 3H), 1.30–1.18 (m, 1H), 1.09 (s, 3H), 0.65–0.56 (m, 2H), 0.54–0.35 (m, 6H); ¹³C NMR (75
25 MHz, DMSO-d₆) δ = 167.0, 160.1, 160.0, 150.0, 142.4, 137.0, 132.9, 126.7, 116.3, 114.7, 103.4, 47.7,
26 37.1, 30.9, 23.9, 13.0, 10.9, 9.3, 3.7. HRMS (ESI) *m/z* [M + Na]⁺ calcd for C₂₁H₂₄N₄O₅SNa: 467.1360.
27 Found: 467.1349.

28
29
30
31
32
33
34
35
36
37 **N-(1-Methylcyclopropyl)-3-[(3-methylisoxazol-5-yl)methyl]-1-(oxetan-3-ylmethyl)-2,4-dioxo-**
38 **quinazoline-6-sulfonamide (35d)**

39
40 Prepared by General method C (using the alkyl tosylate), using **32c** as a starting material, to afford a
41 white powder, 42%. ¹H NMR (300 MHz, DMSO-d₆) δ = 8.42 (d, *J*=2.3 Hz, 1H), 8.36 (s, 1H), 8.06
42 (dd, *J*=2.4, 8.9 Hz, 1H), 7.76 (d, *J*=9.0 Hz, 1H), 6.33 (s, 1H), 5.21 (s, 2H), 4.61 (dd, *J*=6.1, 7.8 Hz,
43 2H), 4.53–4.42 (m, 4H), 3.45–3.39 (m, 1H), 2.18 (s, 3H), 1.09 (s, 3H), 0.60 (s, 2H), 0.43–0.38 (m,
44 2H); ¹³C NMR (75 MHz, DMSO-d₆) δ = 167.0, 160.1, 159.7, 150.4, 142.3, 137.1, 132.7, 126.6, 116.0,
45 115.0, 103.4, 73.8, 45.7, 37.1, 33.3, 30.9, 24.0, 13.0, 10.9. HRMS (ESI) *m/z* [M + Na]⁺ calcd for
46 C₂₁H₂₄N₄O₆SNa: 483.1309. Found: 483.1296.

47
48
49
50
51
52
53
54
55
56 **1-[(2,5-Dimethylpyrazol-3-yl)methyl]-N-(1-methylcyclopropyl)-3-[(3-methylisoxazol-5-**
57 **yl)methyl]-2,4-dioxoquinazoline-6-sulfonamide (35e)**

1
2
3 Prepared by General method C (using the alkyl mesylate), using **32c** as a starting material, to afford a
4 white powder, 39%. ¹H NMR (300 MHz, DMSO-d₆) δ = 8.44 (d, *J*=2.3 Hz, 1H), 8.23 (s, 1H), 8.06
5 (dd, *J*=2.3, 8.8 Hz, 1H), 7.60 (d, *J*=8.9 Hz, 1H), 6.36 (s, 1H), 5.80 (s, 1H), 5.38 (s, 2H), 5.23 (s, 2H),
6 3.81 (s, 3H), 2.18 (s, 3H), 2.00 (s, 3H), 1.08 (s, 3H), 0.64–0.55 (m, 2H), 0.44–0.36 (m, 2H); ¹³C NMR
7 (75 MHz, CDCl₃) δ = 166.0, 160.1, 159.8, 150.1, 147.8, 142.0, 137.9, 136.6, 133.7, 128.8, 115.6,
8 115.2, 105.4, 104.4, 39.7, 37.0, 36.7, 31.8, 24.6, 14.1, 13.3, 11.4. HRMS (ESI) *m/z* [M + H]⁺ calcd for
9 C₂₃H₂₇N₆O₅S: 499.1758. Found: 499.1747.

10
11
12
13
14
15
16
17
18 **3-(Cyanomethyl)-N-(1-methylcyclopropyl)-2,4-dioxo-1-prop-2-ynyl-quinazoline-6-sulfonamide**
19
20 **36b**

21 Prepared by General method C (using the alkyl bromide), using **32d** as a starting material, to afford a
22 white powder, 37%.

23
24
25
26 ¹H NMR (300 MHz, CDCl₃) δ = 8.75 (d, *J*=2.3 Hz, 1H), 8.25 (dd, *J*=2.3, 8.9 Hz, 1H), 7.55 (d, *J*=8.9
27 Hz, 1H), 5.03–4.95 (m, 5H), 2.41 (t, *J*=2.4 Hz, 1H), 1.28 (s, 3H), 0.83–0.72 (m, 2H), 0.59–0.50 (m,
28 2H); ¹³C NMR (75 MHz, CDCl₃) δ = 159.2, 148.9, 141.4, 138.3, 134.2, 128.9, 115.5, 115.3, 114.0,
29 75.7, 74.8, 34.2, 31.9, 29.3, 24.6, 14.1. HRMS (ESI) *m/z* [M + Na]⁺ calcd for C₁₇H₁₆N₄O₄SNa:
30 395.0784. Found: 395.0776.

31
32
33
34
35
36
37 **3-(Cyanomethyl)-1-(cyclopropylmethyl)-N-(1-methylcyclopropyl)-2,4-dioxo-quinazoline-6-**
38 **sulfonamide (36c)**

39 Prepared by General method C (using the alkyl bromide), using **32d** as a starting material, to afford a
40 white powder, 60%. ¹H NMR (300 MHz, DMSO-d₆) δ = 8.44 (d, *J*=2.3 Hz, 1H), 8.25 (s, 1H), 8.11
41 (dd, *J*=2.3, 8.9 Hz, 1H), 7.85 (d, *J*=9.0 Hz, 1H), 4.97 (s, 2H), 4.10 (d, *J*=6.9 Hz, 2H), 2.09 (s, 1H),
42 1.09 (s, 3H), 0.92–0.78 (m, 1H), 0.65–0.56 (m, 2H), 0.56–0.44 (m, 4H), 0.44–0.36 (m, 2H); ¹³C NMR
43 (75 MHz, CDCl₃) δ = 159.7, 149.7, 142.6, 137.6, 134.1, 129.0, 115.2, 115.1, 114.3, 48.9, 31.8, 29.2,
44 24.6, 14.1, 9.3, 4.2. HRMS (ESI) *m/z* [M + Na]⁺ calcd for C₁₈H₂₀N₄O₄SNa: 411.1097. Found:
45 411.1088.

46
47
48
49
50
51
52
53
54
55
56 **3-(Cyanomethyl)-1-[(2,5-dimethylpyrazol-3-yl)methyl]-N-(1-methylcyclopropyl)-2,4-dioxo-**
57 **quinazoline-6-sulfonamide (36e)**

Prepared by General method B, using **32d** as a starting material, to afford a white powder, 17%. ¹H NMR (300MHz, DMSO-d₆) δ = 8.44 (d, *J*=2.2 Hz, 1H), 8.25 (br s, 1H), 8.06 (dd, *J*=2.3, 8.9 Hz, 1H), 7.58 (d, *J*=9.0 Hz, 1H), 5.84 (s, 1H), 5.39 (s, 2H), 4.98 (s, 2H), 3.83 (s, 3H), 2.00 (s, 3H), 1.08 (s, 3H), 0.63–0.55 (m, 2H), 0.43–0.37 (m, 2H); ¹³C NMR (75 MHz, CDCl₃) δ = 159.2, 149.4, 148.0, 141.9, 138.3, 136.0, 134.2, 129.0, 115.4, 115.2, 114.0, 105.4, 39.9, 36.7, 31.9, 29.3, 24.6, 14.1, 13.3. HRMS (ESI) *m/z* [M + Na]⁺ calcd for C₁₈H₂₀N₄O₄SNa: 465.1315. Found: 465.1305.

2-Amino-N-[(5-methyl-1,3,4-thiadiazol-2-yl)methyl]benzamide (37)

(5-Methyl-1,3,4-thiadiazol-2-yl)methanamine **42** (2.4 g, 17 mmol) was added to a magnetically stirred solution of isatoic acid anhydride **29** (2.7 g, 17 mmol) and triethylamine (2.5 mL, 18 mmol) in DMF (20 mL) at 0 °C. After the addition, the resulting mixture was heated to 60 °C for 5 h and then stirred at RT for 16 h. The solvent was removed in vacuo to give a light brown solid, which was preabsorbed onto silica and columned, eluting with 0–5% MeOH/DCM to afford **37** (3.0 g, 65%) as a light brown solid. ¹H NMR (300 MHz, DMSO-d₆) δ = 9.12 (t, *J*=5.8 Hz, 1H), 7.51 (dd, *J*=1.4, 8.0 Hz, 1H), 7.16 (ddd, *J*=1.5, 7.0, 8.3 Hz, 1H), 6.71 (dd, *J*=1.1, 8.2 Hz, 1H), 6.59–6.43 (m, 3H), 4.72 (d, *J*=5.9 Hz, 2H), 2.67 (s, 3H).

3-[(5-Methyl-1,3,4-thiadiazol-2-yl)methyl]-1H-quinazoline-2,4-dione (38)

A solution of **37** (3.0 g, 11 mmol) in THF (100 mL) was cooled to 0 °C and treated with triphosgene (1.6 g, 5.4 mmol), causing precipitate formation. The mixture was stirred in the cool bath for 15 min and then stirred at RT for 18 h. The mixture was quenched with sat. aq. K₂CO₃ (50 mL) and stirred at RT for 24 h. The resulting precipitate was collected by filtration, washed with water and oven-dried to afford **24** (1.7 g, 58%) as an off-white solid. ¹H NMR (300 MHz, DMSO-d₆) δ = 11.80 (br s, 1H), 7.96 (d, *J*=7.8 Hz, 1H), 7.69 (dt, *J*=1.5, 7.7 Hz, 1H), 7.28–7.16 (m, 2H), 5.44 (s, 2H), 2.67 (s, 3H).

3-[(5-Methyl-1,3,4-thiadiazol-2-yl)methyl]-2,4-dioxo-1H-quinazoline-6-sulfonyl chloride (39)

A solution of **38** (1.7 g, 6.2 mmol) in chlorosulfonic acid (5 mL, 6.2 mmol) was heated to 50 °C for 2 h and then allowed to cool to RT. The reaction mixture was then added dropwise to crushed ice (~20 mL) at –10 °C and stirred for 20 min. The precipitated solid was collected by filtration, washed with water and oven-dried to give a sticky solid. This was azeotroped with toluene (×3) to give the desired

product (1.6 g, 69%) as a pale yellow solid. ¹H NMR (300 MHz, DMSO-*d*₆) δ = 11.76 (s, 1H), 8.16 (d, *J*=2.0 Hz, 1H), 7.88 (dd, *J*=2.0, 8.4 Hz, 1H), 7.17 (d, *J*=8.5 Hz, 1H), 5.44 (s, 2H), 2.67 (s, 3H).

N-(1-Methylcyclopropyl)-3-[(5-methyl-1,3,4-thiadiazol-2-yl)methyl]-2,4-dioxo-1H-quinazoline-6-sulfonamide (40)

A mixture of **39** (411 mg, 1.1 mmol) and 1-methylcyclopropanamine hydrochloride (130 mg, 1.2 mmol) in DCM (20 mL) was cooled in an ice bath and treated with triethylamine (0.34 mL, 2.4 mmol). The reaction mixture was allowed to warm to RT and was stirred for 18 h. The reaction mixture was then concentrated, pre-absorbed onto silica and columned, eluting with 0–5% MeOH in DCM afford **40** (142 mg, 32%) as a white powder. ¹H NMR (300 MHz, DMSO-*d*₆) δ = 12.07 (s, 1H), 8.33 (s, 1H), 8.16 (s, 1H), 8.04 (br d, *J*=8.7 Hz, 1H), 7.37 (d, *J*=8.6 Hz, 1H), 5.44 (s, 2H), 2.68 (s, 3H), 1.07 (s, 3H), 0.63–0.55 (m, 2H), 0.43–0.34 (m, 2H).

1-Ethyl-N-(1-methylcyclopropyl)-3-[(5-methyl-1,3,4-thiadiazol-2-yl)methyl]-2,4-dioxo-quinazoline-6-sulfonamide (41a)

Prepared by General method C (using the alkyl iodide), using **40** as a starting material, to afford a white powder, 20%. ¹H NMR (300 MHz, DMSO-*d*₆) δ = 8.44 (d, *J*=2.3 Hz, 1H), 8.19 (br s, 1H), 8.11 (dd, *J*=2.3, 8.9 Hz, 1H), 7.76 (d, *J*=8.9 Hz, 1H), 5.50 (s, 2H), 4.20 (q, *J*=7.1 Hz, 2H), 2.68 (s, 3H), 1.24 (t, *J*=7.0 Hz, 3H), 1.08 (s, 3H), 0.63–0.56 (m, 2H), 0.43–0.37 (m, 2H); HRMS (ESI) *m/z* [M + H]⁺ calcd for C₁₈H₂₂N₅O₄S₂: 436.1108. Found: 436.1096.

1-[(2,5-Dimethylpyrazol-3-yl)methyl]-N-(1-methylcyclopropyl)-3-[(5-methyl-1,3,4-thiadiazol-2-yl)methyl]-2,4-dioxo-quinazoline-6-sulfonamide (41e)

Prepared by General method C (using the alkyl chloride), using **40** as a starting material, to afford a white powder, 44%. ¹H NMR (300 MHz, DMSO-*d*₆) δ = 8.45 (d, *J*=2.3 Hz, 1H), 8.25 (s, 1H), 8.07 (dd, *J*=2.4, 8.9 Hz, 1H), 7.61 (d, *J*=8.9 Hz, 1H), 5.79 (s, 1H), 5.52 (s, 2H), 5.40 (s, 2H), 3.82 (s, 3H), 2.68 (s, 3H), 2.00 (s, 3H), 1.08 (s, 3H), 0.63–0.56 (m, 2H), 0.42–0.37 (m, 2H); ¹³C NMR (75 MHz, CDCl₃) δ = 166.6, 163.7, 159.8, 150.1, 147.5, 142.0, 138.1, 133.8, 129.0, 124.6, 115.7, 115.1, 105.6, 40.2, 39.7, 36.6, 31.9, 24.7, 15.6, 14.1, 13.0. HRMS (ESI) *m/z* [M + H]⁺ calcd for C₂₂H₂₆N₇O₄S₂: 516.1482. Found: 516.1470.

PARG Biochemical Assay

This assay was conducted according to the published protocol.²¹ Briefly, PARG in vitro assays were conducted in a total volume of 15 μ L in a standard 384-well format. 5 μ L of human full length PARG (AstraZeneca),¹⁶ used at a final reaction concentration of 65 pM, was added to 5 μ L of Bt-NAD ribosylated PARP1 substrate (AstraZeneca) at a final reaction concentration of 4.8 nM in assay buffer (50 mM Tris pH 7.4, 0.1 mg/mL BSA, 3 mM EDTA, 0.4 mM EGTA, 1 mM DTT, 0.01% Tween 20, 50 mM KCl). The reaction was incubated at room temperature for 10 min and then 5 μ L detection reagent was added. Detection reagent consists of 42 nM MAb anti-6HIS XL665 (CisBio: 61HISXLB) and 2.25 nM streptavidin europium cryptate (CisBio: 610SAKLB), both at 3 \times working stock concentrations (final concentrations of 14 nM and 0.75 nM respectively), in detection buffer (50 mM Tris pH 7.4, 0.1 mg/mL BSA and 100 mM KF). Following incubation at room temperature for 60 min in the dark, TR-FRET signal was measured at λ Ex 340 nm and λ Em 665 nm and λ Em 620 nm using a PHERAstar FS plate reader (BMG Labtech). The ratio was calculated as $[\text{Em665}/\text{EM620}]\times 10^4$ for each well and used to calculate percent inhibition for test compounds.

Cellular PAR chain Assay

This assay was carried out according to the published protocol³¹ Briefly, HeLa cells were seeded into 384-well plates and 16–24 h later, were treated with inhibitors (8 pt dose response, 0.01–30 μ M) or vehicle (DMSO) control. After 1 h cells were co-dosed with MMS at 50 μ g/mL (final) and incubated for 1 h at 37 $^{\circ}$ C. Cells were fixed with ice-cold 95% methanol/ phosphate buffered saline (PBS) for 15 min at -20 $^{\circ}$ C and then washed once with PBS at room temperature. Cells were then permeabilized using PBS/Triton 0.1% for 20 min, and washed once in PBS before incubating with anti-PAR antibody (10H, Merck-Millipore) overnight at 4 $^{\circ}$ C. Cells were then incubated with anti-mouse Alexofluor 488-conjugated secondary antibody (A11029, ThermoFisher) at 1:1000 and Hoechst 33342 (1:5000) and images were captured on a CellInsight (ThermoFisher Scientific, Northumberland, UK) and analyzed using proprietary software. The mean of the intensity of nuclear

1
2
3 spots at 488 nM was reported with 25 fields captured from duplicate wells and approximately 1100
4
5 cells analyzed per well.
6
7

8 For details of the enzyme assay – cell assay correlation, see Supporting Information Figure S1.
9

10 11 **Cytotoxicity Assay** 12

13
14 HeLa cells were seeded in 30 μ L media at 1×10^4 cells/mL in Greiner (#781091) 384-well plates. 16–
15
16 24 h later, cells were treated with inhibitors (8 point dose response, 0.01–30 μ M, triplicates) or
17
18 vehicle (DMSO) control. The outer wells were left un-dosed to account for edge effects. After 72 h,
19
20 50 μ L of 3.7% formaldehyde/PBS was added to each well and cells were fixed for 20 min. Cells were
21
22 then rinsed twice with PBS and stained for 1 h with Hoechst 33342/PBS (1:2000) in the dark. After
23
24 two further rinses with PBS, images were captured and nuclei counted on a CellInsight
25
26 (ThermoFisher). The maximum number of fields (25) were captured from each triplicate well which
27
28 approximated to at least 1000 nuclei in vehicle-dosed wells.
29
30

31 32 **Cytotoxicity and Selectivity** 33

34 See reference 12 for methods to measure PARP1 selectivity and ARH3 selectivity.
35
36
37

38 39 **Pharmacokinetics** 40

41 All studies were conducted after review by the Animal Welfare and Ethical Review Body at CRUK-
42
43 MI and in accordance with the University of Manchester Policy on the use of animals in research. All
44
45 work was carried out in compliance with the Animals (Scientific Procedures) Act 1986 and EU
46
47 Directive 2010/63/EU.

48 Pharmacokinetics were studied in male CD-1 mice following single intravenous or oral
49
50 administration. Compounds were formulated as solutions comprising up to 10% DMSO with up to
51
52 10% Tween80 in saline at a concentration of approximately 1 mM. Doses were administered at 1
53
54 mg/kg (IV) or 5 mg/kg (oral). Blood samples were collected as dried blood spots and assayed
55
56 following solvent extraction through a phospholipid removal plate followed by LC-MS/MS analysis.
57
58 The time-points for blood collection were as follows: oral (0.5, 1, 3, 5 and 24 h); IV (0.1, 0.25, 0.75,
59
60

1
2
3 2, 5 and 24 h). The resulting concentration-time data were analyzed by non-compartmental methods
4
5 (PK Solver, Excel Add-In).
6
7
8
9

10 **Structure-based Virtual screening and Library Design**

11
12

13 The X-ray crystal structure of the anthraquinone **8a** in complex with the human PARG catalytic
14 domain (PDB 6HMM) was the basis for virtual screening and protein-ligand docking studies using the
15 Schrödinger modelling suite (Schrödinger, LLC, New York, NY, 2012-2015 releases). The Maestro
16 Protein Preparation Wizard was used for initial processing of the X-ray crystal structure, applying
17 default settings for hydrogen addition, optimization of hydrogen bonding networks and constrained
18 geometry refinement, followed by visual assessment of the final protein model. Crystallographic
19 solvent molecules were removed prior to generation of a receptor grid file for use in Glide docking. A
20 grid box was defined based on the crystallographic pose of **8a**, extending the inner grid box to 14 Å in
21 the direction of the PARG ribose-binding site so as to encompass the bound pose of ADP-ribose and
22 hence to facilitate docking of ligands larger than the relatively compact anthraquinone **8a**. Hydrogen
23 bonding constraint sites were defined as the protein atoms interacting with the sulfonamide moiety of
24 **8a** (Glu727 carboxylate, Gln754 sidechain NH₂, Ile726 backbone NH).
25
26
27
28
29
30
31
32
33
34
35
36
37
38

39 For the initial virtual screen, a set of commercially available aryl sulfonamides was generated by
40 searching an in-house compilation of individual supplier catalogues, filtered for general drug-like
41 property profiles.²⁷ Prompted by the steep SAR we had observed around the sulfonamide moiety of
42 **8a**, the substructure search was limited to aryl sulfonamides bearing a small *N*-alkyl substituent, as
43 represented by the SMILES string *cS(=O)(=O)[NH]CC*. After removal of duplicates and checking of
44 physicochemical property profiles using Canvas, a set of approximately 30,000 compounds was
45 prepared for docking using LigPrep and subsequently docked to the PARG protein grid using Glide
46 SP, using default docking parameters other than inclusion of at least one of the H-bonding constraints
47 around the sulfonamide moiety. From the docked poses, a selection was made on the basis of docking
48 score, visually plausible binding interactions, lead-like property profile and chemical diversity.
49
50
51
52
53
54
55
56
57
58
59
60

1
2
3 To extend the diversity of aryl sulfonamides for virtual screening, several rounds of virtual library
4 building and docking were pursued, based on lists of commercially available aryl sulfonyl chlorides,
5 initially obtained by searching our internal vendor catalogue and subsequently the eMolecules
6 Building Blocks collection (<https://www.emolecules.com>, accessed Oct 24, 2018). These lists were
7 the basis for virtual library enumeration with favoured *N*-alkyl substituents (typically
8 methylcyclopropyl) using PipelinePilot (BIOVIA, San Diego, CA), followed by processing in
9 LigPrep and docking in Glide as before. Ligand interaction diagrams in Figures 5, 7, 8 and 10 were
10 generated within Maestro and images of protein-ligand complexes within the PyMOL Molecular
11 Graphics System (Schrödinger, LLC, New York, NY).
12
13
14
15
16
17
18
19
20
21
22
23
24

25 AUTHOR INFORMATION

26 27 28 **Corresponding author**

29
30
31 *Telephone: +44 (0)161-306-6280. Email: allan.jordan@cruk.manchester.ac.uk.
32
33

34 **Notes**

35
36
37 The authors declare no competing financial interest.
38
39

40 #BW, KMS, AMcG and AMJ contributed equally to the content and preparation of this manuscript.
41
42

43 **Acknowledgments**

44
45 This work was supported by Cancer Research UK (Grant C480/A11411 and C5759/A17098). We
46 thank AstraZeneca for triaging HTS output and Mentxu Aiertza and Samantha Hitchin for assistance
47 with compound logistics. We thank Ivan Ahel for helpful discussions regarding PARG biology.
48 HRMS spectra were generated by Gareth Smith, School of Chemistry, University of Manchester, M13
49 9PL, UK. LogD and turbidimetric solubility were provided by Cyprotex Discovery, Macclesfield,
50 UK. We thank Giles Hassall (AstraZeneca) for expression and purification of the human PARG
51 catalytic domain, Claire Brassington (AstraZeneca) for assistance with crystallization, Diamond Light
52
53
54
55
56
57
58
59
60

1
2
3 Source for beamtime, and the AstraZeneca Alderley Park Protein Structure team and the staff of
4 beam-line I04-1 for assistance with crystal testing and X-ray diffraction data collection. JChem for
5
6
7
8
9
10
11
12
13
14
15
16
17
18
19
20
21
22
23
24
25
26
27
28
29
30
31
32
33
34
35
36
37
38
39
40
41
42
43
44
45
46
47
48
49
50
51
52
53
54
55
56
57
58
59
60

Source for beamtime, and the AstraZeneca Alderley Park Protein Structure team and the staff of beam-line I04-1 for assistance with crystal testing and X-ray diffraction data collection. JChem for Excel was used for structure property prediction and calculation and general data handling (JChem for Excel, version 6.1.5.781, 2008–2013, ChemAxon (<http://www.chemaxon.com>)). We thank Rae Lawrence for help in re-formatting the graphics in this manuscript.

ABBREVIATIONS USED

SAR Structure-Activity Relationship

HTS High-Throughput Screen

ASSOCIATED CONTENT

Supporting Information

The supporting information is available free of charge via the Internet at <http://pubs.acs.org>. Molecular formula strings (CSV). LC-MS methods and solvent gradients; preparative HPLC instrument and solvent gradients; summary of purity data; additional core-hops identified from virtual screening; preparative methods and spectroscopic data for key intermediates and compounds **S1-S17**; exemplar NMR and LC data; PARG co-crystal structure determination and refinement details for **8a**, **22h**, **27t** and **33f** (PDF).

ACCESSION CODES

Atomic coordinates and structure factors for X-ray crystal structures of **8a** (PDB 6HMM), **22h** (PDB 6HMN), **27t** (PDB 6HMK) and **33f** (PDB 6HML) in complex with the human PARG catalytic domain have been deposited in the Protein Data Bank. Authors will release the atomic coordinates and experimental data upon article publication.

1
2
3 **REFERENCES**
4
5
6

- 7 ¹ Lord, C. J.; Ashworth, A. The DNA Damage Response and Cancer Therapy. *Nature* **2012**, *481*,
8 287–294.
- 9
10
11 ² Hosoya, N.; Miyagawa, K. Targeting DNA Damage Response in Cancer Therapy. *Cancer Sci.* **2014**,
12 *105*, 370–388.
- 13
14
15 ³ O'Connor, M. J. Targeting the DNA Damage Response in Cancer. *Mol. Cell* **2015**, *60*, 547–560.
- 16
17
18 ⁴ Mortusewicz, O.; Fouquerel, E.; Amé, J.-C.; Leonhardt, H.; Schreiber, V. PARG is Recruited to
19 DNA Damage Sites Through Poly(ADP-ribose)- and PCNA-dependent Mechanisms. *Nucleic Acids*
20 *Res.* **2011**, *39*, 5045–5056.
- 21
22
23
24
25 ⁵ Barkauskaite, E.; Jankevicius, G.; Ladurner, A. G.; Ahel, I.; Timinszky, G. The Recognition and
26 Removal of Cellular Poly(ADP-ribose) Signals. *FEBS J.* **2013**, *280*, 3491–3507.
- 27
28
29 ⁶ Feng, X.; Koh, D. W. Chapter Five - Roles of Poly(ADP-Ribose) Glycohydrolase in DNA Damage
30 and Apoptosis. *Int. Rev. Cell Mol. Biol.*, Kwang, W. J., Ed. Academic Press: **2013**, *304*, 227–281.
- 31
32
33
34 ⁷ Davar, D.; Beumer, J. H.; Hamieh, L.; Tawbi, H. Role of PARP Inhibitors in Cancer Biology and
35 Therapy. *Curr. Med. Chem.* **2012**, *19*, 3907–3921.
- 36
37
38 ⁸ Ricks, T. K.; Chiu, H.-J.; Ison, G.; Kim, G.; McKee, A. E.; Kluetz, P.; Pazdur, R. Successes and
39 Challenges of PARP Inhibitors in Cancer Therapy. *Front. Oncol.* **2015**, *5*, 222.
- 40
41
42 ⁹ Frampton, J. E. Olaparib: A Review of Its Use as Maintenance Therapy in Patients with Ovarian
43 Cancer. *BioDrugs* **2015**, *29*, 143–150.
- 44
45
46 ¹⁰ Fauzee, N. J. S.; Pan, J.; Wang, Y.-I. PARP and PARG Inhibitors—New Therapeutic Targets in
47 Cancer Treatment. *Pathol. Oncol. Res.* **2010**, *16*, 469–478.
- 48
49
50
51 ¹¹ Anuradha, P.; Pooja, M.; Prakash, G. C.; Anil, B. G. PARG Inhibitors' Success: A Long Way to
52 Go! *Curr. Enz. Inhib.* **2014**, *10*, 81–93.
- 53
54
55 ¹² James, D. I.; Smith, K. M.; Jordan, A. M.; Fairweather, E. E.; Griffiths, L. A.; Hamilton, N. S.;
56 Hitchin, J. R.; Hutton, C. P.; Jones, S.; Kelly, P.; McGonagle, A. E.; Small, H.; Stowell, A. I. J.;
57
58
59
60

1
2
3
4 Tucker, J.; Waddell, I. D.; Waszkowycz, B.; Ogilvie, D. J. First-in-Class Chemical Probes against
5 Poly(ADP-ribose) Glycohydrolase (PARG) Inhibit DNA Repair with Differential Pharmacology to
6
7 Olaparib. *ACS Chem. Biol.* **2016**, *11*, 3179–3190.

10
11 ¹³ Slade, D.; Dunstan, M. S.; Barkauskaite, E.; Weston, R.; Lafite, P.; Dixon, N.; Ahel, M.; Leys, D.;
12
13 Ahel, I. The Structure and Catalytic Mechanism of a Poly(ADP-ribose) Glycohydrolase. *Nature*,
14
15 **2011**, *477*, 616–620.

16
17 ¹⁴ Dunstan, M. S.; Barkauskaite, E.; Lafite, P.; Knezevic, C. E.; Brassington, A.; Ahel, M.;
18
19 Hergenrother, P. J.; Leys, D.; Ahel, I. Structure and Mechanism of a Canonical Poly(ADP-ribose)
20
21 Glycohydrolase. *Nat. Commun.* **2012**, *3*, 878.

22
23 ¹⁵ Kim, I.-K.; Kiefer, J. R.; Ho, C. M. W.; Stegeman, R. A. Classen, S.; Tainer, J. A.; Ellenberger, T.
24
25 Structure of Mammalian Poly(ADP-ribose) Glycohydrolase Reveals a Flexible Tyrosine Clasp as a
26
27 Substrate-binding Element. *Nat. Struc. Mol. Biol.* **2012**, *19*, 653–656.

28
29 ¹⁶ Tucker, J. A.; Bennett, N.; Brassington, C.; Durant, S. T.; Hassall, G.; Holdgate, G.; McAlister, M.;
30
31 Nissink, J. W. M.; Truman, C.; Watson, M. Structures of the Human Poly(ADP-Ribose)
32
33 Glycohydrolase Catalytic Domain Confirm Catalytic Mechanism and Explain Inhibition by ADP-
34
35 HPD Derivatives. *PLoS ONE*, **2012**, *7*, e50889.

36
37 ¹⁷ Barkauskaite, E.; Brassington, A.; Tan, E. S.; Warwicker, J.; Dunstan, M. S.; Banos, B.; Lafite, P.;
38
39 Ahel, M.; Mitchison, T. J.; Ahel, I.; Leys, D. Visualization of Poly(ADP-ribose) Bound to PARG
40
41 Reveals Inherent Balance Between *Exo*- and *Endo*-Glycohydrolase Activities. *Nat. Commun.* **2013**, *4*,
42
43 2164.

44
45 ¹⁸ Žaja, R.; Mikoč, A.; Barkauskaite, E.; Ahel, I. Molecular Insights into Poly(ADP-ribose)
46
47 Recognition and Processing. *Biomolecules*, **2013**, *3*, 1–17.

48
49 ¹⁹ Wang, Z.; Gagné, J.-P.; Poirier, G. G.; Xu, W. Crystallographic and Biochemical Analysis of the
50
51 Mouse Poly(ADP-ribose) Glycohydrolase. *PLoS ONE*, **2014**, *9*, e86010.

52
53 ²⁰ Rack, J. G.; Perina, D.; Ahel, I. Macrod domains: Structure, Function, Evolution, and Catalytic
54
55 Activities. *Annu Rev Biochem.* **2016**, *85*, 431–454.

- 1
2
3
4 ²¹ Stowell, A. I. J.; James, D. I.; Waddell, I. D.; Bennett, N.; Truman, C.; Hardern, I. M.; Ogilvie, D. J.
5
6 A High-throughput Screening-compatible Homogeneous Time-resolved Fluorescence Assay
7
8 Measuring the Glycohydrolase Activity of Human Poly(ADP-ribose) Glycohydrolase. *Anal. Biochem.*
9
10 **2016**, *503*, 58–64.
- 11
12 ²² Koh, D. W.; Coyle, D. L.; Mehta, N.; Ramsinghani, S.; Kim, H.; Slama, J. T.; Jacobson, M. K. SAR
13
14 Analysis of Adenosine Diphosphate (Hydroxymethyl)pyrrolidinediol Inhibition of Poly(ADP-ribose)
15
16 Glycohydrolase. *J. Med. Chem.* **2003**, *46*, 4322–4332.
- 17
18 ²³ Formentini, L.; Arapistas, P.; Pittelli, M.; Jacomelli, M.; Pitozzi, V.; Menichetti, S.; Romani, A.;
19
20 Giovannelli, L.; Moroni, F.; Chiarugi, A. Mono-galloyl Glucose Derivatives are Potent Poly(ADP-
21
22 ribose) Glycohydrolase (PARG) Inhibitors and Partially Reduce PARP-1-dependent Cell Death. *Br. J.*
23
24 *Pharmacol.* **2008**, *155*, 1235–1249.
- 25
26 ²⁴ Steffen, J. D.; Coyle, D. L.; Damodaran, K.; Beroza, P.; Jacobson, M. K. Discovery and Structure-
27
28 Activity Relationships of Modified Salicylanilides as Cell Permeable Inhibitors of Poly(ADP-ribose)
29
30 Glycohydrolase (PARG). *J. Med. Chem.* **2011**, *54*, 5403–5413.
- 31
32 ²⁵ Finch, K. E.; Knezevic, C. E.; Nottbohm, A. C.; Partlow, K. C.; Hergenrother, P. J. Selective Small
33
34 Molecule Inhibition of Poly(ADP-Ribose) Glycohydrolase (PARG). *ACS Chem. Biol.* **2012**, *7*,
35
36 563–570.
- 37
38 ²⁶ Islam, R.; Koizumi, F.; Kodera, Y.; Inoue, K.; Okawara, T.; Masutani, M. Design and Synthesis of
39
40 Phenolic Hydrazide Hydrazones as Potent Poly(ADP-ribose) Glycohydrolase (PARG) Inhibitors.
41
42 *Bioorg. Med. Chem. Lett.* **2014**, *24*, 3802–3806.
- 43
44 ²⁷ Baell, J. B.; Holloway, G. A. New Substructure Filters for Removal of Pan Assay Interference
45
46 Compounds (PAINS) from Screening Libraries and for Their Exclusion in Biosassays. *J. Med. Chem.*
47
48 **2010**, *53*, 2719–2740.
- 49
50 ²⁸ McGonagle, A. E.; Jordan, A. M.; Waszkowycz, B.; Hutton, C. P.; Waddell, I. D.; Hitchin, J. R.;
51
52 Smith, K. M.; Hamilton, N. M. 2,4-Dioxo-Quinazoline-6-Sulphonamide Derivatives as Inhibitors of
53
54 PARG. *PCT Int. Appl. WO2015079251* June 4, 2016.
- 55
56
57
58
59
60

1
2
3
4
5
6
7
8
9
29 McGonagle, A. E.; Jordan, A. M.; Waszkowycz, B.; Hutton, C. P.; Waddell, I. D.; Hitchin, J. R.;
Smith, K. M.; Hamilton, N. M. PARG Inhibitory Compounds. *PCT Int. Appl. WO2016097749* June
23, 2016.

10
11
12
13
14
30 Lipshutz, B. H.; Chung, D. W.; Rich, B.; Corral, R. Simplification of the Mitsunobu Reaction. Di-
p-chlorobenzyl Azodicarboxylate: A New Azodicarboxylate. *Org. Lett.* **2006**, *8*, 5069–5072.

15
16
17
18
19
20
21
22
23
24
25
26
27
31 James, D. I.; Durant, S.; Eckersley, K.; Fairweather, E.; Griffiths, L. A.; Hamilton, N.; Kelly, P.;
O'Connor, M.; Shea, K.; Waddell, I. D.; Ogilvie, D. J. An Assay to Measure Poly(ADP ribose)
Glycohydrolase (PARG) Activity in Cells. *Fl1000Research*, **2016**, *5*, 736–746.

28
29
30
31
32
33
34
35
36
37
38
39
40
41
42
43
44
45
46
47
48
49
50
32 Gibson, D.; Gean, K. F.; Ben-Shoshan, R.; Ramu, A.; Ringel, I.; Katzhendler, J. Preparation,
Characterization, and Anticancer Activity of a Series of *cis*-PtCl₂ Complexes Linked to
Anthraquinone Intercalators. *J. Med. Chem.* **1991**, *34*, 414–420.

28
29
30
31
32
33
34
35
36
37
38
39
40
41
42
43
44
45
46
47
48
49
50
33 Lipophilic Ligand Efficiency calculated as biochemical pEC₅₀ - XlogP

30
31
32
33
34
35
36
37
38
39
40
41
42
43
44
45
46
47
48
49
50
51
52
53
54
55
56
57
58
59
60
34 Talele, T. T. The “Cyclopropyl Fragment” is a Versatile Player that Frequently Appears in
Preclinical/Clinical Drug Molecules. *J. Med. Chem.* **2016**, *59*, 8712–8756.

35
36
37
38
39
40
41
42
43
44
45
46
47
48
49
50
51
52
53
54
55
56
57
58
59
60
35 <https://ximbio.com/reagent/152787/parg-inhibitor-pdd00017273-small-molecule-tool-compound>,
accessed Oct 24, 2018

36
37
38
39
40
41
42
43
44
45
46
47
48
49
50
51
52
53
54
55
56
57
58
59
60
36 See, for example, Gogola, E; Duarte, A.A.; de Ruiter, J.R.; Wiegant, W.W.; Schmid, J. A.; de
Bruijn, R.; James, D. I.; Llobet, S.G.; Vis, D.J.; Annunziato, S.; van den Broek, B.; Barazas, M.;
Kersbergen, A.; van de Ven, M.; Tarsounas, M.; Ogilvie, D.J.; van Vugt, M.; Wessels, L.F.A.;
Bartkova, J.; Gromova, I.; Andújar-Sánchez, M.; Bartek, J.; Lopes, M.; van Attikum, H.; Borst, P.;
Jonkers, J.; Rottenberg, S. Selective Loss of PARG Restores PARylation and Counteracts PARP
Inhibitor-Mediated Synthetic Lethality. *Cancer Cell*, **2018**, *33*, 1078–1093

51
52
53
54
55
56
57
58
59
60
37 See Supporting Information for correlation between biochemical and cellular pEC₅₀s for the whole
quinazolinedione series.

38 <http://www.chemicalprobes.org/pdd00017273>, accessed Oct 24, 2018

39 XLogP calculated using Dotmatics suite, Bishop's Stortford, UK.

1
2
3
4 ⁴⁰ Chan, D. M. T.; Monaco, K. L.; Wang, R.-P.; Winters, M. P. New N- and O-arylations with
5
6 Phenylboronic Acids and Cupric Acetate. *Tetrahedron Lett.* **1998**, *39*, 2933–2936.

7
8 ⁴¹ McLeod, M.; Boudreault, N.; Leblanc, Y. Synthetic Application of Monoprotected Hydrazines
9
10 toward the Synthesis of 1-Aminopyrroles. *J. Org. Chem.* **1996**, *61*, 1180–1183.
11
12
13
14
15
16
17
18
19
20
21
22
23
24
25
26
27
28
29
30
31
32
33
34
35
36
37
38
39
40
41
42
43
44
45
46
47
48
49
50
51
52
53
54
55
56
57
58
59
60

Table of Contents Graphic.